NMR STUDIES OF INTRACELLULAR SODIUM IN THE PERFUSED FROG HEART

by

Deborah Burstein

Bachelor of Arts
Physics
Queens College of the City University of New York (1979)

Master of Science
Physics
Massachusetts Institute of Technology (1982)

SUBMITTED TO THE HARVARD-MASSACHUSETTS INSTITUTE OF TECHNOLOGY
DIVISION OF HEALTH SCIENCES AND TECHNOLOGY
IN PARTIAL FULFILLMENT OF THE REQUIREMENTS FOR THE DEGREE OF
DOCTOR OF PHILOSOPHY

at the
Massachusetts Institute of Technology
May, 1986

Signature of Author _____
Harvard-Massachusetts Institute of Technology
Division of Health Sciences and Technology
May 2, 1986

Certified by _____
Eric T. Fossel
Thesis Supervisor

Accepted by _____
Roger G. Mark
Chairman, Graduate Committee

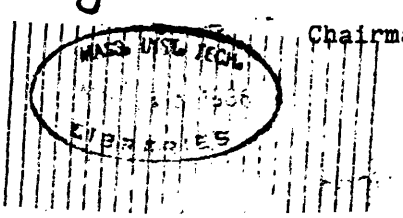

NMR STUDIES OF INTRACELLULAR SODIUM IN THE PERFUSED FROG HEART

by

Deborah Burstein

Submitted to the Harvard-Massachusetts Institute of Technology
Division of Health Sciences and Technology
on May 2, 1986 in partial fulfillment of the
requirements for the Degree of Doctor of Philosophy in
Medical Physics

ABSTRACT

Nuclear magnetic resonance (NMR) spectroscopy provides a means of noninvasively observing intracellular sodium, one of the principal ions responsible for the electrical activity of the heart. The NMR parameters of resonant frequency, spin density, and the relaxation times T_1 and T_2 yield information regarding the number of sodium ions in the sample as well as the interactions between the ions and their environment. However, the difficulty in differentiating between the NMR signals originating from the intracellular and from the extracellular sodium ions has, until now, precluded quantitative analysis of the above parameters for the intracellular sodium. In this study, a shift reagent (dysprosium tripolyphosphate) was used to alter the resonant frequency of the extracellular contributions to the NMR spectrum. Mathematical filtering or presaturation of the extracellular resonance was used to separate more completely the intra- and extracellular sodium NMR signals, thereby allowing for the quantitative investigation of the intracellular sodium in the perfused frog heart.

Sodium NMR spectra were obtained on a Bruker 360 AM spectrometer operating at 95.26 MHz. The results presented here demonstrate the feasibility of using NMR spectroscopy to measure changes in the intracellular sodium levels with pharmacologic and physiologic interventions. 1) The three interventions of adding 10μM ouabain to the perfusate, perfusing with a zero potassium buffer, and replacement of 66% of the sodium in the perfusate with lithium, resulted in the following percent changes in the intracellular sodium levels (mean ± S.D.): ouabain, +(460±60), n=6; zero potassium, +(300±30), n=3; lithium, -(51±6), n=3. 2) The ability to monitor reversible events was demonstrated by returning to the normal buffer after perfusing with zero potassium; the sodium level was shown to return to its initial level within 30 minutes. 3) Smaller changes in the intracellular sodium were observed when the hearts were paced at varying rates. An increase of 45% in the intracellular sodium was observed when changing the pacing rate from 0 to 60 beats per minute, and proportional changes were measured for intermediate pacing rates. These results are comparable to those in the literature which utilize microelectrode measurements. In the experiments reported here, the extracellular calcium was below the normal levels due to binding of the calcium to the shift reagent; compensation for this effect is possible and should allow this

technique to be extended to further physiologic studies and to mammalian systems.

Motional restriction, or binding, of sodium results in multicomponent NMR relaxation times, primarily affecting T_2. The relaxation times of the intracellular sodium were measured under both control conditions and after a 5 fold increase in the intracellular sodium (due to ouabain exposure). T_1 was measured with the standard inversion recovery technique, yielding a single exponential decay with a time constant of 22.4 ± 3.0 msec (n=5, control) or 24.2 ± 1.5 msec (n=5, ouabain). The T_2 of the intracellular sodium was measured using the standard Hahn echo technique, both with and without the modification of presaturation of the extracellular resonance. The T_2 decay was not well fit by a single exponential; a double exponential fit yielded time constants and relative amplitudes of 2.0 ± 1.3 msec (46 ± 8%) and 16.3 ± 4.3 msec (54 ± 8%) for the control hearts (n=5) and 2.1 ± 0.6 msec (43 ± 5%) and 16.8 ± 4.0 msec (57 ± 5%) for the ouabain treated hearts (n=7). The short relaxation times and the biexponential T_2 decays demonstrate that there is some restriction of the sodium ions within the cell relative to ions in free solution, and that these interactions are not affected by a five fold increase in the sodium level. However the relative amplitudes of the different time constants are inconsistent with those which would be expected from a homogeneous pool of nuclei. These results are therefore indicative of restriction and compartmentation of sodium within the cell, information which is not available from microelectrode studies. In addition, the results presented here, along with further studies, may enable the NMR identification of at least a component of the intracellular sodium on the basis of its short T_2 relaxation time, and thus, may eliminate the need for the shift reagent for in-vivo studies. They may also help form the basis for the interpretation of clinically obtained sodium images, in which contrast is determined by the sodium content, T_1, and T_2.

Thesis Supervisor: Dr. Eric T. Fossel

Title: Associate Professor of Radiology,
Harvard Medical School

ACKNOWLEDGEMENTS

This thesis represents the culmination of my student days in the MEMP program of HST. The educational opportunities provided to me over the years have been unique, and have only been enriched by the dedication of the faculty and staff, and by the comraderie and talents of the students. As such, I am grateful to the faculty, staff, and students of the Division of HST for making this a rewarding and unforgettable experience. I hope that, in this past year, I have been able to reciprocate for at least a small fraction of what I have received from the outstanding group of individuals associated with HST.

Several individuals deserve special thanks for their help with this thesis:

Dr. Eric Fossel, for introducing me to the world of NMR, for his constant encouragement which kept me believing that the magnet would eventually arrive, and for the experimental support once it did arrive. Finally, for giving me the room to expand and pursue my own ideas.

Drs. Richard Cohen, Martin Kushmerick, and Leo Neuringer, the other members of my thesis committee, for their help with the aspects of the thesis work with which they were familiar, and for taking the time to learn about those aspects which were at first unfamiliar to them.

Drs. Moshe Reis and Michael Koskinen, for many helpful discussions and suggestions.

Dr. Sven Paulin, for his constant cheerfulness and encouragement, and for the general support of the radiology department

at Beth Israel Hospital.

Steve Gladstone and Ivan Jemelka, for their technical assistance. Special thanks to Steve for the superb job done in building the perfusion apparatus, and for all the other aspects of his work which keeps the lab running so smoothly.

Dr. Bernard Ransil, for his help with the data analysis which was performed at the Core lab computer facilities at the Beth Israel Hospital.

I'd like to acknowledge the financial support of the Whitaker Foundation (the Whitaker Health Sciences Fund Fellowship), the American Heart Association (Grant in Aid 83-1186), and NIH (Grants HL34684 and HL28432).

Many others have contributed indirectly to the completion of this thesis. I extend my gratitude to:

Dr. Ernest Cravalho. I am indebted to Ernie for his constant advice, support, source of motivation, and friendship. Ernie always put the welfare of the student first; his concern has been felt and appreciated by all. I also thank him for never taking advantage of the many opportunities which I gave him to say "I told you so".

Dr. Roger Mark. Despite the huge increase in his administrative duties of the past year, Roger has managed to remain a sincere and concerned scientist, physician, and friend. I value his judgement and opinions, and I thank him for the countless occasions on which he managed to give me "just a few minutes" of his time.

Dr. Fred Bowman, Keiko Oh, and Patty Cunningham. Their diligence enabled me to miraculously avoid all contact with the administrative paper mill at MIT.

Gloria McAvenia. Any time that I asked Gloria to do me a favor, it was done, with a smile, and done well. I took advantage of this many times over the past few years, and am very appreciative.

My colleagues. It is difficult to express how much the MEMPs have added to my experience at HST. Although I have become close to many, my classmates are very special to me:

Jon Bliss. "Bliss" helped me right from the start with practical information, such as the shortest bike route to HMS. His presence in the office, especially in the first few years, made the work seem much easier, and certainly more enjoyable.

Paul Albrecht. Paul has a wonderful way of balancing work and pleasure, and I am grateful for his constantly reminding me to enjoy the latter. I will always remember his phrase, "He who laughs, lasts". I also thank him for all of the selfless help which he has given me in the preparation of this thesis.

Joe Smith. Joe has been my closest friend and colleague; I doubt that I could have finished this work without his support. I thank him for being there to share my frustrations and achievements, for knowing when to argue and when to just listen, and for sharing the more enjoyable sides of Boston with me.

In addition, I thank my friends who continuously accomodated my erratic schedule into their plans. In particular, I thank Shirley Warter and Rena and Ken Kirshenbaum, who were always there when I needed to get away from it all.

Most importantly, let me thank those who have been a source of unending love and support for much longer than my years at HST - my family. I thank them for their patience as I worked on this "project", and for pretending to believe me every time I told them that it would be done in just a few months. Finally, I thank them for teaching me that what one achieves is not as important as how one achieves it.

TABLE OF CONTENTS

1. INTRODUCTION

Nuclear magnetic resonance (NMR) spectroscopy has recently become an important tool in physiologic and medical research. The dominant ionic species responsible for the electrical activity of the heart, sodium, potassium, calcium, and chloride, are all NMR observable. Of these, sodium has the highest NMR sensitivity (Table 1.1). Sodium also plays a major role in the control of the electrical activity of the heart, in that it is the primary charge carrier involved in initiation and conduction of the cardiac electrical activity. For these reasons, the study of intracellular sodium constitutes an important first step in the study of intracellular ions by NMR.

	NMR Frequency at 8.5 Tesla (MHz)	Relative Sensitivity	Natural Abundance	Absolute Sensitivity	Spin Number	Quadrupolar Moment ($10^{-28}m^2$)
H-1	360.13	1.00	99.98	1.00	1/2	0.0
Li-7	139.84	0.29	92.58	0.27	3/2	-0.03
Na-23	95.26	9.25×10^{-2}	100.00	9.25×10^{-2}	3/2	0.14
Mg-25	22.03	2.67×10^{-3}	10.13	2.71×10^{-4}	5/2	0.20
Cl-35	35.23	4.70×10^{-3}	75.53	3.55×10^{-3}	3/2	-0.08
Cl-37	29.16	2.70×10^{-3}	24.47	0.70×10^{-3}	3/2	-0.06
K-39	16.81	5.08×10^{-4}	93.10	4.73×10^{-4}	3/2	0.11
Ca-43	24.25	6.40×10^{-3}	0.15	9.28×10^{-6}	7/2	0.06

Table 1.1 NMR obervable ions of interest in cardiology. The relative sensitivity is given for an equal number of nuclei, with protons assigned a relative sensitivity of 1.00. The absolute sensitivity is given as the natural abundance multiplied by the relative sensitivity. The spin and the (electric) quadrupole moment are properties which can strongly affect the NMR spectrum, as will be discussed in chapter 2.

Microelectrode based techniques have been the mainstay of previous efforts to study intracellular sodium. By their nature, however, such techniques are highly invasive and are therefore largely limited

to in-vitro preparations. Microelectrodes measure ionic activity in single cells, and are insensitive to compartmentation or small amounts of bound ions within cells. However, events within single cells, or those of single ion channels, can be observed with microelectrodes.

NMR spectroscopy now offers a noninvasive method of studying intracellular sodium which can be used for in-vitro or in-vivo studies. The NMR studies yield information regarding the sodium content of the sample, as well as the interactions between the sodium and its surroundings. In particular, NMR can be very sensitive to binding or compartmentation of ions within cells. At present, NMR spectroscopy is a bulk technique, however in the future the study of single cells may be feasible. Therefore, the techniques of microelectrodes and NMR should complement eachother both in terms of the types of experiments which are feasible and the information which is obtainable from the studies.

A fundamental difficulty with the use of NMR in the study of intracellular ions has been that of separating the NMR signals arising from the intracellular and from the extracellular ions. The recent development of shift reagents has enabled this separation on the basis of the altered resonant frequency of the extracellular ions in the presence of the shift reagent. However, in preparations of perfused hearts, the separation has in general not been large enough to avoid interference between the very large signal arising from the extracellular sodium with the much smaller intracellular sodium signal.

The studies presented here utilized either mathematical filtering or the NMR technique of presaturation to better separate the intra-

and extracellular sodium NMR signals. These methods allowed for the first non-invasive, quantitative, investigation of intracellular sodium in the perfused frog heart by NMR.

The first set of experiments involved monitoring intracellular sodium levels during pharmacologic and physiologic interventions. The effects of; 1) the addition of 10μM ouabain to the perfusate, 2) perfusing with a zero potassium perfusate, 3) replacing 2/3 of the sodium in the perfusate with lithium, and 4) varying the pacing rates of the hearts, were investigated.

The second set of experiments were those of measuring the NMR relaxation times of intracellular sodium. It is these NMR relaxation times which contain information regarding the interaction of sodium with its surroundings. The relaxation times were measured under both control conditions and after equilibration with 10 μM ouabain.

Sodium imaging by NMR has recently become feasible. The contrast within images is determined by the sodium content, as well as the relaxation times. Therefore, in addition to providing information about the inherent properties of intracellular sodium, these studies may aid in the interpretation of clinically obtained sodium images.

Finally, intracellular potassium and lithium have been observed by NMR in these studies. The intracellular potassium concentration as determined by NMR was compared to that of sodium, and intracellular lithium was observed when the hearts were perfused with a lithium perfusate. In the future, simultaneous, quantitative studies of several ions within the heart may extend even further the usefulness of NMR as a tool in the study of cardiac electrophysiology.

2. THEORY OF NUCLEAR MAGNETIC RESONANCE

Basic Principles:

The phenomenon of NMR is a consequence of a nucleus with an odd number of protons, an odd number of neutrons, or both, possessing a net nuclear magnetic moment and angular momentum ("spin"). Due to the angular momentum, the magnetic moment will precess around a static magnetic field, $\vec{B}_0$. Let us assume that $\vec{B}_0$ is in the z direction. Quantum mechanical constraints on a nucleus are such that the angular momentum is quantized, with quantum number I. The z component is also quantized, with quantum number m such that m = -I, -(I-1), ... I. Consequently, a spin 1/2 (I=1/2) nucleus can precess around the field in one of two possible orientations, corresponding to m = 1/2 and m = -1/2 (Figure 2-1). The different configurations correspond to different energy levels, due to the energy of interaction between the magnetic moment and the magnetic field.

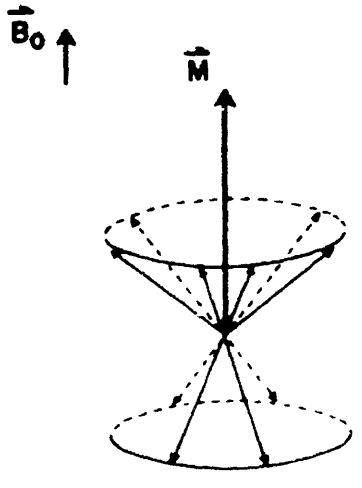

Figure 2-1 Collection of spin 1/2 nuclei in the presence of a magnetic field $\vec{B}_0$.

The frequency of precession is obtained by noting that the rate

of change of angular momentum ($\vec{L}$) is equal to the torque of the magnetic field ($\vec{B_0}$) on the magnetic moment ($\vec{\mu}$), or

$$\frac{d\vec{L}}{dt} = \vec{\mu} \times \vec{B_0}. \tag{2.1}$$

The angular momentum is related to the magnetic moment by a constant, the magnetogyric ratio, γ , such that $\vec{\mu} = \gamma\vec{L}$, and therefore

$$\frac{d\vec{\mu}}{dt} = \gamma\vec{\mu} \times \vec{B_0} \tag{2.2}$$

The moment precesses around the z axis with a precessional frequency

$$\omega_0 = \gamma B_0, \tag{2.3}$$

which is referred to as the Larmor frequency. The value for this frequency could have been similarly obtained by noting that the difference in the energy levels of the two configurations, in a quantum mechanical sense, is $\Delta E = \gamma\hbar B_0 = \hbar\omega$. Therefore transitions of nuclei between these levels, the quantum mechanical resonance, will involve frequencies of $\omega_0 = \gamma B_0$.

At absolute zero temperature the spins would all be precessing with their z components parallel to $\vec{B_0}$, in the lower energy state. However, in real situations the thermal energy precludes this total alignment from occuring, and the proportion of spins in the parallel and antiparallel states are given by the Boltzmann distribution,

$$\frac{n1}{n_2} = e^{-\Delta E/kT} \tag{2.4}$$

where n_1 = number of nuclei with their z components antiparallel to $\vec{B_0}$
n_2 = number of nuclei with their z components parallel to $\vec{B_0}$
$\Delta E = \gamma\hbar B_0$
k = Boltzmann's constant

T = temperature in degrees Kelvin

We are left with a collection of spins precessing around the z axis with random phase, and with an excess of spins in the parallel configuration. This excess is on the order of 1 in 10^6 for the magnetic fields and temperatures involved in typical NMR experiments, but the result is still a net bulk magnetic moment, $\vec{M}$, in the z direction (Figure 2-1).

In order to describe the phenomenon of NMR classically, we need only concentrate on this net magnetization vector, $\vec{M}$. In equilibrium, the bulk magnetization is stationary along the z axis. In terms of the torque equations,

$$\frac{d\vec{M}}{dt} = (\gamma\vec{M}) \times (\vec{B_0}) = 0 \qquad (2.5)$$

In order to study the characteristics of the nuclei, we must disturb this equilibrium. The universally used method is that of applying a transient radiofrequency field, $\vec{B_1}$, which disturbs the nuclei directly. The return the nuclei to equilibrium in $\vec{B_0}$ is then observed.

In order for $\vec{B_1}$ to affect $\vec{M}$, it must have a component perpendicular to $\vec{M}$. Since $\vec{M}$ is initially in the same direction as $\vec{B_0}$, defined to be in the z direction, $\vec{B_1}$ is applied in the xy plane. During the time that B_1 is on,

$$\frac{d\vec{M}}{dt} = (\gamma\vec{M}) \times (\vec{B_0}+\vec{B_1}). \qquad (2.6)$$

If we describe the process in a reference frame rotating with frequency ω,

$$\frac{d\vec{M}}{dt} = (\frac{\partial\vec{M}}{\partial t})_{rot} + \vec{\omega} \times \vec{M} \qquad (2.7)$$

$$(\frac{\partial \vec{M}}{\partial t})_{rot} = (\gamma \vec{M}) \times [(\vec{B}_0 + \vec{B}_1) + \vec{\omega}/\gamma]. \qquad (2.8)$$

If we let the reference frame rotate with the Larmor frequency $\vec{\omega_0} = -\gamma \vec{B_0}$ (the negative sign is due to the rotation vector being in the opposite direction as $\vec{B_0}$), we have

$$(\frac{\partial \vec{M}}{\partial t})_{rot} = (\gamma \vec{M}) \times (\vec{B}_1) \qquad (2.9)$$

In this reference frame $\vec{M}$ will precess around $\vec{B_1}$ with frequency γB_1. In order for this to be a simple precession, $\vec{B_1}$ must be stationary in this rotating frame, and therefore must be rotating with the Larmor frequency in the laboratory frame. The Larmor frequency in typical experiments is on the order of 100 MHz; accordingly, $\vec{B_1}$ must be a radiofrequency field, as stated.

The effect of $\vec{B_1}$ is therefore to rotate $\vec{M}$ such that it has a component in the xy plane. In terms of the individual nuclei, they now have phase coherence in the xy plane, and the proportion of nuclei in the upper and lower states has been disturbed.

When $\vec{B_1}$ is turned off, the nuclei begin to return to their initial state of equilibrium in $\vec{B_0}$. The moments dephase in the xy plane due to the nuclei exchanging energy with one another; therefore the time constant for M_{xy} to return to zero is referred to as the spin-spin relaxation time, or T_2. Dephasing can also take place due to inhomogeneities in $\vec{B_0}$, in which case the nuclei in different physical and/or chemical locations precess at slightly different frequencies. The spin-spin relaxation time including this inhomogeneity effect is referred to as T_2^*. The spins also exchange energy with their environ-

ment and return to the thermal equilibrium of the Boltzmann distribution. The time constant for M_z to return to its original value by this process is referred to as the spin-lattice relaxation time, or T_1.

In the pulsed NMR experiment, we prepare the system by placing it into a nonequilibrium state with a pulse of a $\vec{B_1}$ field and observe the return of the spin system to equilibrium. The detector coil is set up to detect the x or y component of the changing magnetization vector which is rotating with the Larmor frequency and decaying with an exponential time constant T_2^*. This can be written in complex form as

$$f(t) = A e^{-t/T_2^*} e^{j\omega_0 t} \tag{2.10}$$

The complex Fourier Transform of the above is given by

$$F(\omega) = \int_0^\infty A e^{-t/T_2^*} e^{j\omega_0 t} e^{-j\omega t} dt \tag{2.11}$$

where t=0 is defined as the time of excitation. This yields

$$F(\omega) = A\left[\frac{T_2^*}{1+(\omega_0-\omega)^2 T_2^{*2}} - j\frac{(\omega_0-\omega)T_2^*}{(\omega_0-\omega)^2 T_2^{*2}}\right] \tag{2.12}$$

where the coefficient A will be determined by the initial conditions set up by the pulse. The real part of $F(\omega)$ is referred to as the v mode and the imaginary part is referred to as the u mode; these are shown as a function of frequency in Figure 2-2. The v mode has a maximum at $\omega=\omega_0$; the linewidth at half maximum amplitude can easily be shown to be $2/T_2^*$. This linewidth is usually given in units of Hertz, with the symbol $\Delta\nu_{1/2}$, with which it has the value $1/\pi T_2^*$.

It is well known that the area under the curve in the frequency domain is proportional to the initial value of the time domain func-

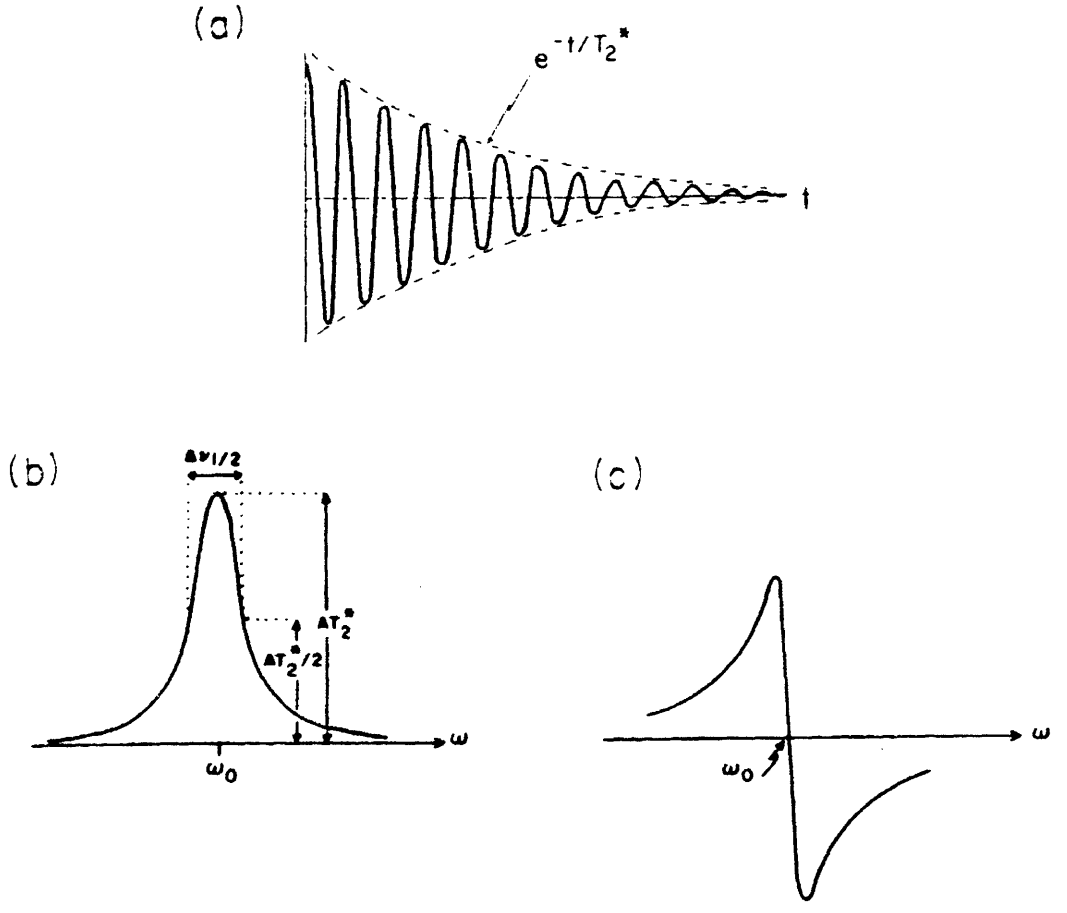

Figure 2-2 (a) A decaying sinusoid of frequency ω_0 with exponential time constant T_2^*. (b) The real (v mode) and (c) imaginary (u mode) parts of the Fourier transform of the function shown in (a).

tion; therefore this area is proportional to the initial magnetization induced in a coil after the excitation pulse, which is proportional to the net equilibrium magnetization, or the number of nuclei in the sample. The real part of the Fourier transform accordingly yields the following information (see Figure 2-3): a) ω_0, the resonant frequency of the nuclei, which is proportional to the magnetic field at the nucleus. This magnetic field consists mainly of B_0, and is modified by the fields due to surrounding molecules in the local environment the

nucleus. b) The area, which is proportional to the number of nuclei in the sample. c) The linewidth at half height, which is indicative of the time constant of the decay T_2^*. A more detailed description of these parameters is to follow.

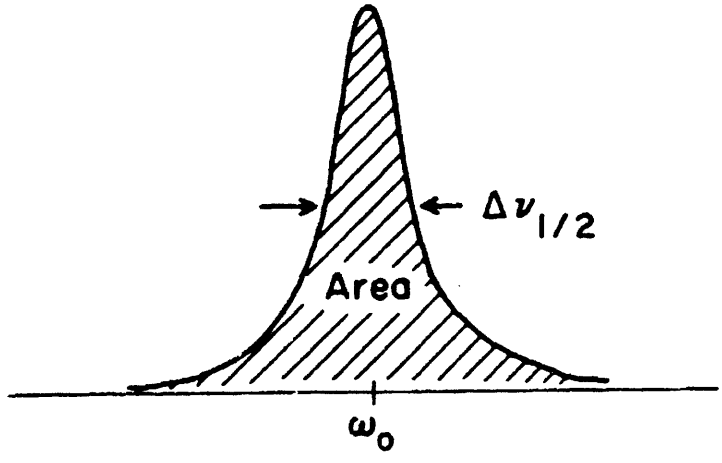

Figure 2-3 Parameters of interest in the NMR spectrum: ω_0, area, and $\Delta\nu_{1/2}$

NMR of Quadrupolar Nuclei:

The discussion until now has been based on spin-1/2 systems. However, many nuclei of interest to medical research, such as sodium, potassium, and lithium, have a spin of 3/2. Others, such as magnesium and calcium, have even higher spin numbers (5/2 and 7/2, respectively). While the analysis of the NMR experiment can still be performed on the basis of the motion of the net magnetization vector, the quantum mechanical effects of the higher spin level must be incorporated into this picture. Under certain conditions these effects may result in more than one resonant frequency and relaxation time for a homogeneous population of nuclei. The discussion which follows will be restricted to spin 3/2 nuclei; the general principles can also be applied to nuclei with higher spin numbers.

A nucleus with a spin of I = 3/2 has four possible values for m (m= -3/2, -1/2, 1/2, and 3/2), and hence four possible orientations in the presence of a static magnetic field. These orientations correspond to four possible energy levels; transitions are allowed only between adjacent levels, which are equally spaced (Figure 2-4a).

Nuclei with spin greater than 1/2 also posess electric quadrupole moments (and are therefore referred to as quadrupolar nuclei). The electric quadrupole moments interact strongly with electric field gradients, therefore the orientation of the nucleus relative to the electric field gradient will result in different energy levels for the different m states of the nucleus. If we assume that this quadrupolar interaction is small compared to the interaction of the nucleus with the static magnetic field, we can write the energy levels of the

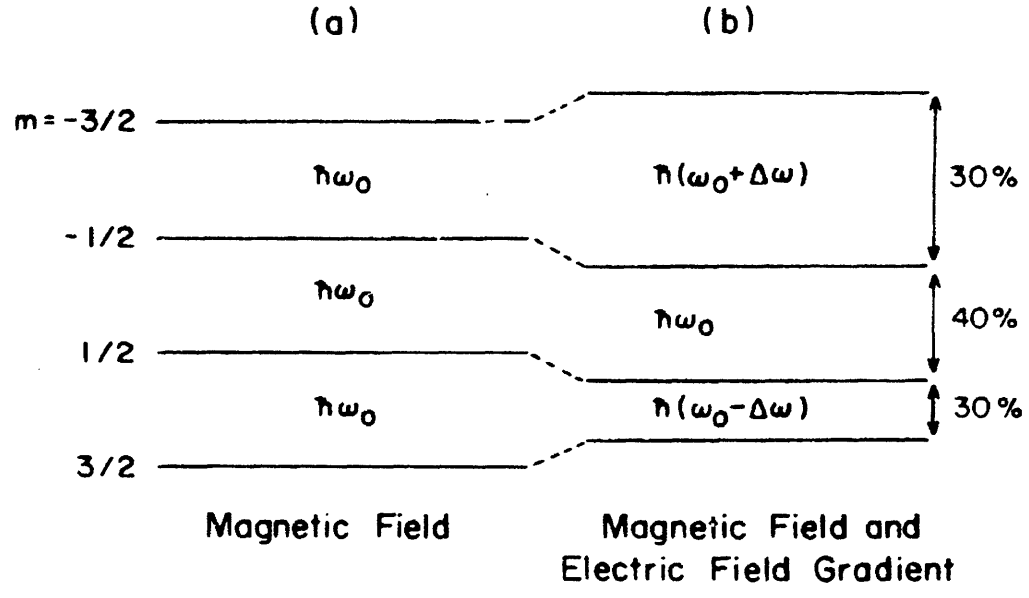

Figure 2-4 Energy levels of a spin 3/2 nucleus in the presence of (a) a static magnetic field, and (b) a static magnetic field and an electric field gradient. The numbers on the right correspond to the percentage of total transitions which occur between the indicated levels.

combined effect to first order as (Slichter, 1980)

$$E_m = -\gamma\hbar B_0 m + \left(\frac{e^2qQ}{4I(2I-1)}\right)\left(\frac{3\cos^2\theta-1}{2}\right)(3m^2-I(I+1)) \qquad (2.13)$$

where q is the electric field gradient

Q is the quadrupolar moment of the nucleus

θ is the angle between the axis of the electric field gradient (assumed to be axially symmetric) and the magnetic field.

For a given value of θ, the levels m = -1/2, 1/2 are displaced in one direction relative to their levels in the absence of an electric field gradient, while m = -3/2, 3/2 are displaced in the opposite direction by an equal amount. This yields the energy levels of Figure 2-4b. It has been shown that the transition probability for the m = -1/2 to

m = 1/2 transition is 0.4 while the others have a transition probability of 0.3 (Abragam, 1961).

When the nuclei are rotating relative to the electric field gradient, the effects of the electric field gradient on the energy levels will average out and there will be only one transition frequency (ω_0). This is the condition which is expected to be relevant in studies of physiologic systems. From this point on, the discussion will be based on a system with only one resonant frequency.

However, even if the effect of the electric field gradient on the resonant frequencies averages out, the quadrupolar interaction can profoundly affect the relaxation rates between the levels. In fact the interaction between the electric quadrupole moment of the nucleus and the electric field gradient is expected to be the dominant mechanism responsible for relaxation of quadrupolar nuclei. General equations describing the relaxation times will now be given, and the specific expressions for the relaxation times of spin 3/2 nuclei will be presented.

Relaxation Times:

Nuclear relaxation can only occur through stimulated transitions of the nuclei. A fluctuating field which may provide a mechanism for nuclear relaxation can be described by a function of time, f(t). Its correlation function, C(t), gives an indication of the time evolution of this field. Similarly, the Fourier transform of C(t), J(ω), describes the spectral density of the time varying field.

In order for a transition to be stimulated, there must be a field

fluctuating at the resonant frequency. Therefore the expressions for the relaxation times will involve the term $J(\omega_0)$. If the nucleus is rotating in the opposite sense of a field fluctuating at $2\omega_0$, the relative fluctuation will again be one of the resonant frequency, ω_0. Hence the term $J(2\omega_0)$ will also be important in the description of the relaxation times. In addition, local static fields will result in a variation of the precession frequency among nuclei. This leads to dephasing of the nuclei and T_2 relaxation. Consequently, expressions for T_1 can be given in terms of the spectral density function evaluated at the frequencies of ω_0 and $2\omega_0$, while expressions for T_2 will also involve the spectral density function evaluated at 0.

For a spin 3/2 system with a single resonant frequency, T_1 and T_2 were each shown to be composed of two components (Hubbard, 1970), with 80% of the nuclei relaxing with a T_1 of

$$\frac{1}{T_1'} = 2\left(\frac{eq}{\hbar}\right)^2 J(2\omega_0) \tag{2.14}$$

and 20% with a T_1 of

$$\frac{1}{T_1''} = 2\left(\frac{eq}{\hbar}\right)^2 J(\omega_0) \tag{2.15}$$

Similarly 60% decay with a T_2 of

$$\frac{1}{T_2'} = \left(\frac{eq}{\hbar}\right)^2 [J(0) + J(\omega_0)] \tag{2.16}$$

while 40% have a T_2 of

$$\frac{1}{T_2''} = \left(\frac{eq}{\hbar}\right)^2 [J(\omega_0) + J(2\omega_0)] \tag{2.17}$$

Before presenting a formal description of the spectral density, $J(\omega)$, a few observations can be made. For the case of free ions, there will

be a wide range of motions and hence the spectral density function will have approximately equal values at 0, ω_0, and $2\omega_0$. In this case $J(0)=J(\omega_0)=J(2\omega_0)$, and there will be only one value of T_1 and one value of T_2, which are equal. When ionic motion is restricted, the field fluctuations due to the motions take on higher values at low frequencies, and $J(0)$ becomes larger than $J(\omega_0)$ or $J(2\omega_0)$. This yields two distinct values of T_2 and two values of T_1 which are relatively close in value. Note that only one component of T_2 of spin 3/2 systems contains the $J(0)$ term. Therefore, there will be a component of T_2 for a spin 3/2 system that will not be as significantly shortened when nuclear motion is restricted.

There have been several attempts to identify the mechanisms responsible for relaxation. A thorough analysis was presented by Engstrom et. al. (1982) for lithium, sodium, and chloride ions in dilute aqueous solutions. They concluded that the field fluctuations are due to both translational and rotational motions of the water molecules in the first hydration shell. While the fast (translational) motions may dominate the fluctuations of the field gradients, the slower (rotational and exchange) motions may be responsible for a large part of the relaxation. This idea of relaxation by a two step process was proposed earlier (Wennerstrom et. al., 1974; Lindman, 1978).

The effect of exchange on relaxation will be described in the next section. The spectral density function corresponding to rotational motion is given as

$$J(\omega) = \frac{(eq)^2}{20} \frac{\tau_c}{(1+\omega^2\tau_c^2)} \qquad (2.18)$$

where τ_c (the correlation time) is the characteristic decay time of the correlation function, essentially an indicator of the duration of interaction. This spectral density function is shown in Figure 2-5.

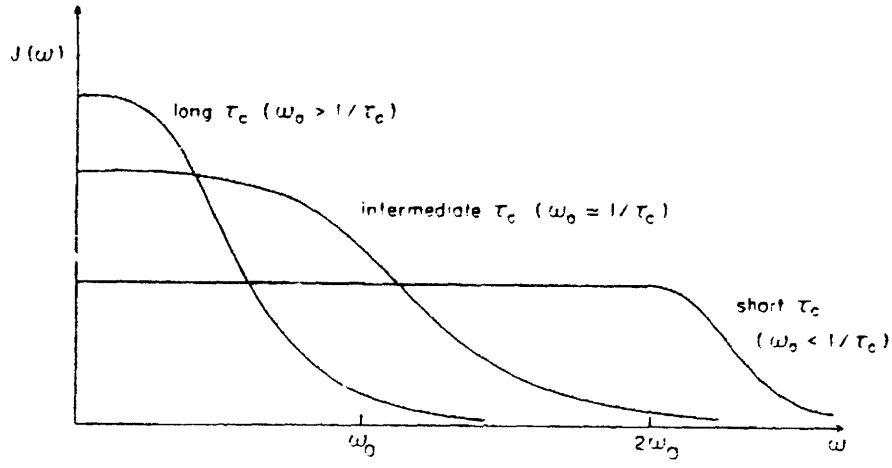

Figure 2-5 The spectral density function corresponding to rotational motion plotted for various values of the correlation time.

The equations for spin 3/2 nuclei can now be written as

$$\frac{1}{T_1'} = \frac{1}{10}\left(\frac{e^2qQ}{\hbar}\right)^2 \frac{\tau_c}{(1+4\omega_0^2\tau_c^2)} \qquad (80\%) \qquad (2.19)$$

$$\frac{1}{T_1''} = \frac{1}{10}\left(\frac{e^2qQ}{\hbar}\right)^2 \frac{\tau_c}{(1+\omega_0^2\tau_c^2)} \qquad (20\%) \qquad (2.20)$$

$$\frac{1}{T_2'} = \frac{1}{20}\left(\frac{e^2qQ}{\hbar}\right)^2 \left(\tau_c + \frac{\tau_c}{(1+\omega_0^2\tau_c^2)}\right) \qquad (60\%) \qquad (2.21)$$

$$\frac{1}{T_2''} = \frac{1}{20}\left(\frac{e^2qQ}{\hbar}\right)^2 \left(\frac{\tau_c}{(1+\omega_0^2\tau_c^2)} + \frac{\tau_c}{(1+4\omega_0^2\tau_c^2)}\right) \qquad (40\%) \qquad (2.22)$$

This serves to demonstrate the intuitive notions above. For free ions, the correlation time is approximately 10^{-11} sec. The resonant frequencies are typically on the order of 100 MHz, and therefore $\tau_c << 1/\omega_0$ and

$$\frac{1}{T_1'} = \frac{1}{T_1''} = \frac{1}{T_2'} = \frac{1}{T_2''} = \frac{1}{10}\left(\frac{e^2qQ}{\hbar}\right)^2 \tau_c \qquad (2.23)$$

This condition of $\tau_c << 1/\omega_0$ is referred to as extreme narrowing. Bound ions will have long correlation times and $\tau_c \geq 1/\omega_0$, such that there are two distinct values of T_2 and two distinct values of T_1 which are closer in value.

Spectra of Spin 3/2 Nuclei:

With the above T_2 information, the NMR spectra of spin 3/2 nuclei can be described for cases in which field inhomogeneity effects are not the dominant factor in the linewidths. For the case of samples with very short correlation times, such as pure aqueous solutions with very rapidly rotating molecules, the T_2 relaxation times will be relatively long for the whole population and thus there will be one sharp resonance in the spectrum (Figure 2-6a). As the ions become motionally restricted, the correlation times increase and hence the relaxation times will decrease with 60% of the nuclei being more strongly affected than the other 40%. Thus there will be a superposition of two resonances in the spectra, with forty percent of the energy in the sharper resonance and sixty percent in the broad resonance (Figure 2-6b). The broad resonance may be undetectable under standard experimental conditions, which has led to the general claim that 60% of the sodium or potassium in tissues may be "invisible" by NMR. When the correlation times are very long, the quadrupolar interactions have a stable effect on the energy levels and there are three distinct resonances in the spectrum (Figure 2-6c). The equations presented above do not apply for this last case, which has only been reported in a few isolated instances in biological systems (Edzes et. al., 1972; Fossel

et. al., 1985).

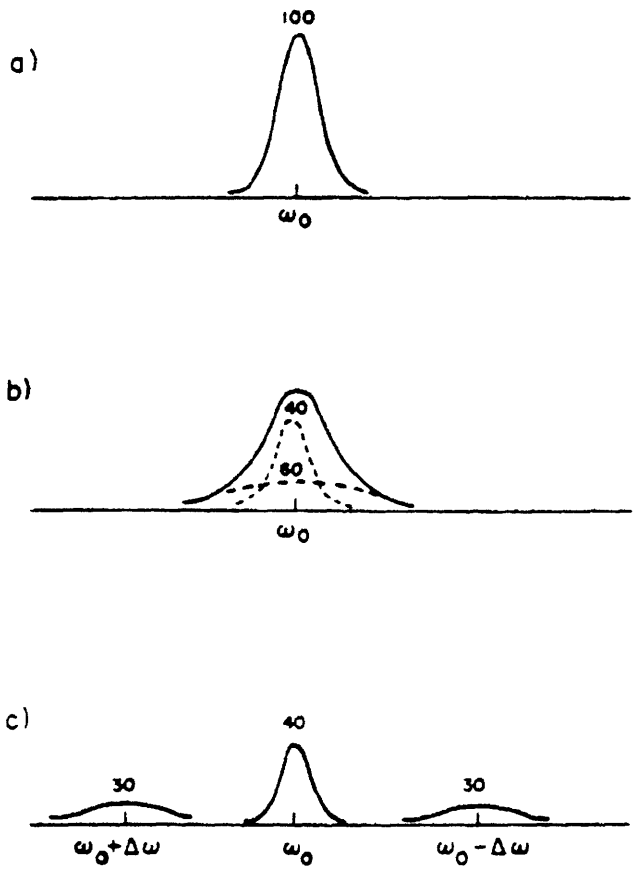

Figure 2-6. Three general classes of spectra for spin 3/2 nuclei: (a)$\tau_c << 1/\omega_0$,, with a single resonance; (b) $\tau_c \simeq 1/\omega_0$, with 2 superimposed resonances; and (c) $\tau_c << 1/\omega_0$, with 3 separate resonances. The numbers represent the relative areas for the different resonances.

It should be noted that the definitions of slow and fast discussed above are relative to the inverse of the resonant frequency, as demonstrated in the equations by the comparison of ω_0 to τ_c.

Variations Among Quadrupolar Nuclei:

Several predictions concerning the variation of the electric field gradient fluctuations at the nuclei of different ions have been made. Lindblom and Lindman (1973) suggest that the hydration properties of the ions affect the electric field gradient such that it increases from Li^+ to Cs^+ in the order

$$Li^+ < Na^+ < K^+ < Rb^+ < Cs^+ \qquad (2.24)$$

The relaxation times of these ions in solution would therefore be expected to decrease in the above order. Persson et. al. (1974) also suggest that ions interact with amphiphilic molecules with the order

$$K^+ > Na^+ > Rb^+ > Cs^+ \geq Li^+ \qquad (2.25)$$

Therefore, in comparable solutions, we would expect that potassium would exhibit quadrupolar effects before sodium or lithium.

Chemical Exchange:

The analysis of the previous sections holds for a single pool of nuclei, with all of the nuclei experiencing the same environment. However, the sodium and potassium ions in physiologic systems are located in a heterogeneous cellular environment, with different intra- and extracellular environments, possibly ionic binding sites, intracellular compartments, and an unknown amount of exchange between the various pools of ions. Since a single spectrum is obtained from the composite NMR signal of all of these nuclei, the effects of compartmentation and possible exchange between the pools must be considered. This exchange can affect the relaxation times and resonant frequencies of the nuclei in the various pools.

Exchange rates can be functionally described as being slow, intermediate, or fast, with the time scales being defined relative to the differences in relaxation times and resonant frequencies between the pools. Without exchange, or in the limit of slow exchange, the individual pools of ions can be thought of as being independent; the relaxation times are insignificantly affected and the NMR spectrum consists of a superposition of the individual spectra. In the limit of fast exchange, the relaxation times and resonant frequencies consist of a weighted average of the individual components.

It is clear that as long as we have no independent knowledge of the percentage of ions bound or compartmentalized with differing exchange rates, it will not be possible to definitively describe the state of the system from a single spectrum or relaxation time measurement. However, we can characterize the effects that exchange will have

on the relaxation times and spectra, and search for the effects, if present.

The problem of defining the relaxation times of nuclei in chemical exchange was addressed for a system of two pools of nuclei, each with single relaxation time in the absence of exchange (Leigh, 1971). This would apply to quadrupolar nuclei in the extreme narrowing case. Generalized equations for the relaxation rates were derived which showed that the relaxation of each species is affected by the exchange (this was also pointed out by Marshall, 1970), and that while T_2 is affected by the difference in resonant frequencies of the two species, T_1 is not. A complete analysis of the relaxation times for different cases of slow and fast exchange was later given by McLaughlin and Leigh (1973). They first defined the conditions of slow and fast exchange explicitly. For T_1, slow (fast) exchange is defined as the case in which the rate of exchange is much slower (faster) than the difference between the T_1 relaxation rates of the nuclei in the absence of exchange. This definition also holds for T_2, however the difference in resonant frequencies of the two pools must also be taken into account, and the rate of exchange is also slow (fast) relative to the difference between the resonant frequencies of the nuclei in states A, B. Fast exchange relative to the difference in resonant frequencies is referred to as exchange narrowing.

McLaughlin and Leigh show explicitly that for two populations in slow exchange there will be two distinct T_1s, given by

$$\frac{1}{T_1} = \frac{1}{T_{1A}} + \frac{1}{\tau_A} \quad ; \quad \frac{1}{T_1} = \frac{1}{T_{1B}} + \frac{1}{\tau_B} \qquad (2.26)$$

where T_{1A} is the T_1 of the ions in state A in the absence of exchange, and τ_A is the lifetime of the ions in this state, with similar definitions for state B. For fast exchange, there will be an averaged T_1, given by

$$\frac{1}{T_1} = \frac{f_A}{T_{1A}} + \frac{f_B}{T_{1B}} \tag{2.27}$$

where f_A, f_B are the fractions of nuclei in states A, B.

T_2 may be discussed in terms of the appearance of the spectra as well as the measured relaxation rates. For two pools of nuclei in slow exchange, there will be two distinct resonances, with the total spectrum being a superposition of the separate resonances. The relaxation times of the two resonances are given as

$$\frac{1}{T_2} = \frac{1}{T_{2A}} + \frac{1}{\tau_A} \quad ; \quad \frac{1}{T_2} = \frac{1}{T_{2B}} + \frac{1}{\tau_B} \tag{2.28}$$

with similar definitions as above for the case of T_1. If the populations are in fast exchange and exchange narrowed there will be one resonance at a frequency given by

$$\omega = \omega_A f_A + \omega_B f_B \tag{2.29}$$

and a T_2 of

$$\frac{1}{T_2} = \frac{f_A}{T_{2A}} + \frac{f_B}{T_{2B}} + f_A f_B \tau_{AB} \Delta\omega_{AB}^2 \tag{2.30}$$

where $\omega_{A(B)}$ is the resonant frequency of the ions in state A (B), τ_{AB} is the rate of equilibration of the ions between the two environments, and $\Delta\omega_{AB}$ is the frequency separation between the two resonances in the absence of exchange. This reduces to a weighted average of the separate resonances if the separation of the two intrinsic resonances

is small.

If the two populations are in fast exchange but not exchange narrowed there will again be two resonances with the same T_2s as given above for the case of slow exchange. Therefore it is possible to have a situation in which there will be an averaged T_1 while simultaneously there may be two separate resonances and two separate T_2s.

The effect of increasing the exchange rate of the nuclei within two resonances in a spectrum is shown in Figure 2-7. The resonances will at first be negligibly affected by the exchange, will begin to broaden, and will coalesce into one peak which will then begin to narrow (hence the term exchange narrowing). Note that the smaller resonance will broaden and shift more than the large resonance (Sandstrom, 1982).

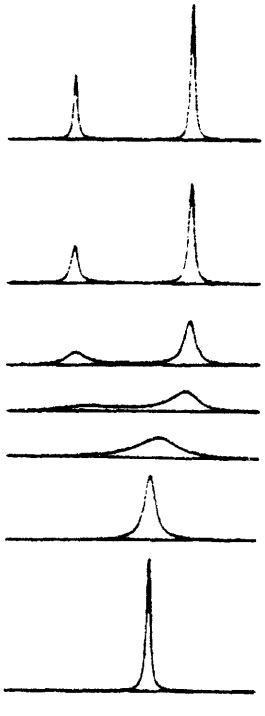

Figure 2-7 From top to bottom; effect of increasing the exchange rate between the nuclei of two resonances. Adapted from Sandstrom, 1982.

Exchange Between Quadrupolar Nuclei:

In this section we will consider the case of quadrupolar nuclei which may have more than one relaxation time in the absence of exchange, i.e. if they are not in the region of extreme narrowing. The general problem of exchange between quadrupolar nuclei under these conditions is understandably complex. General equations describing the relaxation rates were developed in 1972 (Bull, 1972) for systems in which all of the nuclei resonate at the same resonant frequency. It was found that for two pools of spin 3/2 nuclei which are not under conditions of extreme narrowing, the relaxation consists of the sum of four exponentials.

The equations were later expanded and written explicitly (Goldberg and Gilboa, 1978a). It was shown that for a system with equal populations of bound and free ions in slow exchange there exist three exponentials in the T_2 decay curve while there are two exponentials in the case of fast exchange. This can be interpreted to be the relaxation of the free ions, which consists of one exponential, added to the exponentials of the bound ions in the case of slow exchange to yield three exponentials while it is averaged with each of the two exponentials of the bound ions to yield two exponentials in the fast exchange case. However, the authors continue to point out that the three curves in the first case may not be differentiated experimentally. In terms of the spectra, this will yield three superimposed resonances for the slow exchange case and two for the fast exchange case (Figure 2-8). The curves for T_1 show the presence of more than one exponential, however the effect is very small in the limit of fast or intermediate

exchange rates.

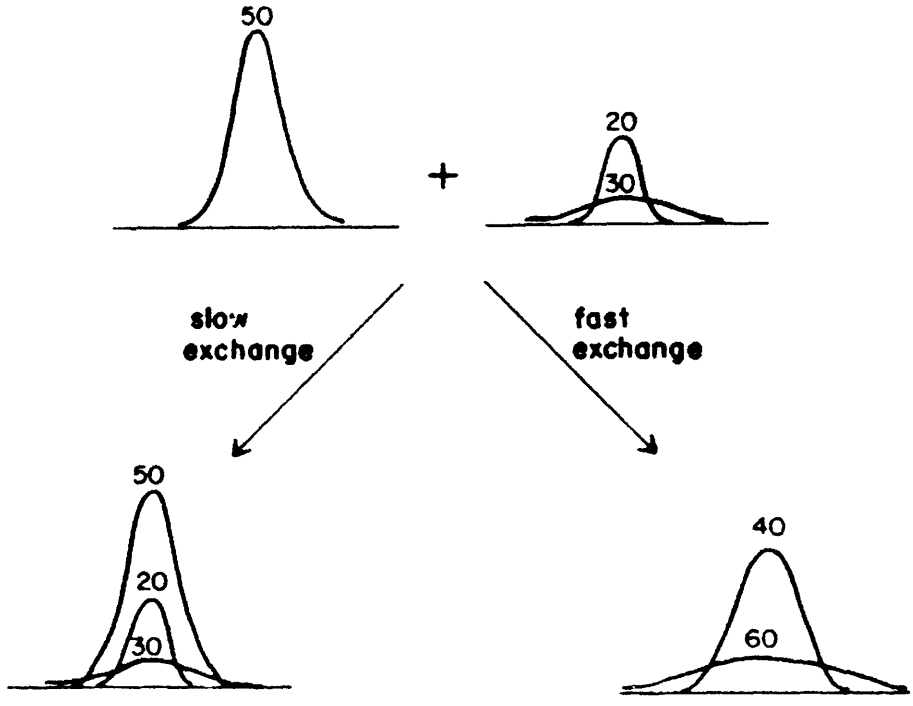

Figure 2-8 The effects of exchange on a spin 3/2 system in which 50% of the nuclei are relatively free (with one component of T_2) and 50% of the nuclei are restricted (with two T_2 components). When the populations are in slow exchange there is a superposition of the spectra and when the populations are in fast exchange there is a weighted average of the spectra.

The case of the system with 1% bound ions was also addressed (Goldberg and Gilboa, 1978a), and it was shown that the slow exchange case yields one exponential decay for T_2 while two components are distinguished in the fast exchange case. This is because the effect of the small amount of bound ions is not noticeable until its broadened linewidth is averaged with the sharp peak of the remaining 99% in the fast exchange case. The above study also noted that experimental results from a system in intermediate exchange could be very similar

to those in fast exchange, and therefore using the fast exchange equations may lead to false conclusions.

3. THE NMR EXPERIMENT:

The NMR Probe and Excitation:

Having described the theoretical basis of the NMR experiment, we will now describe how these principles are put to practice. A static magnetic field, $\vec{B_0}$, is produced in the z direction. In the experiments reported here, a superconducting magnet was used to produce a magnetic field strength of approximately 8.45 Tesla. Within the bore of the magnet is the probe which contains the circuit to transmit and detect the resonant fields in the xy plane. While the resonance condition requires a circularly polarized magnetic field, this is in practice obtained by transmitting a linearly polarized wave which can be broken up into two circularly polarized components;

$$\vec{B} = 2\vec{B_1}\cos(\omega_0 t) \tag{3.1}$$

$$= B_1[\cos(\omega_0 t)\vec{x} + \sin(\omega_0 t)\vec{y}\,] + B_1[\cos(\omega_0 t)\vec{x} - \sin(\omega_0 t)\vec{y}\,] \tag{3.2}$$

The first rotates at ω_0, which is close to the resonant frequency of the spins, while the second one rotates at $-\omega_0$, or $-2\omega_0$ relative to the spins, and will not affect the spin system as long as B_1 is much less than B_0. This condition is always met in our experiments, in which B_0 is 8.45 Tesla and $\vec{B_1}$ is approximately 10^{-3} Tesla.

In simplest form, the resonant circuit consists of two capacitors and an inductor, such as those shown in Figure 3-1. The inductor, or rf coil, surrounds the sample and is used to apply the B_1 field. Variable capacitors allow this circuit to be tuned over a wide range of frequencies, enabling one to use the same probe for studies of

different nuclei. The resonance of the circuit itself is much broader than the range of frequencies in a given spectrum of interest.

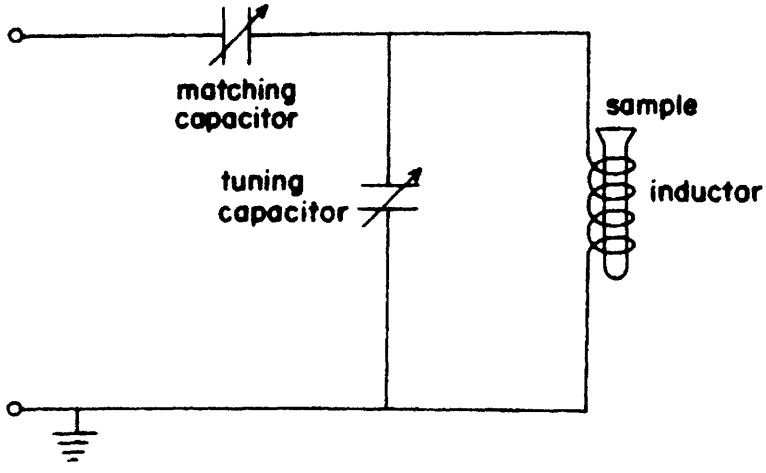

Figure 3-1 Basic resonant circuit for use in the NMR probe. Variable capacitors enable the circuit to be tuned to the resonant frequency of the nuclei of interest and to be matched to the impedance of the transmitter and receiver circuit. The coil surrounds the sample and thus produces the magnetic field for excitation of the nuclei and detects the rotating magnetization vector of the nuclei during relaxation.

Also of importance is the quality factor, or Q, of the circuit, which is an indication of the efficiency of the circuit. The Q is affected by the loading of the coil by the sample, and thus the same tranmsmitter settings may yield different B_1 field strengths for different samples. While the transmitter pulse can be lengthened to accomodate for a loss in Q due to loading of the coil by the sample, the loss on the efficiency of the receiver cannot be precisely determined and therefore compensated. Consequently, if signals from two different samples are to be compared quantitatively, the tuning, matching, and Q of the circuit must be checked for each sample.

In order to simultaneously observe the NMR response of a group of nuclei with similar Larmor frequencies, the transmitted signal is given as a pulse of radiofrequency ω_0, which actually contains a range of frequencies (Figure 3-2). The durations of the pulses used in these experiments are on the order of 10 to 100 μsec. Consequently, the frequency range of interest in the spectrum, which is several KHz, is within the flat region surrounding ω_0.

The length of the pulse, in addition to determining the frequency content, will determine the angle through which $\vec{M}$ tips. We have seen that $\vec{M}$ rotates around $\vec{B_1}$ with frequency $\omega_1 = \gamma B_1$, so the angle through which $\vec{M}$ tips in a time T is given by

$$\theta = \omega_1 T = \gamma B_1 T \qquad (3.3)$$

The flip angle is therefore proportional to the strength and duration of the pulse. A pulse which tips $\vec{M}$ into the xy plane is referred to as a 90 degree pulse; one which inverts $\vec{M}$ is called a 180 degree pulse, and so on.

$\vec{B_1}$ Homogeneity:

We would like $\vec{B_1}$ to be homogeneous across the sample, such that all groups of nuclei in the sample experience the same flip angle for a given transmitter pulse. In practice, this cannot be perfectly achieved. As will be discussed shortly, the signal is obtained from the component of the magnetization in the xy plane, and thus a 90 degree pulse will yield the maximum signal. If we assume that the B_1 field is inhomogeneous such that this bulk 90 degree signal actually represents 1/3 of the nuclei rotating by 90-θ, 1/3 by 90, and 1/3 by

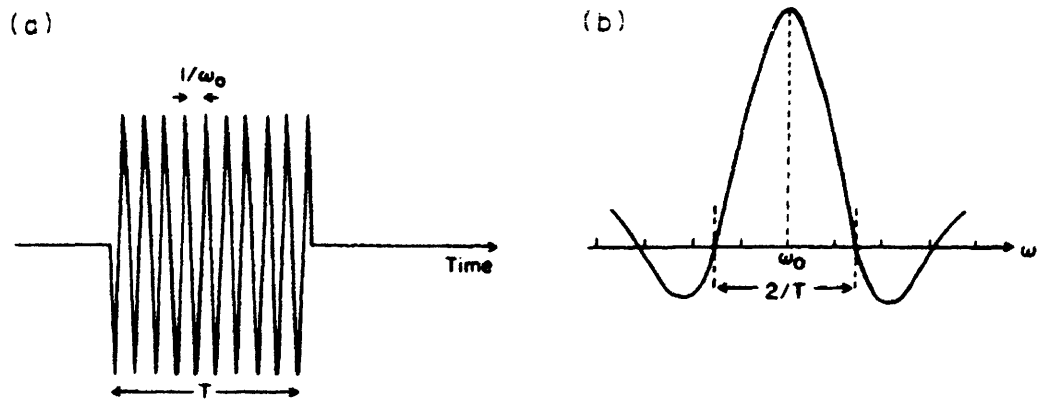

Figure 3-2 A pulse of a radiofrequency field of frequency ω_0 and duration T represented in the (a) time and (b) frequency domains.

90+θ degrees, a bulk 450 degree pulse, given as 5 times the length of the bulk 90, would yield rotations of 450-5*θ, 450, and 450+5*θ degrees. The signal derived from the first case will be

$$\frac{1}{3}M_0\cos(\theta) + \frac{1}{3}M_0 + \frac{1}{3}M_0\cos(\theta) \qquad (3.4)$$

with a similar expression using 5*θ for the second case. This is compared to a signal of M_0 for a perfectly homogeneous $\vec{B_1}$ field, and therefore a perfect 90 degree pulse. Table 3.1 shows the relative signals obtained from a perfect 90, a bulk 90, and a bulk 450 degree pulse for several values of θ. We see that very little error is incurred due to inhomogeneity in B_1 for the bulk 90 degree pulse versus the perfect 90 degree pulse. However, the effect of the inhomogeneity in $\vec{B_1}$ is enhanced and easily observed with a bulk 450 degree pulse. The ratio of the experimentally yielded signals obtained with a bulk 90 and a bulk 450 degree pulse will determine θ, and therefore will yield an estimate of the error incurred by assuming a homogeneous

B_1.

θ	perfect 90	bulk 90	bulk 450
0	1	1.000	1.00
5	1	0.997	0.94
10	1	0.989	0.76
15	1	0.977	0.51
20	1	0.960	0.22

Table 3.1 Relative signals obtained in a perfectly homogeneous B_1 field versus various degrees of inhomogeneities. See text for details.

Detection and Fourier Transformation of the NMR Signal:

After the excitation pulse the magnetization returns to equilibrium exponentially. The time varying component of net magnetization in the xy plane (which is varying at a rate of approximately 100 MHz) induces a current in a receiving coil, which in this case is the same as the transmitting coil. The resultant voltage, referred to as the Free Induction Decay (FID), is fed into a phase sensitive detector (PSD), which uses the transmitting oscillator as the reference. The output of the PSD is digitized in an analog to digital converter (ADC), and this signal is displayed. Thus while the actual voltages induced in the receiving coil are on the order of 100 MHz, the displayed FID appears as a low frequency signal, with the frequency equal to the offset of the true resonant frequency from the center frequency of the transmitter.

In practice, if we used only one phase sensitive detector, we would have difficulty determining if the resonance signal was higher or lower than the reference, and thus the full spectrum of interest

would have to be of either higher or lower frequency than the reference. To circumvent this problem, two phase sensitive detectors are used, with the second reference being obtained by shifting the phase of the transmitter by 90 degrees. The final signal is obtained by adding the outputs of the two phase sensitive detectors, such that frequencies higher and lower than the reference frequency can be differentiated. This is referred to as quadrature phase detection (QPD), and has the advantage of an improvement of $\sqrt{2}$ in signal/noise over the use of one detector. This is because the reference is in the center of the frequency range of interest and therefore the needed frequency bandwidth is only 1/2 of that which would be necessary without QPD. In addition, by having the frequency synthesizer in the middle of the range of frequencies of interest, we increase the range of frequency over which $\vec{B}_1$ is uniform (see Figure 3-2). In reality, however, this in general is not a problem with the short pulse lengths and hence broad frequency band of the typical excitation pulses, relative to the narrow frequency band of the NMR spectrum.

The FID is then Fourier transformed. If the signal is in phase with the transmitter, the output of the PSD will be maximal at t=0, and the real part of the transform will be the same as that in eqn. 2.12, with a typical Lorentzian shape. However, in order to avoid damaging the receiver with the large transmitter pulse the receiver must be gated off for a certain delay time after the transmitter pulse. This, and other instrumental delays, is equivalent to a phase difference in the Fourier Transform of the data such that the real and imaginary parts of the Fourier transform are mixed. A phase shift correction can be applied mathematically to correct for this effect.

Note that for a given delay time the phase shift, i.e. the fraction of a cycle that has passed, is dependent on the frequency. Therefore the phase correction that will be needed will be linear with frequency. In addition, misadjustments of the PSD will require a constant phase correction, and thus in general zero and first order phase corrections (constant and linear with frequency) are used. Phase correction is usually done visually by observing the real part of the spectrum and correcting the phase mathematically until the typical Lorentzian shape is observed.

Some point within the spectrum, usually at a reference peak, is defined to be at zero frequency. The spectrum as a whole is displayed either on a frequency scale, in Hertz, or on a parts per million (ppm) scale, defined as the resonance frequency divided by the carrier frequency, multiplied by 10^6.

Experimental Parameters:

From a practical standpoint, it is advantageous to minimize the time required to obtain the spectra. The parameters of interest in this regard which are under the experimenter's control are the spectral width (SW) and block size (number of memory locations allocated for data storage, or SI). The data is sampled at intervals equal to the dwell time, DW. By Nyquist's theorem, the digitization rate 1/DW must be at least equal to or greater than twice the spectral width, or

$$1/DW = 2(SW) \qquad (3.5)$$

In most cases this digitization rate is automatically set by computer to fulfill the above criterion once the spectral width is chosen by

the investigator.

The acquisition time, ACQ, will be equal to the product of the dwell time and the number of samples, or

$$ACQ = DW \times SI = \frac{SI}{2(SW)} \qquad (3.6)$$

As we increase the number of data points we increase the acquisition time, and as we increase the spectral width we decrease the acquisition time by increasing the digitization rate. However, it is important to take into account what effect this has on our spectral resolution, which is given as

$$\Delta\nu = \frac{2(SW)}{SI} = \frac{1}{ACQ} \qquad (3.7)$$

There is a direct trade off between acquisition time and spectral resolution.

Data Manipulation:

Certain mathematical methods of improving either the signal to noise (S/N) or resolution of the spectra are available to us. It is possible to increase the S/N of a spectrum by multiplying the FID by a decreasing exponential before performing the Fourier Transform. This is because the beginning of the FID, with the higher S/N, will be emphasized relative to the poor S/N region in the tail of the FID. However, the improved S/N is at the expense of resolution, due to the added exponential time constant and hence increased linewidth. The time constant used in the exponential is referred to as the line broadening constant, and is denoted by LB. It has been shown that the optimal exponential filter is one with a time constant equal to the

time constant of the FID, or T_2^* (Becker et. al., 1979).

It is also possible to increase the S/N of a spectrum by zero-filling the FID after the signal has decreased into the noise. In practice, the FID is acquired into a given number of time domain (TD) points; the remainder of the SI points are zero filled.

Conversely, it is possible to enhance the resolution while decreasing the S/N by multiplying the FID by an increasing exponential. In practice, this resolution enhancement is done by multiplying the FID by a function of the form $\exp(-at-bt^2)$, where a is chosen as $-1/T_2^*$ and b is positive. This yields a signal of the form $\exp(-bt^2)$ which is a Gaussian and therefore has less prominent wings than the original Lorentzian. In practice, $a = (\pi)(LB)$ and $b = (-a)/(2)(GB)(ACQ)$ where GB is the Gaussian Broadening factor.

Pulse Sequences:

In general the S/N of a single FID does not yield sufficient S/N in the spectrum for practical purposes, and therefore averaging of many FIDs is performed before transforming the data. However, one must be careful to allow the system to return to equilibrium between the excitation pulses. In general, this means allowing a recycle delay, RD, of $5T_1$ between each 90 degree pulse. It is possible to use a pulse width, PW, such that the nuclei tip less than 90 degrees, in which case the nuclei are not as far from equilibrium and a shorter recycle delay time is required. The pulse sequence used for averaging of the FIDs is shown in Figure 3-3. The transform is performed on the averaged FID.

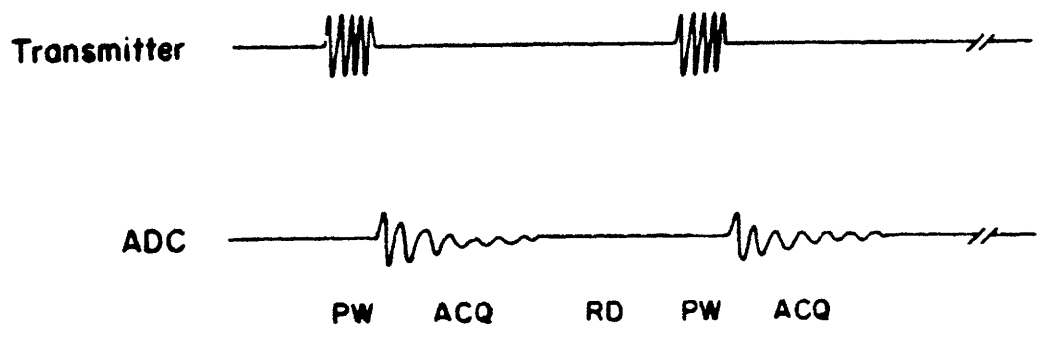

Figure 3-3 Pulse sequence for averaging of many FIDs before Fourier Transformation.

Shift Reagents:

In many of the physiologic studies, it would be desirable to be able to differentiate between the intracellular and extracellular nuclei by NMR. Unfortunately, these nuclei resonate at the same NMR frequency. In order to observe their separate contributions to the spectra, various shift reagents have been developed. These shift reagents are highly negatively charged molecules with paramagnetic centers; when a positive ion is in contact with the shift reagent the magnetic field at its nucleus is slightly altered. Therefore, positive ions in contact with the shift reagent will resonate at a much higher/lower frequency than the free ions. Since the ions which are in contact with the shift reagent are in a very fast exchange with the free ions in the same solution, the result is an intermediate resonant frequency for all of the ions, with the frequency shift proportional to the relative amounts of shift reagent and ions in solution. When added to cellular systems, the shift reagent is not expected to enter

the cells, as cell membranes are impermeant to polyanions. Therefore the intracellular ions should resonate at the original frequency if there is no significant exchange between the intracellular and extracellular ions and if there is no bulk susceptibility effect from the shift reagent, i.e. if the shift reagent does not effect the bulk magnetic field in the medium. Since a molecule of shift reagent in contact with an ion will shift the resonance by many times the linewidth, the shift reagent can be added to the extracellular space in small concentrations and yield an averaged shift which allows for the separation of the NMR resonances from the intracellular and extracellular ions (see Figure 3-4).

Suppression of a Resonance:

Situations frequently arise in which a large resonance interferes with a nearby smaller resonance. In the case of a perfused heart, the resonance from the extracellular ions, even in the presence of a shift reagent, interferes with the resonance from the much smaller intracellular ionic pool. There are several methods of reducing this interference. In marginal cases, mathematical resolution enhancement can be performed to separate the two resonances. Another means of reducing the interference is to suppress the large (extracellular) resonance through a method referred to as presaturation. A long (narrow frequency) pulse is transmitted at the frequency of the resonance to be eliminated. This long pulse, on the order of several relaxation times of the nuclei, or typically 75 msec in these studies, combined with the relaxation phenomena, totally randomizes the selected spins with no remaining net magnetization. (The nuclei are referred to as being

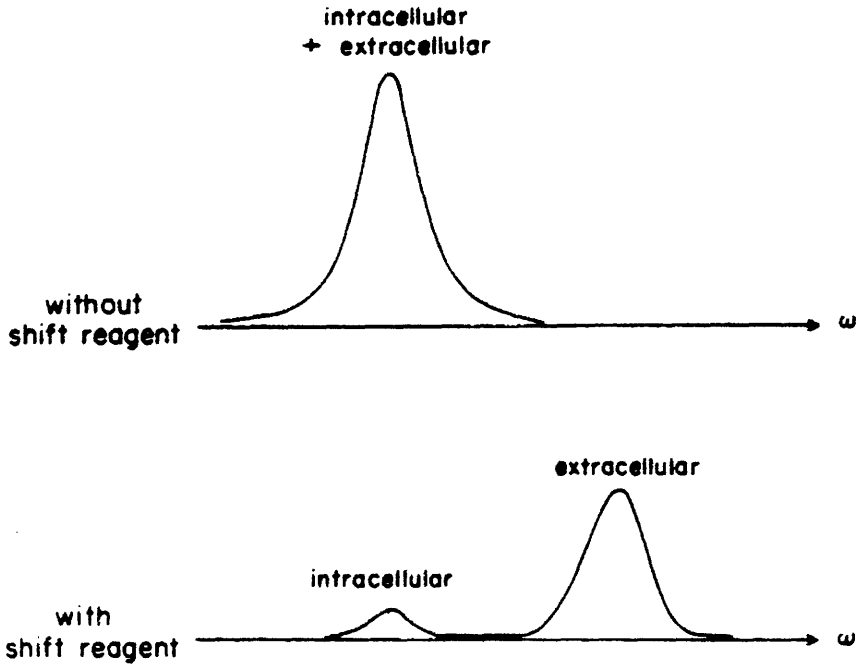

Figure 3-4 Schematic spectra obtainable from a cellular system (a) in the absence of shift reagents; all of the ions resonate at the same frequency, and (b) in the presence of shift reagents that do not enter the cells; the resonant frequency of the extracellular ions is shifted and two distinct resonances are observed.

saturated.) Therefore a short (broad-band) excitation pulse directly following this presaturation pulse will not affect these nuclei, and the corresponding resonance in the spectrum will be suppressed. It should be noted that the transmitter must be on a lower power setting for the presaturation pulses than for the broad-banded (μsec) excitation pulses.

If the method of presaturation is used the possible effects of exchange between the two pools should be kept in mind. If there is exchange between the two resonances which is on the order of magnitude

of T_1, some of the saturated spins will transfer to the second resonance in their saturated states; accordingly the second resonance will also be affected by the presaturation.

T_1 Measurement:

Various methods have been developed to measure the relaxation times, T_1 and T_2. The most common technique to quantitatively determine T_1 is a pulse sequence referred to as Inversion-Recovery. A 180 degree pulse is applied which inverts $\vec{M}$ to lie along the -z axis. After a given delay, τ, during which the nuclei relax by T_1 mechanisms along the z axis, a 90 degree pulse is applied which flips $\vec{M}$ to the xy plane. An FID is collected which reflects the magnitude of $\vec{M}$ a time τ after inversion. After the nuclei have completely recovered the sequence can be repeated for signal averaging. The process is then repeated with a different delay time (see Figure 3-5). If we assume that M is initially equal to $-M_0$ after the 180 degree pulse and recovers with an exponential decay rate $1/T_1$, the equation describing the z component of $\vec{M}$ is given as

$$M = M_0 - 2M_0 e^{(-\tau/T_1)} \tag{3.8}$$

$$\ln(M_0-M) = \ln(2M_0)-\tau/T_1 \tag{3.9}$$

This z component is measured as the area of the resonance obtained after the 90 degree pulse. Thus a plot of $\ln(M_0-M)$ versus τ will yield a slope of $-1/T_1$.

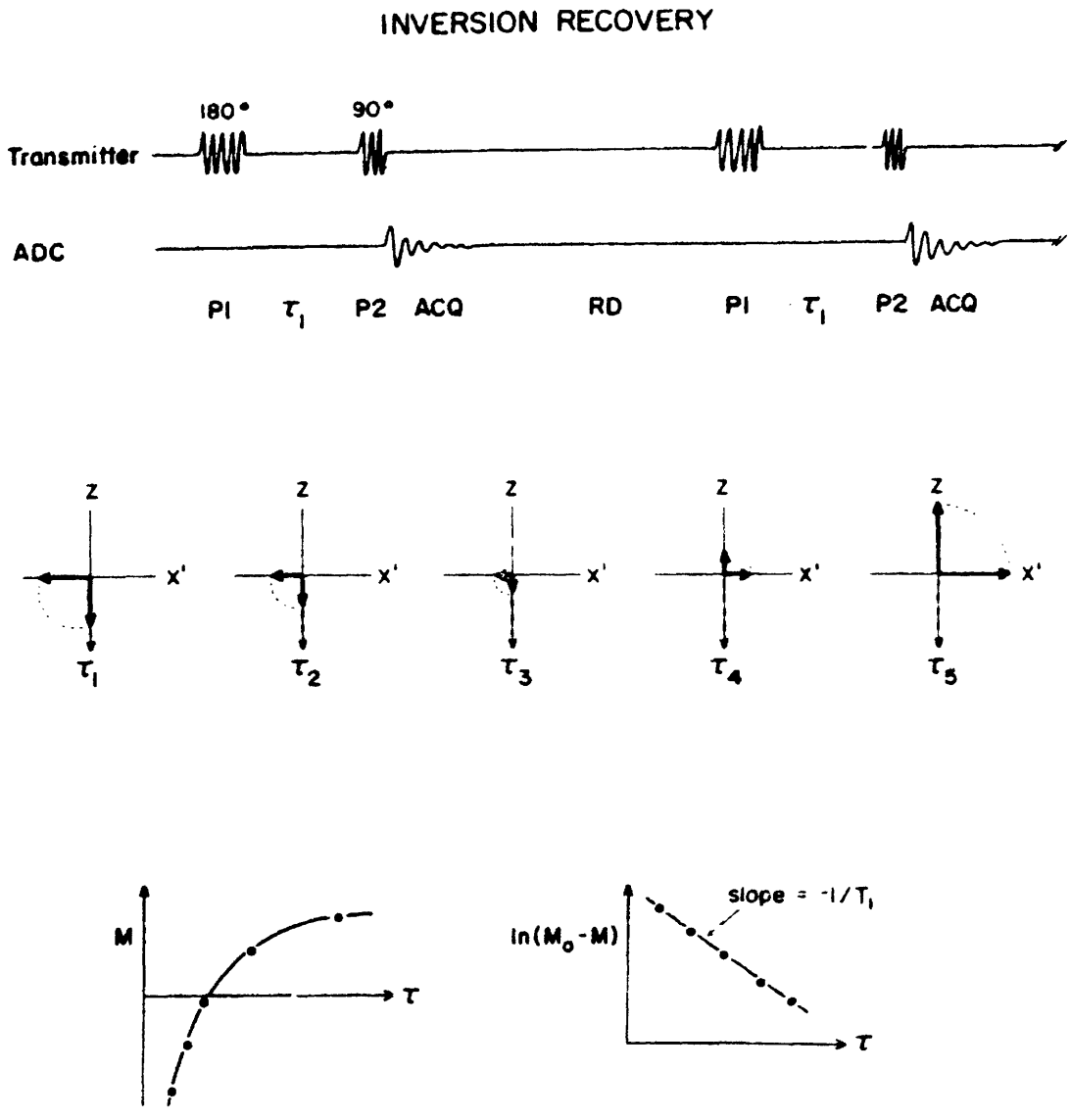

Figure 3-5 Inversion Recovery: Top: the 180 - τ - 90 pulse sequence to measure T_1. The sequence for one value of τ is shown, repeated for signal averaging. Middle: The behavior of M in the rotating frame. The magnetization is inverted to lie along the -z axis by the 180 degree pulse; during the time τ it relaxes along z; the 90 degree pulse then flips the magnetization (in a clockwise rotation) to lie along the x' axis, and the magnetization is then detected. The behavior of M for different values of τ is shown. Bottom: Plots of M vs τ and $\ln(M_0-M)$ vs. τ.

T_2 Measurement:

While the decay rate of the FID is reflected in the width of the spectral peak, in many cases the time constant of this decay, T_2^*, is primarily a function of the static field inhomogeneity. In order to eliminate this effect and determine the inherent T_2 of the spin system, a spin echo pulse sequence is used. In this sequence, a 90 degree pulse is applied which tips the magnetization into the xy plane. Due to the field inhomogeneity, some spins are precessing faster than others and they begin to dephase. In a rotating frame (the primed coordinate system), it appears as if some spins are moving in a clockwise rotation away from the x' axis (which is rotating with a frequency equal to the mean precessional frequency of the spin system) and some are moving in a counterclockwise rotation. After a time τ a 180 degree pulse is transmitted which rotates the spins around the y' axis. The spins have exchanged positions relative to x', however they are still precessing in the same direction. Therefore, they will rephase along the -x' axis after another time τ. A phase sensitive detector which is set up to detect the -x' magnetization will record a "spin echo" with a maximum at a time 2τ.

This echo will compensate for the decay of the x' magnetization due to field inhomogeneities, however the x' magnetization will also decay due to the inherent T_2 effects. Therefore as the τ values increase, the echo amplitudes will decrease. The decay of the echo amplitudes with increasing τ values reflects the inherent T_2 of the spin system, neglecting diffusion effects (see discussion below). This is represented by

$$M = M_0 \exp^{(-2\tau/T_2)} \tag{3.10}$$

$$\ln(M) = \ln(M_0) - 2\tau/T_2 \tag{3.11}$$

Thus a plot of ln(M), where M is taken as the amplitude of the echo at time 2τ, versus 2τ, will yield a slope of $-(1/T_2)$ (Figure 3-6).

Note that the above assumes that the nuclei remain in the same region of field during the course of the experiment so that the precessional frequency of the nuclei are constant. If, however, the nuclei diffuse through regions of different field strengths (or the field inhomogeneities are time variant), the spins will not rephase completely and the echo amplitude will decrease at a rate faster than expected from natural T_2 effects.

The sequence described above is referred to as the Hahn spin echo pulse sequence for measuring T_2 (Hahn, 1950). A modification of this sequence is referred to as the Carr Purcell spin echo sequence (Carr and Purcell, 1954), in which a series of 180 degree pulses are transmitted at equal time intervals with a resulting series of echos. The series of echos are sampled, and again the decay of the echo amplitudes represents the inherent T_2 of the system. With this method the spins are continuously being refocussed, such that diffusion effects are minimized. A further modification is the Carr-Purcell-Meiboom-Gill (CPMG) (Meiboom and Gill, 1958) sequence, in which the 180 degree pulses are shifted 90 degrees relative to the initial 90 degree pulse, which serves to minimize the errors due to inaccurate 180 degree pulses.

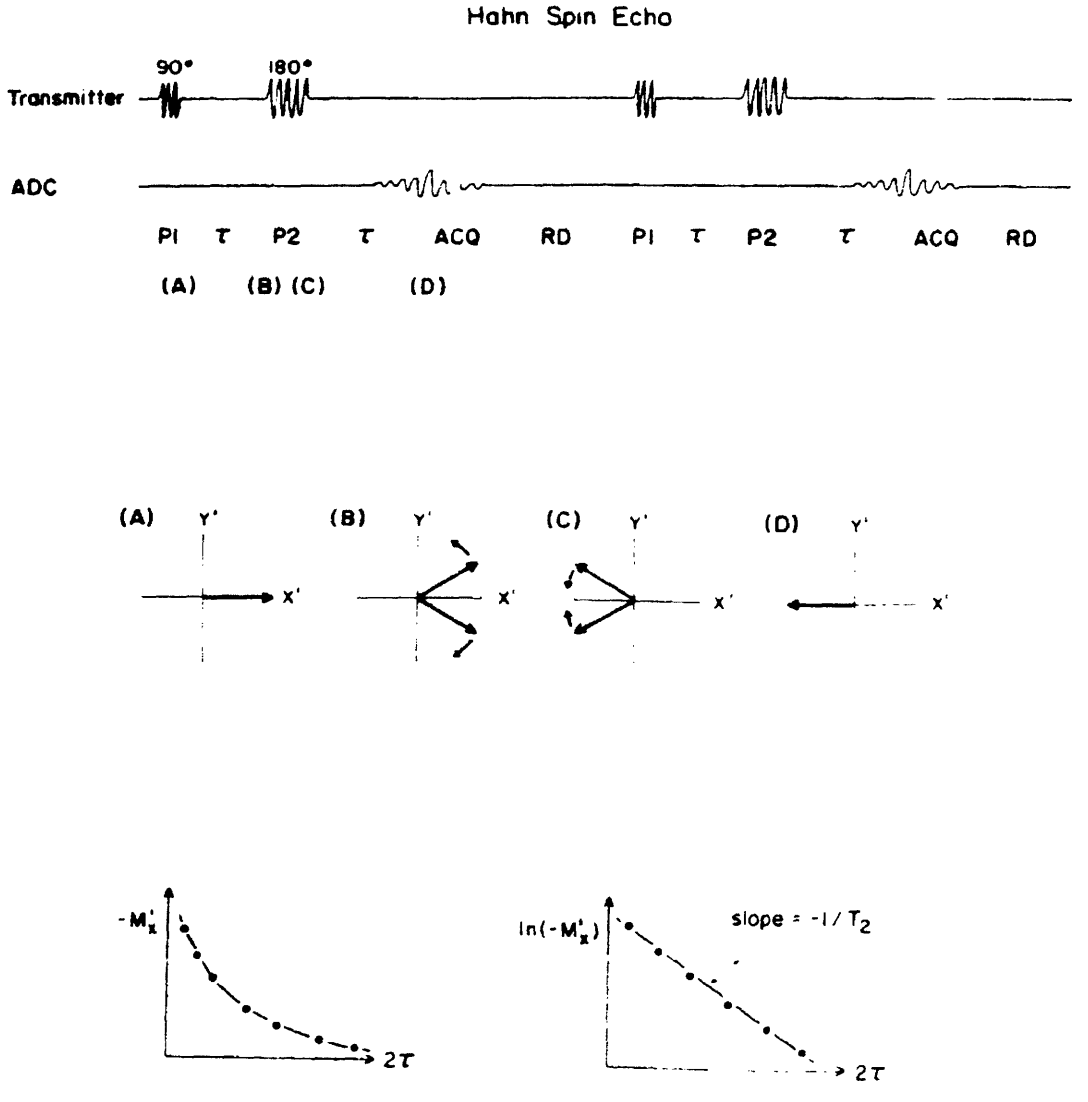

Figure 3-6 Hahn spin echo: Top: The 90–τ–180–τ–echo pulse sequence for measuring T_2. The sequence for one value of τ is shown, repeated for signal averaging. Middle: The behavior of $\bar{M}$ for one value of τ is shown. At (A), the 90 degree pulse has flipped $\bar{M}$ to lie along the x' axis. During τ, the spins begin to dephase in the x'y' plane (B). The 180 degree pulse rotates the spins around the y' axis so that they are now moving towards eachother (C). They rephase to form a spin echo (D). The receiver is turned on at 2τ, at the peak of the echo. Bottom: Plots of $-M_{x'}$ vs. 2τ and $\ln(-M_{x'})$ vs. 2τ.

The above sequences for measuring T_2 are compatible with the technique of presaturation described previously. The initial 90 degree pulse of the T_2 pulse sequences can be transmitted directly after a presaturation pulse, and therefore the presaturated resonance will not be affected. Subsequent 180 degree pulses may affect this resonance after it has recovered, however the 180 degree excitations will not yield a component of magnetization in the xy plane, or therefore a measurable signal, from the original presaturated resonance.

4. REVIEW OF PREVIOUS WORK:

Sodium and potassium NMR has been in use for almost 30 years in the study of biological systems. However, the experimental conditions of the early studies varied widely and in general involved molecular solutions or unviable tissue. Thus it is difficult to extrapolate those results to present day studies. The early work was mainly concerned with the question of the NMR visibility of sodium and potassium within tissue and the evaluation of the correlation times of these ions within biological solutions. More recently, the studies have involved the question of invisible sodium and potassium, the monitoring of ionic fluxes across membranes by NMR, the analysis of the relaxation times for intracellular ions, and NMR sodium imaging. The early studies will be briefly presented, and the later studies will be presented in more detail. There are several excellent reviews which may also be consulted (Shporer and Civan, 1977b; Forsen and Lindman, 1981; Laszlo, 1982; Gupta et. al., 1984).

Early Studies:

The first NMR observation of sodium in a biological system was that of Jardetzky and Wertz in 1956. On the basis of the lineshapes of the sodium spectra they concluded that while sodium in whole blood seemed to be in ionic form, it appeared to be complexed in red blood cell hemolysate. This provoked little notice. However, interest in sodium NMR of biological systems was revived with Cope's report in 1965 that 72% of muscle sodium was invisible to NMR observation. Other studies on various biological tissues (Cope, muscle and kidney, 1967; Martinez et. al., muscle and liver, 1969; Cope, myelinated nerve,

1970; Czeisler et. al., muscle, 1970; Reisin et. al., epithelial tissue, 1970) showed that either less than 100 per cent of the sodium was visible by NMR, or that the sodium relaxation times were significantly different than those in aqueous solution. The conclusion drawn from these studies was that there were two pools of sodium in the tissue, bound and free, and that the bound sodium was invisible by NMR. The same was reported for potassium in bacteria (Cope and Damadian, 1970).

In 1972 Shporer and Civan first suggested that the interpretation of earlier results should include quadrupolar effects, and that perhaps 60% of the total sodium pool was invisible due to quadrupolar broadening. Subsequently, quadrupolar effects in hydrated oriented DNA were clearly demonstrated (Edzes et. al., 1972). A complete theory of quadrupolar effects in biological systems was put forth by Berendsen and Edzes (1973). They predicted that the ions in biological tissue experienced medium range order with slow diffusion, in which $J(0)$ would be much greater than either $J(\omega_0)$ or $J(2\omega_0)$, which would be comparable. In this case one T_1 would be observed while T_2 would have two components, one of which might be too broad to detect under normal NMR conditions.

Many other studies were reported the same year, both with and without quadrupolar effects in mind. Yeh et. al. (1973) measured the sodium in frog muscle and found 53% to be visible, which they attributed to be a combination of the signals from the extracellular sodium and a fraction of the intracellular sodium. The same investigators determined that all of the sodium in red blood cells was visible. Magnuson and Magnuson (Magnuson J.A. and Magnuson N.S., 1973) reported

that 60 to 70% of sodium in frog muscle was invisible, as well as most of the potassium in H. salinarium. They also studied the predictions of a system of bound and unbound ions in fast exchange, that of sodium interacting with a bacterial surface (Magnuson, N. S., and Magnuson, J. A., 1973), and found that in fact the linewidth varied linearly with the bound fraction of sodium. The same investigators (Magnuson J. A., and Magnuson, N. S., 1973, Magnuson et. al., 1973) similarly studied the fast exchange of sodium in etiolated pea stems, while also reporting an increase in the sodium linewidth due to the presence of bovine erythrocytes, other membrane systems, and E Coli, which they explained as a demonstration of the presence of fast exchange.

An argument in favor of slow exchange between two pools of sodium in tissue was put forth by the comparison of the sodium signal from muscle with that of sodium in an ion exchange resin (Czeisler and Swift, 1973). A similar conclusion was drawn for potassium by the comparison of the potassium spectra of muscle and brain to those of an ion exchange resin (Cope and Damadian, 1974).

Meanwhile, NMR was being used to study the interaction of sodium and potassium with biological molecules in solution. James and Noggle (1969) described the interaction between sodium and soluble RNA, Magnuson et. al. (1970) noted the increase in linewidth of sodium interacting with erythrocyte membrane proteins, and the line broadening of potassium spectra in a solution of inorganic phosphates and ATP was similarly noted (Bryant, 1970). Other studies which reported on sodium complexed to molecular solutions were those of Kielman and Leyte (polyphosphates, 1973), Shporer et. al. (valinomycin, 1974), and

Ostroy et. al., (ATPase, 1974).

At the same time, the theory of quadrupolar NMR was being developed. Bull et. al. used this theory in 1973 to analyze the spectra obtained from sodium, lithium, and chloride bound to oxy and carbon monoxyhaemoglobin, with the conclusion that chloride interacts strongly with haemoglobin, as opposed to sodium which showed no evidence of binding in concentrations up to 0.5 Molar. Shporer and Civan (1974) investigated the effects of temperature and field strength on the sodium NMR signal of frog striated muscle, and with an estimate of the quadrupolar coupling constant for the bound sodium and the simplest model which could account for the data, concluded that less than a few percent of the intracellular sodium was bound, and that this was in fast exchange with the free sodium. They reported the presence of one T_1 and two T_2 relaxation times in their data, as Berendsen and Edzes had done earlier. A later study (Civan et. al., 1976) of potassium in frog striated muscle showed similar temperature dependencies as sodium. From this the authors concluded that the binding of potassium was also insubstantial.

Monoi (1974a) studied rat liver homogenate and concluded that the sodium signal reflected quadrupolar interactions, and that at most 20 to 30 percent of the sodium in tissue was bound. However, he also acknowledged the possibility of more than one explanation for the same experimental results. A second paper presents the theoretical basis for his conclusions (Monoi, 1974b). A later study (Monoi, 1976a) demonstrated that one component of the loss of sodium resonance in the rat liver homogenate could be abolished with the addition of cesium,

which suggested that there are sites whose affinity for cesium were greater than their affinity for sodium. Unlike previous reports, he showed that erythrocyte ghosts could decrease the NMR sodium intensity (Monoi and Katsukura, 1976). Chang and Woessner (1978), using Hubbard's theory (Hubbard, 1970) to analyze the sodium NMR signals of rat skeletal muscle, concluded that most of the sodium ions were associated with macromolecular charged sites. They also noted that the NMR signals contained a single T_1 while T_2 consisted of two components.

Various studies followed which attempted to utilize the model of fast exchange with an estimate of the quadrupolar coupling constant in order to get an estimate of the correlation time of the sodium ions bound to various molecules. In most cases this was found to be on the order of nanoseconds (Reuben et. al., DNA, 1975; Monoi, muscle, 1976b; Rose and Bryant, lysozyme, hemoglobin, and albumin, 1978; Delville et. al., 5' guanosine monophosphate nucleotide, 1979; Grandjean and Laszlo, parvalbumin, 1977). A study of potassium in ionophore complexes (Neurohr et. al., 1983) showed the correlation times to be on the order of 10 to 100 picoseconds, while a study of the binding of sodium and potassium to egg yolk phosvitin yielded a calculation of a correlation time of 0.5 nanoseconds, with sodium determined to be in the "nearly exponential" decay region (Braunlin et. al., 1984). Studies of sodium in solutions of double helical DNA also yielded correlation times on the order of nanoseconds, and the spectra displayed non-Lorentzian and assymetric properties. The authors suggested that the model of a single correlation time may not apply for this case, and that second order frequency shifts may be important (Braunlin and Nordenskiold, 1984; Nordenskiold et. al., 1984).

Reports continued of the observation of one T_1 component with two T_2 components in the sodium or potassium spectra of biological material (Shporer and Civan, potassium, bacteria, 1977a; Monoi and Uedaira, sodium, micellar solutions, 1980). In addition, similar findings were reported in the NMR spectra of gramicidin, a polypeptide which has the capability of transporting cations across membranes (Cornelis and Laszlo, 1979; Monoi and Uedaira, 1979; Urry et. al., 1980; Venkatachalam and Urry, 1980). Two studies utilized the linewidths of sodium NMR spectra to indirectly study the binding of other ions to DNA via a displacement of the sodium ions (Bleam et. al., 1980; Burton et. al., 1981).

Goldberg and Gilboa (1978a,b) reviewed Bull's theory (Bull, 1972) and analyzed a system of sodium and bacteria. The data was interpreted in terms of three pools of sodium; two pools of ions, bound and free, which were in intermediate exchange, and one pool of ions, bound, which was in slow exchange with the others. A correlation time for the intermediate exchanging bound ions was given as 100 nanoseconds, and they warned of errors which may be incurred by assuming the fast exchange model when in fact intermediate exchange rates may be applicable. A similar warning was put forth by Feeney (1979). Delville et. al. (1981) evaluated the chemical shifts and quadrupolar coupling constants of sodium with various amines.

Application to Medicine:

The application of sodium NMR to medical problems was becoming apparent. Damadian and Cope (1974) reported a difference in the T_1 of potassium in normal versus cancerous tissue, and later a difference

between the T_1 of sodium in normal versus cancerous tissue was also demonstrated (Goldsmith and Damadian, 1975). The binding affinity of sodium to the erythrocyte ghosts of hypertensives was demonstrated to be different than that of normals (Urry et. al., 1980), and the binding of sodium in human serum was investigated and discussed in terms of possible pathologies (Kissel et. al., 1982). In perfused hearts, halothane was shown to increase the myocardial sodium concentration (Dedrick and Allen, 1983).

The ability to use sodium NMR in an imaging capacity was demonstrated in the case of a perfused heart in 1981 (DeLayre et. al., 1981) and later in brain (Martino and Damadian, 1983; Hilal et. al., 1983, Hilal et. al., 1984; Hilal et. al., 1985). The studies by Hilal et. al. demonstrated that the sodium content increased in the vicinity of an infarct. This they attributed in part to increased NMR visibility of sodium as a result of decomplexation from proteins. An increase in the sodium content in the region of an infarct was also demonstrated with the use of surface coil imaging in a rat head (Moseley et. al., 1985), and in an imaging study of an excised heart after coronary artery occlusion and reperfusion (Cannon et. al., 1986). In the normal canine kidney, the sodium in the medulla was shown to be greater than in the cortex (Hilal et. al., 1984). The sodium distribution in an in-vivo rat kidney was also demonstrated by Bogusky et. al. (1986) using a localized spectroscopy technique.

One of the major differences between imaging of protons and sodium is that due to the short relaxation times of sodium. (The contrast between sodium and proton imaging has recently been reviewed by

Feinberg et. al., 1985.) Two T_2s values of 3 and 30 msec were found in the Na-23 NMR signal from the brain (Hilal et. al, 1985), and a warning was put forth that the portion of the signal with the shorter T_2 may be missed if signal aquisition starts too late (Maudsley and Hilal, 1984; Hilal et. al., 1985). A method of imaging athe sodium with the shorat T_2 component has recently been presented (Ra et. al., 1986).

Shift Reagent Studies:

In 1978 Antholine et. al. first suggested using dysprosium as a nuclear spin relaxation agent for sodium in biological tissues. The same year, Degani and Elgavish used Gd(EDTA) as a relaxation agent to study the transport of sodium across membranes.

It was later discovered that some agents would predominantly shift the sodium resonant frequency without significantly decreasing its relaxation time, yielding two peaks in the NMR spectra of cellular systems; one which could be identified with intracellular sodium and one with extracellular sodium. This technique was first demonstrated on a perfused rat heart, using Gd(EDTA) as a shift reagent (Malloy et. al., 1981). The sodium peak was shown to split with the introduction of the shift reagent, and the identified intracellular and extracellular resonance responded appropriately to physiologic interventions. Various compounds which could be used as relaxation and shift reagents were compared by Pike and Springer (1982), by Pike et. al. (1983), by Chu et. al. (1984), and by Brown et. al. (1986).

In 1982 Gupta and Gupta introduced dysprosium tripolyphosphate as

a shift reagent, and showed that it was effective in shifting the extracellular peaks of human red blood cells and frog skeletal muscle. The relatively large shifts obtained with dysprosium tripolyphosphate made it attractive as a shift reagent in biological work, and the majority of studies of the past few years involving shift reagent work in biological systems have utilized this shift reagent. In the following discussion, unless explicitly stated otherwise, it will be assumed that the shift reagent utilized in the studies was $Dy(PPP)_2^{7-}$.

The effect of the shift reagent on the physiologic integrity of the cells was investigated in several studies. It was shown to have no effect on the morphology (Pettegrew et. al., 1984) or phosphate metabolism of erythrocytes (Pettegrew et. al. 1984; Ogino et. al., 1985). The sodium pump in cultured myocytes was not inhibited by the shift reagent (Gupta and Wittenberg, 1983). A suspension of rat outer medullary kidney tubule segments within the shift reagent buffer showed significant levels of ATP (Rayson and Gupta, 1985), while in rabbit proximal tubules the ATP levels were shown to be 80 to 85 percent of those without the shift reagent, with the same total calcium concentration but 1/15 of the free calcium in the case of the shift reagent buffer relative to normal (Gullans et. al., 1985). Oocytes suspended in shift reagent buffers showed no change in their transmembrane potentials (Gupta et. al., 1985; Morrill et. al, 1985) conductances, or creatine phosphate levels for periods of up to two hours (Morrill et. al., 1985). With a perfused rat heart system, one group has found the $Dy(PPP)_2^{7-}$ shift reagent buffer to be toxic, however they were able to successfully perfuse the hearts with a dysprosium triethylenetetramine hexaacetic acid ($Dy(TTHA)^{3-}$) shift reagent buffer

(Pike et. al., 1985). Another group, however, successfully used the $Dy(PPP)_2^{7-}$ on a perfused rat heart (Fossel and Hoefeler, in press).

The additional information provided by the use of shift reagents allowed the question of invisible sodium or potassium within cells to be readdressed. By stimulating a release of potassium from yeast, it was determined that only 40 percent of the potassium (Ogino et. al., 1983, 1984) and sodium (Ogino et. al., 1984) in yeast is visible by NMR. Similarly, only 40 percent of the sodium in E. Coli was found to be visible by conventional NMR (Ogino et. al., 1984). The concentration of potassium in red blood cells as seen by NMR was shown to be similar to that obtained with flame photometric techniques (Brophy et. al., 1983). Several studies concluded that all of the sodium in red blood cells is visible by NMR (Pettegrew et. al., 1984; Pike et. al., 1984; Ogino et. al., 1985; Cowan et. al., 1985). Ogino et. al. (1985) concluded the same for potassium in red blood cells. However one study concluded that only 80 percent of the sodium in the erythrocytes of rat, man, dog, and sheep is detected by NMR (Boulanger et. al., 1985). Wittenberg and Gupta (1985) determined that the intracellular sodium concentration in mammalian cardiac myocytes as measured by NMR is similar to the values reported in other studies which have utilized microelectrodes as the measuring technique. Similarly, Fossel and Hoefeler (in press) demonstrated that the intracellular sodium level as measured by NMR was consistent with the literature values obtained with microelectrodes, while the potassium was only 21 percent of that expected from the microelectrode studies. However, Pike et. al. (1985) found that in a perfused rat heart both the sodium and potassium were less than 20 percent visible. All of the sodium was shown to

be visible in a suspension of rabbit proximal tubule cells (Gullans et. al., 1985), while less than 19 percent of the expected sodium NMR signal from rat outer medullary tubule segments was lost (Rayson and Gupta, 1985). A study of a suspension of oocytes concluded that only 14 to 17 percent of the intracellular sodium was visible by NMR, with the conclusion that a large fraction of the sodium must be bound and in slow exchange in this system (Gupta et. al., 1983). A later study concluded that there are different compartments in the oocytes with varying degrees of NMR visibility for sodium (Gupta et. al., 1985).

Separation of the intracellular and extracellular resonances also allowed for the study of NMR characteristics of the intracellular ions, apart from the question of visibility. These studies focussed on the determinations of the relaxation times of the ions, either by examining the appearance of the spectra (the linewidths) or through direct measurement of the relaxation times. Pike et. al. (1984), using $Tm(PPP)_2^{7-}$ as a shift reagent, showed there to be a sharp and narrow component to the intracellular sodium resonance in human erythrocytes, indicating a multicomponent T_2 in this system. Fossarello et. al. (1985) found there to be a broad and narrow component to the sodium resonance of human lenses. They attributed this to compartmentation within the lense. A comparison of the ratio of the linewidth at 1/8 and 1/2 the peak height of intracellular sodium in erythrocytes to that in saline demonstrated that the ratio was higher in the first case, again indicating a multicomponent T_2 (Boulanger et. al., 1985).

In red blood cells, Shinar and Navon (1984) demonstrated that the

intracellular sodium relaxation times were independent of the intracellular sodium concentration (as seen by a comparison of the values for human and canine red blood cells, which have different intracellular sodium concentrations). T_2 was found to be less than T_1, with T_1 values of 20.7 and 23 msec (canine and human, respectively), and T_2 values of 11.3 and 11.6 msec (canine and human, respectively). The T_2 could be fit with a double exponential, with values of 6.6 and 23.6 msec for the two components. Pettegrew et. al. (1984) also showed T_2 to be less than T_1 in red blood cells, and demonstrated that the linewidth of the intracellular peak was broader than would be expected from consideration of this measured inherent T_2. The T_1 of both the intracellular and extracellular sodium in a suspension of rabbit proximal tubule cells was found to be 10 msec (Gullans et. al., 1985), and the T_1 of the intracellular sodium of a perfused rat heart was found to be 25 msec (using $Dy(TTHA)^{3-}$ as a shift reagent) (Pike et. al., 1985).

Several studies have utilized the technique of shift reagent NMR to obtain physiologic information. Ting et.al. (1981) used paramagnetic lanthanide ions to study the transport of ions across vesicle membranes. Similarly, sodium transport into and out of egg lecithin vesicles was studied with the use of dysprosium nitrilotriacetate ion as a shift reagent (Pike et. al., 1982), as well as sodium transport in yeast cells (Balschi et. al., 1982) and sodium transport across the brush border membrane of the renal proximal tubule (using $Dy(EDTA^-$, Elgavish and Elgavish, 1985). A later study correlated the sodium efflux from yeast with intracellular pH changes, as seen by phosphorus NMR (Balschi et. al., 1984). The efflux and influx of sodium, potassium, and protons in yeast , E. Coli, and red blood cells was also

followed with the use of shift reagents (Ogino et. al., 1984). By examining the broadening of the sodium lines due to exchange phenomena and also by using the method of magnetization transfer, the time course of transport of sodium across unilamellar vesicles was determined (Riddell and Hayer, 1985). Values obtained by NMR for the intracellular and extracellular sodium concentrations in erythrocytes were applied to the Nernst equation to calculate the sodium membrane potential (Cowan et. al. 1985) and Wittenberg and Gupta (1985) followed the effect of calcium deficiency and insulin on the intracellular sodium of myocytes. The intracellular sodium in a perfused rat heart was followed with perfusion by a zero potassium buffer and with ouabain administration by Pike et. al. (1985) using $Dy(TTHA)^{3-}$ as a shift reagent.

There are two recent reviews on the use of shift reagent in physiologic systems (Gupta et. al., 1984; Springer et. al., 1985).

Nuclei Other than Sodium and Potassium:

There have also been several physiologic studies on ions other than sodium and potassium. Lithium has a very high NMR sensitivity (Table 1.1), and has been observed in several studies. The transport of lithium through the phospholipid membranes of vesicles has been observed by Degani and Elgavish (1978), and lithium binding to ATPase was observed by Grisham and Hutton (1978). In the presence of a shift reagent, two lithium resonances were observed in a yeast suspension by Balschi et. al. (1982), while the three resonances due to quadrupolar interactions with the lithium ions were observed by Edzes et. al. (oriented DNA, 1972) and Fossel et. al. (phospholipid suspension,

1985). In-vivo lithium imaging has also been accomplished, with an observation that the T_2 relaxation for lithium was biphasic with time constants of 10 and 100 msec (Renshaw et. al., 1985). Finally, calcium and magnesium were observed in a perfused heart preparation (Fossel, 1984).

5. CARDIAC ELECTROPHYSIOLOGY:

The heart is responsible for the pumping of blood throughout the body. This coordinated mechanical activity relies on a coordinated electrical activity in the myocardium; it is the electrical activity which is of interest in these studies. Most of our information regarding the cardiac electrical activity has been obtained through the use of microelectrodes and the voltage clamp technique. (For reviews of these techniques, see Beeler and McGuigan, 1978; Armstrong and Garcia-Diaz, 1980; Lee, 1981; Tsien, 1983; and Sakmann and Neher, 1984.) A brief review of our present understanding of cardiac electrophysiology is given below.

Cardiac Action Potential:

Under normal conditions, many types of cells can support a potential difference across their membranes by virtue of their selective permeabilities to physiologic ions such as Na^+, K^+, Ca^{++}, and Cl^-. One of the unique characteristics of cardiac cells is that the membrane permeabilities and transmembrane potentials undergo cyclic variations which allow for the repetitive electrical and hence mechanical activity of the heart.

If an ionic concentration gradient is established across a membrane, there will be a tendency for the ions to cross the membrane from the region of higher concentration to that of lower concentration. However, if the membrane i' not permeable to counterions, this movement will lead to a charge separation and will produce a potential difference across the membrane which will impede further ionic move-

ment. At equilibrium, the transmembrane potential is described by the

$$E = -61\frac{mV}{z} \ln\frac{C_i}{C_o} \qquad (5.1)$$

where z = the valence number

C_i = the intracellular concentration of the ion

C_o = the extracellular concentration of the ion

Typical intracellular and extracellular ionic concentrations, with the corresponding equilibrium Nernst potentials, are given in Table 5.1.

	Na^+	K^+	Ca^{++}	Cl^-
Intracellular Concentration (mM)	15	145	0.0001	120
Extracellular Concentration (mM)	145	4	2	5
Nernst Equilibrium Potential (mV)	+ 60	- 94	+ 129	- 80

Table 5.1 Intracellular and extracellular ionic concentrations in the heart and the corresponding equilibrium Nernst potentials (Sperelakis, 1984).

These potentials represent those which would be produced if the membrane was only freely permeable to the ion in question. In the resting state the cardiac membrane permeability to potassium is high, while the permeability to the other ions is low. The resulting transmembrane potential is close to the Nernst potential for potassium, approximately -90 mV. However, the cardiac membrane permeabilities are time and voltage dependent. If the transmembrane potential is raised to a threshold value, either by an external injection of current or by current leakage such as in specialized cardiac cells, the sodium permeability sharply increases and potassium permeability

falls. Thus sodium moves down its concentration gradient into the cell, raising the transmembrane potential. As the transmembrane potential rises so does the sodium permeability, hence with a regenerative effect.

At a certain point in time the sodium permeability begins to fall. There is an increase in chloride permeability, and a relatively long period of calcium and sodium inward currents which offset outward potassium currents. During this time the transmembrane potential stays relatively constant. Potassium permeability then rises while calcium and sodium permeabilities fall, causing the transmembrane potential to return to its resting value.

The above represents a relatively simple view of the cardiac electrical activity. Microelectrode techniques have improved greatly in recent years (Fozzard et. al., 1985), and with these improvements come increased knowledge of the complexity of the cardiac ionic currents. A large number of individual currents have been identified (Noble, 1984; DiFrancesco and Noble, 1985; Fozzard et. al., 1985). In particular, the sodium currents of the action potential are known to be much more complex than originally thought, with sodium currents flowing throughout the action potential (Mullins, 1981).

The total excursion of the transmembrane potential is called an action potential, while the rising phase is referred to as depolarization, the flat region is referred to as the plateau, and the falling phase as repolarization. A typical action potential is shown in Figure 5-1. This transmembrane potential can be monitored through the use of microelectrodes inserted into the cells.

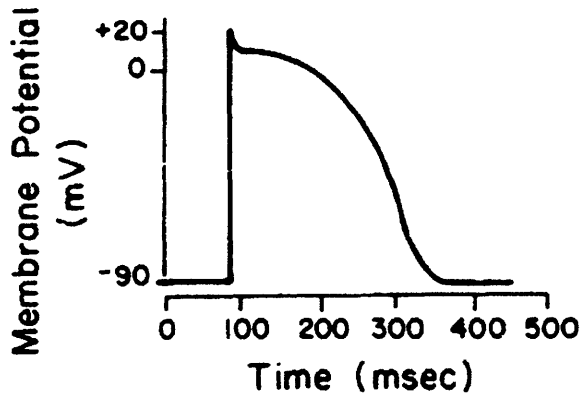

Figure 5-1 A typical cardiac action potential with its rising (depolarization), plateau, and falling (repolarization) phases.

Conduction and Contraction:

Under normal conditions, once an action potential is initiated in one section of the myocardium it spreads uniformly along the cells and between cells. This is because the positive ions which enter the cell at one region will flow within the cell and therefore raise the intracellular potential at adjacent regions, thereby initiating an action potential in these adjacent regions. The current also passes through low resistance junctions between cells to stimulate neighboring cells. Certain cardiac cells have leakage currents which increase their transmembrane potentials to threshold, and thus are natural pacemaker cells.

The atria are the cardiac chambers which receive blood from the body and lungs. The blood is pumped from the atria into the ventricles, from where it is pumped out to the body and lungs. The normal cardiac pacemakers are located in the atria; depolarization spreads across the atria to the atrial-ventricular junction where there is a delay due to the slower action potential in this area, and then the ventricles depolarize. Alternatively, a region can be experimentally

triggered to depolarize with current electrodes placed across the heart preparation such that current is forced into the cells to depolarize them and initiate a conducted action potential.

The velocity of the depolarization wavefront is such that, under normal conditions, the entire myocardium depolarizes, is at rest for a given period, and then repolarizes. The external voltage changes due to the combination of the cellular transmembrane changes can be monitored by placing the heart in an external saline bath. An electrode placed in the saline will monitor the net voltage excursion due to the depolarization current wavefront crossing the myocardium, a period of quiescence when the transmembrane potentials are constant at the plateau levels, and another voltage excursion as the cells repolarize. This is shown in Figure 5-2.

Figure 5-2 Voltage recording from the saline bath surrounding a spontaneously beating frog heart. The first deflection represents the depolarization of the atria, the second arises from depolarization of the ventricle, followed by a small deflection due to depolarization of the bulbus cordis (see chapter 6). The last deflection is that of repolarization of the ventricle. Repolarization of the atria does not yield a measurable voltage in this arrangement.

The rise in intracellular calcium during the plateau phase stimulates mechanical contraction of the cell. Thus the uniform spread of electrical activity leads to a contraction of the heart, with the

mechanical motion ocurring during and after the plateau phase.

Active Transport Mechanisms:

The net ionic movement of any one species per action potential is thought to be very small; for sodium it is estimated to be a net inward movement of 0.016 mM (Cohen et. al., 1982). However, in order for this activity to continue over long periods of times the ions must be returned to their initial conditions, against their concentration gradients. Active transport mechanisms accomplish this at the expense of energy stored in ATP. The most studied of these mechanisms is referred to at the "sodium pump", or more precisely the Na^+/K^+-ATPase. This enzyme moves sodium ions from within the cell to the extracellular space, with an opposite movement of potassium ions. For every two sodium ions which are moved, three potassium ions are transported. (For a review of the sodium pump, see Sweadner and Goldin, 1980; Kaplan, 1985.)

In addition, there are exchange mechanisms which indirectly use the energy of the sodium pump by exchanging ions for the sodium which has been moved by the pump. In particular there is a complex sodium/calcium exchange which may function to transport these ions in both directions at different points in the cardiac cycle (Mullins, 1979; Langer, 1982).

Several interventions are known to inhibit the ionic transport mechanisms. Ouabain, a digitalis glycoside, increases the contractile force of the heart. It is generally agreed that the mechanism of action of ouabain is an inhibition of the sodium pump, with a result-

ing increase in intracellular sodium and a secondary increase in intracellular calcium. This increased calcium leads to the increased contractility of the heart. However, it has also been suggested that the effects of ouabain are due to a change in the permeability of the membrane (Flear et. al., 1975).

Lithium ions have been used as a sodium replacement in the extracellular fluid. In frog sartorius muscle, lithium entered the cells like sodium, but was extruded more slowly, with an accumulation of lithium at the expense of potassium (Keynes and Swan, 1959). This was also shown to be the case in calf Purkinje and cat ventricular fibers; lithium currents were able to replace the sodium currents during depolarization, but there were differences in the later parts of the action potential and the efflux of lithium from the cells was inefficient (Carmeliet, 1964). Later studies indicated that lithium displaced sodium from the sodium/calcium exchange carrier, however it did not promote a calcium exchange (Langer, 1982). There is also evidence that lithium inhibits the sodium pump (Martin and Morad, 1982).

If the heartrate is increased sodium ions enter the cells at an increased rate. If the pumps cannot compensate, sodium builds up inside the cells and potassium accumulates outside. In guinea pig papillary muscle, an increase in rate from 0 to 0.5 Hz led to a change of the intracellular sodium activity from 5.8 to 7.9 mM, with the steady state value being reached one to two minutes after the change in rate (Cohen et. al., 1982).

6. ANATOMY AND ELECTROPHYSIOLOGY OF THE FROG HEART:

The frog heart has many features which make it attractive as an experimental preparation with which to study cardiac physiology. At the same time, the differences between the frog heart and mammalian hearts should be kept in mind before extrapolating results obtained with the former to human cardiac physiology. In this section the anatomy and electrophysiology of the frog heart will be reviewed, and the basic differences between it and a mammalian heart will be pointed out.

Anatomy:

The gross anatomy of the frog heart, shown in Figure 6-1, is composed of two atria and one ventricle. Deoxygenated blood from the body, along with oxygenated blood from the skin and mouth, returns to the right atrium while oxygenated blood from the lungs returns to the left atrium. Blood from both atria enter the ventricle, however it is unclear whether or not separation of oxygenated and deoxygenated blood is maintained there. All blood eventually leaves via the bulbus cordis into both the systemic and pulmonic circulations, where some separation may be maintained through the action of various valves and septa (Robb, 1965). By weight, the atria constitute 20% of the heart, the ventricle makes up 70%, and the bulbus, 10% (Brady, 1964).

As cold blooded animals, frogs respire through both their lungs and skin. Their resting cardiac O_2 consumption is 0.4 to 1 ml/gm hr (Brady, 1964), with a substantially higher glycogen content than mammalian hearts (Ventura-Clapier and Vassort, 1980). There are no

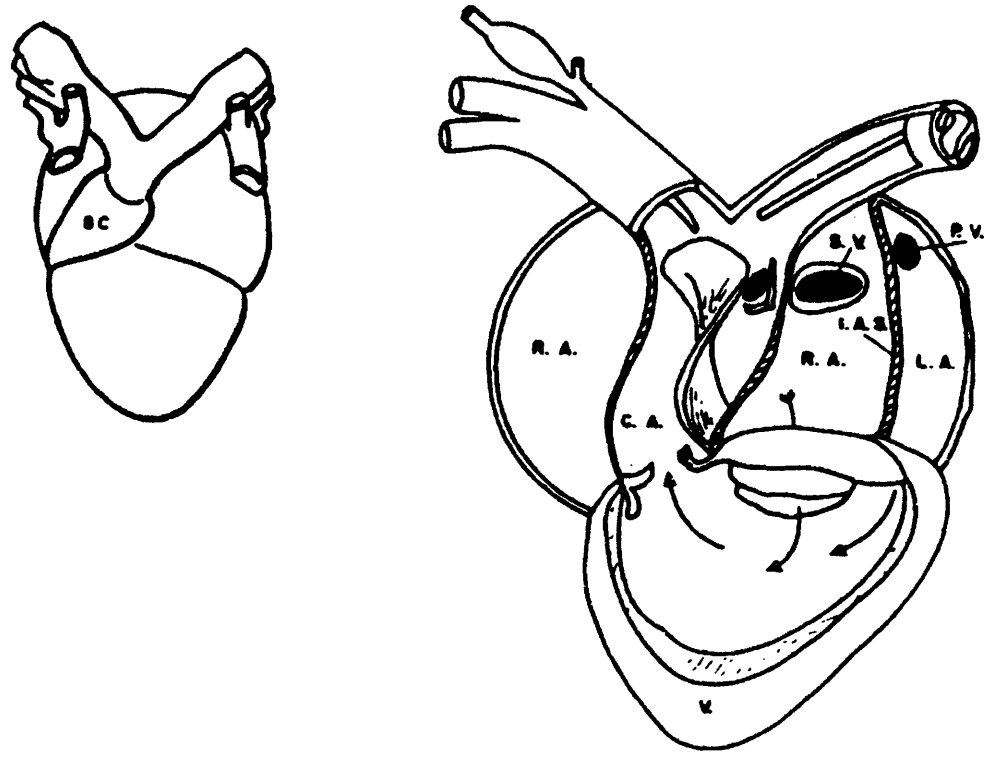

Figure 6-1 Gross Anatomy of the frog heart, ventral view. RA = right atrium, LA = left atrium, IAS = interatrial septum, SV = sinus venosus, PV = pulmonary vein, CA = conus arteriosus, and BC = bulbus cordis. Adapted from Robb, 1965.

coronary arteries, rather the cardiac tissue is very porous with the exchange of substances between the heart cavities and cells obtained via diffusion, with a relatively short diffusion distance for all bundles of tissue (Page and Niedergerke, 1972). Cohen and Kline (1982) summarize the description of frog ventricular muscle given by Page and Niedegerke (1972) as follows:

> Briefly, a strip is organized into fiber bundles or trabeculae with mean cross-sectional areas of about 3000 μm^2 ($\simeq$60μm diameter). Individual fibers are 3-5 μm in diameter, and are closely packed within the bundle. The average separation between fibers, the interfiber space (IFS), is about 150 angstroms. Each bundle is surrounded by a sheath that is several microns thick. Underneath the sheath is the

subendothelial space (SES). This varies between 1 and 5 μm in thickness. The extracellular space outside the trabeculae, labelled the extra-trabecular space (ETS), is contiguous with the bulk solution. The fraction of the total strip volume represented by each of these compartments is the following: interfiber space (IFS) - 1%, subendothelial space (SES) - 10%, extra-trabecular space (ETS) - 15%, and intracellular space (ICS) - 74%.

These cells, as well as the intercellular clefts, are in general smaller than in the mammalian counterpart (Morad and Goldman, 1973). They are, however, similar to those of Purkinje cells, specialized cells of the conducting system in mammals, with intercellular clefts between 100 angstroms and 1 micron in diameter (Kline and Cohen, 1984). The surface to volume ratio of the frog myocyte is equal to 1.27/micron (Page and Niedegerke, 1972), while the value given to the mammalian counterpart is 0.4/micron (Mullins, 1981).

The frog myocytes also differ from the mammalian in that there is a negligible T tubule system in the former (Morad and Goldman, 1973). This is important in considering the availability of calcium for contraction and for the sodium/calcium exchange mechanism in the two systems (Chapman et. al., 1983). In the frog ventricle, the calcium needed to develop tension is obtained primarily from the extracellular space (Klitzner and Morad, 1983).

Electrophysiology:

The electrophysiology of the frog heart also differs in several respects from the mammalian counterpart. The upstroke of the action potential is slower (40 to 80 msec versus 2 to 3 msec for mammalian) and the action potential is longer (600 to 1000 msec versus 200 to 600 msec for mammalian) (Morad and Goldman, 1973). Therefore the heartrate

is slower than that in other commonly used mammalian experimental animals (Hoffman and Cranefield, 1960; Boyett and Jewel, 1980). The frog heart thus lends itself well to the study of the components of the action potential.

In addition, the atrial and ventricular cells of the frog heart normally do not contain pacemaking activity. Therefore removal of the natural pacemaker, which is located near the venous input to the heart, enables the heartrate to be controlled over a wide range with external stimulation (Uchiyama et. al., 1967).

7. METHODS:

In order to study cardiac intracellular sodium by NMR, a method of perfusing a heart within a magnet, within a coil of a resonant circuit, is needed. It is desirable to be able to change the perfusate solution without disturbing the preparation, to monitor the cardiac activity during the experiments, and to pace the hearts within the magnet. This is accomplished with the perfusion apparatus described below. Also described are the NMR techniques used to suppress the extracellular sodium resonance, the pharmacologic and physiologic interventions used in these studies, and the relaxation time experiments and methods of data analysis.

Physiologic Preparation:

Bullfrogs (Rana Catesbeiana) with body lengths of approximately six inches, were stored in the cold (4 degrees Centigrade) until the time of the experiment. At this time they were anesthetized with pentobarbitol per intraperitoneal injection. The hearts were excised and placed in a dish of Ringer's solution at room temperature. Within 2 to 3 minutes, they were mounted on the perfusion apparatus shown in Figure 7-1, as described below. The hearts weighed approximately one gram, on average, after removal of the bulk fluid from the ventricles (upon completion of the experiments).

The perfusion system operated as follows: Perfusate from two different reservoirs (one liter each) was run through separate lines of a Cole Parmer Masterflex pump. Each outflow line from the pump was branched with a 3-way stopcock such that the perfusate could either be

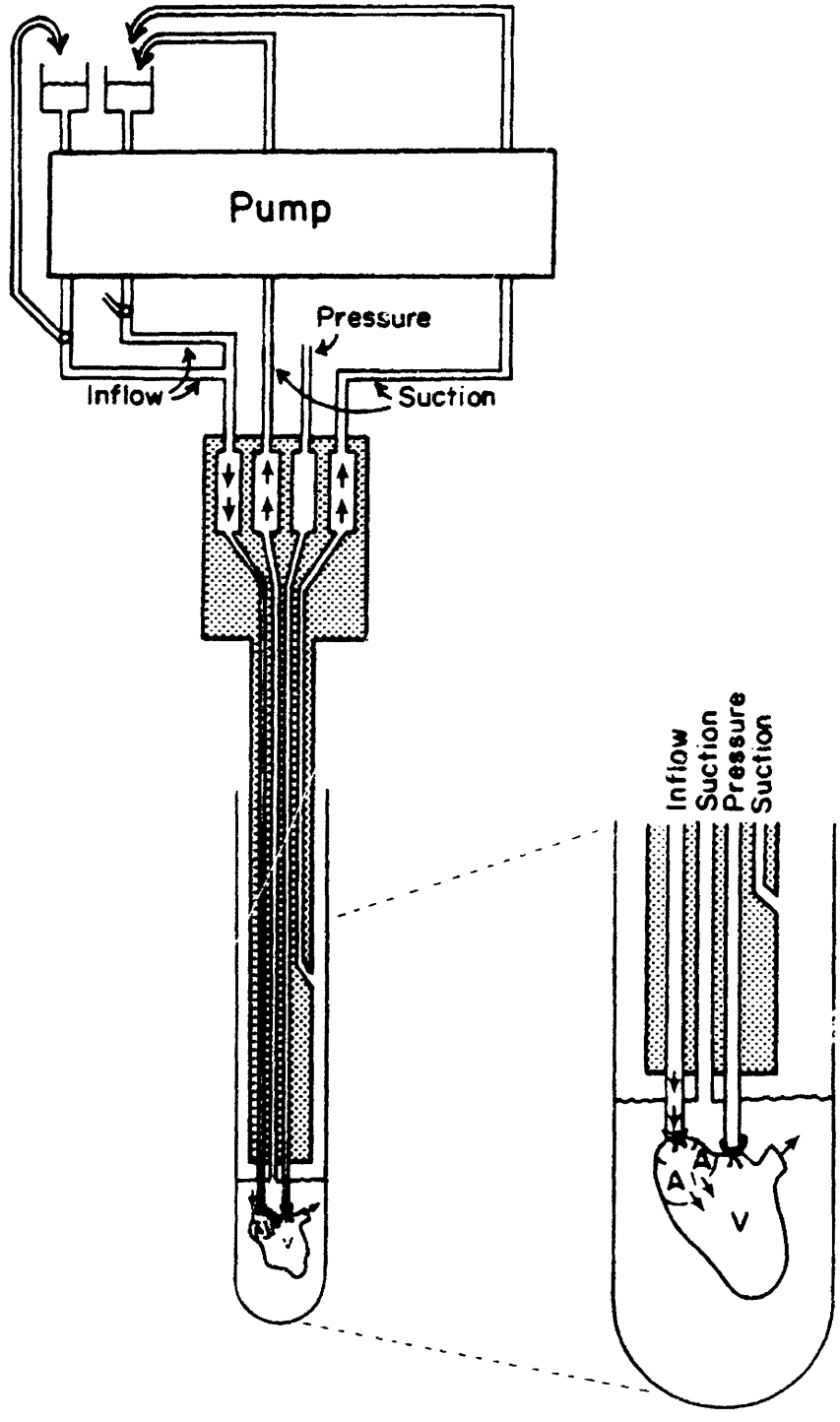

Figure 7-1 Apparatus used for the perfusion of isolated frog hearts. Full description in text.

returned to the reservoir or flow to the heart. The branches of the perfusate lines which continued to the heart were joined near the input to a specially built plastic cannula. At any given time, one perfusate was flowing through this line to the heart while the other was returned from the pump to the reservoir.

The perfusate flowed through one tract within the plastic cannula; a widening in this served as a bubble trap. Tubing was connected to the lower end of the cannula, and was then tied into the sheath containing the venous input to the heart. The perfusate flowed through the atria into the ventricle, and out of the ventricle athrough one of the main arterial branches into a 20 mm O.D. NMR tube. The other arterial branch was tied onto a fluid filled line from a Statham P23 ID pressure transducer to yield an uncalibrated pressure tracing of the heart's contractions. Two tracts of the cannula were used for separate suction lines. One suction line consisted of thin tubing threaded through the cannula; the height of this line could be changed to adjust the fluid level in the NMR tube. The other tract of the cannula served as a direct suction line, as a backup. The adjustable suction line was usually positioned above the level of the heart so that the heart was submerged in the perfusate. The reservoirs were aerated with room air, and the flow was maintained at approximately 8 milliliters per minute. Buffer was recirculated by returning the perfusate from the suction lines to the reservoir in use.

Alternatively, the heart could be perfused as a closed system. Instead of allowing the cardiac efflux to drain into the NMR tube, the arterial output was tied into one tract of the cannula; the adjustable

suction line was positioned within the cannula, several centimeters above the heart. The perfusate thus flowed through the heart as a closed system, and the heart could be suspended in air or in a non-sodium solution.

A Grass (model SD5) stimulator was used for the studies in which the heart was externally stimulated. A shielded twisted pair of wires from the stimulator output was brought to the magnet. At the point of entry into the magnet, these wires were connected with salt bridges to wires which ran almost to the heart. These were then soldered onto silver wire which ran down a groove in the side of the cannula and served as stimulating electrodes.

The salt bridges were used in order to reduce the pickup of stray radiofrequency fields into the probe, and were made as follows: 250 mg of agarose was added to 100 ml of isotonic (0.9%) saline. The mixture was heated and stirred until the agarose was totally dissolved. Tygon tubing (1/16" I.D., 1/8" O.D.) was immersed in the solution in order to equilibrate the temperatures. A blunt ended needle was used to draw the solution into a syringe and inject the solution into the tubing, which was then allowed to cool while still submerged. When fully cooled to room temperature the agarose formed a gel, and the tubing could be removed. The salt bridges were stored refrigerated. A length of tubing approximately six inches long had a D.C. resistance of about 10 kilohm.

The composition of the Ringer's solution is given in Table 7.1. Note the potassium concentration (Biology Data Book, 1974), as compared to that used in many other Ringer's solutions. Also listed are

the compositions of the other perfusate solutions used in the experiments, as discussed below.

	Ringers	3 mM SR Buffer	Li-Buffer	Zero-K^+ Buffer
Li	0	0	80	0
Na	120	120	40	120
K	4.8	4.8	4.8	0
Cl	125	100	100	93
H_2PO_4	0.43	0.43	0.43	0.43
HPO_4	1.58	1.58	1.58	1.58
Ca	1.8	1.8	1.8	0.9
$Dy(PPP)_2$	0	3.0	3.0	3.0
$(PPP)_2$	0	0.68	0.68	0.68

Table 7.1 Composition (in mM concentrations) of the various buffers used throughout tthe experiments, as indicated in the text. The calcium is given as the amount that was added to the solution.

NMR:

The experiments were all performed on a Bruker 360 AM wide-bore spectrometer, operating at 360.13 MHz for protons, 95.262 MHz for sodium-23, 145.786 for phosphorous-31, 16.805 for potassium-39, and 139.96 for lithium-7. The perfusion cannula fit inside a 20 mm O.D. NMR tube, the tube was mounted on an NMR spinner and lowered into a Bruker broad-banded probe, which was used for all of the studies. Typical 90 degree pulse widths were 35 μsec for sodium, 25 μsec for phosphorus, 95 μsec for potassium, and 30 μsec for lithium. Quadrature phase detection was used, and the spectrometer was not field-frequency locked.

Shift Reagents:

Two kinds of shift reagents were used in these experiments. The first was dysprosium triethylenetetramine hexaacetic acid $(DyTTHA)^{3-}$,

and the other was dysprosium tripolyphosphate ($Dy(PPP)_2^{7-}$). A stock solution of $Dy(TTHA)^{3-}$ was prepared as follows: Dysprosium chloride ($DyCl_3 \cdot 6H_2O$, Alfa Products) was dissolved in distilled water to a concentration of 110 mM. Triethylenetetramine Hexaacetic Acid (TTHA, Sigma Chemical Co.) was added in a molar ratio of 1:1. The solution had a pH of approximately 2.0, and the TTHA did not dissolve. Sodium hydroxide was then slowly titrated in over a period of approximately 1.5 hours to bring the pH to 7.0, during which time the solution slowly cleared. Distilled water was added to bring the concentration of $Dy(TTHA)^{3-}$ to 100 mM.

A stock solution of $Dy(PPP)_2^{7-}$ was prepared as follows: Dysprosium chloride was dissolved in water to a concentration of 250 mM, with a pH of 4.8. The pentasodium salt of tripolyphosphate ($Na_5P_3O_{10}$, Sigma Chemical Co.) was added to another beaker with distilled water to a concentration of 550 mM; this did not completely dissolve until the pH was brought from 8 to 7 with the addition of 1N HCl. Separately, sodium tripolyphosphate was prepared to a concentration of 250 mM; this dissolved without the aid of HCl. The $DyCl_3$ solution was added to the 550 mM sodium tripolyphosphate; a precipitate formed with the solution pH at 5.2. The 250 mM solution of sodium tripolyphosphate was added to the above until the precipitate dissolved. The pH was then brought up to 7.0 with the addition of 10N NaOH. This addition of the NaOH (added very slowly) resulted in a transient precipitate. The last step was not absolutely necessary, in that the perfusate was capable of buffering the small amount of shift reagent added to it, and the addition of the NaOH had no effect on the shifting or broadening effects of the shift reagent on the sodium in the perfusate.

The final concentration of shift reagent used in the perfusion buffer was 10 mM for the $Dy(TTHA)^{3-}$ and 3 mM for $Dy(PPP)_2^{7-}$. The NaCl content of the buffer was modified so as to compensate for the excess sodium added by the shift reagent, and thus the ionic content of the shift reagent buffer differs slightly from that of normal Ringer's solution. The final concentrations of the various buffers are given in Table 7.1. The level of calcium listed is the total amount which was added to the solution; however, since the shift reagent is expected to bind calcium, the free calcium in solution was somewhat less for the shift reagent buffers. This was measured with a calcium electrode to be approximately half that of the calcium in the normal Ringer's perfusate.

Suppression of the Extracellular Resonance:

With the perfused frog heart preparation, the extracellular (extramyocardial) volume is much greater than the intracellular. This, combined with the fact that the intracellular sodium concentration is an order of magnitude lower than the extracellular, means that even with a large shift between the intra- and extracellular signals the extracellular resonance may interfere with the much smaller intracellular resonance. Therefore in order to quantitatively study the intracellular sodium, a means of further separating the extracellular and intracellular signals, or eliminating the extracellular signal, is needed. Several methods of achieving this were tried. Mathematical resolution enhancement techniques were used to separate the overlapping peaks. A reduction in the amount of extracellular sodium could be obtained by hanging the heart as a closed system, non-submerged.

However, the degradation of the field homogeneity due to the heart-air interface, and thus the broadening of the peaks, would balance the positive effect of this method. In order to alleviate the homogeneity problem, the heart was submerged as a closed system in a buffer which did not contain sodium.

Presaturation of the extracellular resonance was the method used to suppress the extracellular resonance in the majority of these studies. As described earlier, presaturation involves transmitting a long, low power pulse directly followed by a short, high power (90 degree) pulse, and then acquisition of the NMR signal. The time required to switch a transmitter between low and high power is approximately 10 msec for our instrument. This delay would allow for a significant amount of recovery of the saturated peak before the 90 degree pulse. Therefore, a second synthesizer was used to transmit the presaturation pulse. Both transmitters were connected to the probe simultaneously via a directional coupler. This is shown in Figure 7-2, along with the timing diagram of the pulse sequence.

The various techniques were first attempted on a phantom sample consisting of concentric tubes containing shifted and nonshifted buffer. They were then applied to the heart samples.

Estimation of Intracellular Concentrations:

Rough estimates of the intracellular sodium and potassium concentrations were obtained as follows: The intracellular volume of each heart was determined as a fraction of the total NMR sensitive volume by two different methods to be described below. The intracellular

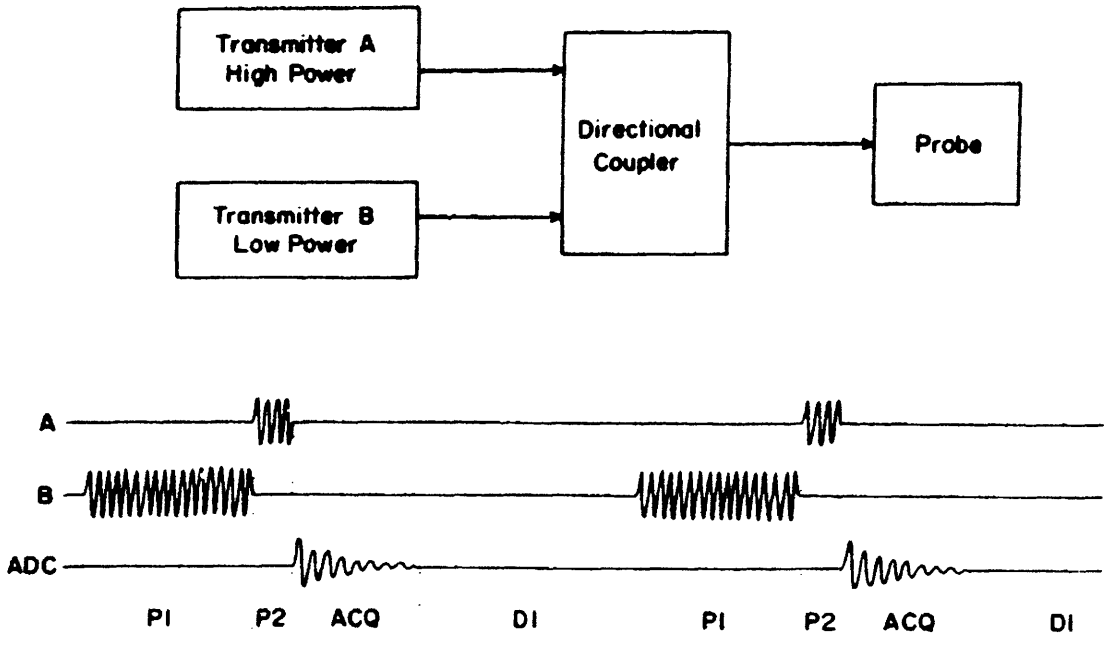

Figure 7-2 Hardware connections and pulse sequence for presaturation of the extracellular resonance in the sodium spectra. P_1 was typically 75 msec, P_2 was 35 μsec, ACQ was 50 ms, and D_1 varied depending on the T_1 of the system.

sodium signal was then scaled up to that which would have been obtained if the intracellular space occupied the entire sensitive volume. A calibration curve was measured relating NMR signal to ionic concentration, for solutions filling the entire sensitive volume. The calibration curve could then be used directly to determine the intracellular concentration.

The first method of determining the intracellular volume was basically one of using the shift reagent as an extracellular tracer. The integral of the resonance from the sample of shift reagent buffer was compared to that of the extracelluiar resonance from a perfused

heart preparation. The volume of the heart preparation which was in contact with the shift reagent could be determined as a fraction of the total NMR volume; the remaining volume was taken to be the intracellular volume, which was then expressed as a percentage of the total volume.

The above assumes that the B_1 field is homogeneous across the sample. In order to determine the homogeneity, the intra- and extracellular resonances obtained from 90, 180, 270, 360, and 450 degree pulses were compared to the theoretical chart given in Table 3.1.

The second method of obtaining the intracellular volume is that of using the literature value for the cell water weight per tissue wet weight for a frog heart, along with the wet weight of the heart as measured after the experiments, to determine the cell water weight, and hence intracellular volume, for the heart. The cell water weight per tissue wet weight for frog hearts has been given as 0.57 (Keenan and Niedergerke, 1967). The sensitive volume of the NMR coil was determined by hanging balloons with various volumes of a standard solution and then extrapolating to determine the volume as seen by the coil when the sample tube was filled with the standard. Therefore, the percentage of the sensitive volume which consisted of the intracellular space could be determined.

The calibration curve relating Na^+ (K^+) concentration versus the area in a resonance was determined by obtaining spectra of various combinations of NaCl and KCl solutions such that the ionic strength remained constant at 150 mM. The ionic strength of the samples was held constant so that it would have no effect on the Q of the probe.

In addition, the tuning and matching of the probe was checked for each sample. The spectra of the Ringers and shift reagent buffers were similarly measured and their Na^+ (and K^+) concentrations verified.

This procedure was followed for five hearts and the results of the two different volume determinations were averaged. The integral of the intracellular resonance was then scaled up tc that which would be obtained if the intracellular space occupied the entire sensitive volume, and the calibration curve was used to determine the intracellular sodium and potassium concentrations.

Pharmacologic and Physiologic Interventions:

Two interventions which are known to raise intracellular sodium were performed. The first was the addition of ouabain, in a dose of 10μM, and the second was the perfusion with a zero potassium buffer with lowered calcium. In addition, the hearts were perfused with a buffer in which approximately 2/3 of the sodium was replaced by lithium. The composition of these buffers is given in Table 7.1.

It was also of interest to see how the rate of electrical activity affected the intracellular sodium. For this purpose, two stimulating wires were brought to the heart, as described previously. The pacing wires were left in contact with the left ventricle, sometimes held in place with sutures. The pacemaker region of these hearts were tied off, and therefore they had no spontaneous activity, but were stimulated at rates up to 60 beats per minute. This study was performed with the normal shift reagent as well as a shift reagent buffer with approximately 1.8 mM excess calcium added. The excess

$CaCl_2$ was added to the final shift reagent solution.

Relaxation Time Experiments:

Sodium and lithium relaxation times were measured for the perfusates as well as the intracellular resonances. T_1 values were obtained with the standard inversion recovery technique. T_2 values were determined with the standard Hahn echo pulse sequence, both with and without the modification of presaturation. Data points were obtained with echo times from 0.5 to 30 msec, and in one case also from 0.1 to 0.5 msec. Due to limitations on the power output of the transmitter, such that the 180 degree pulse could be repeated only at intervals greater than 3 or 4 msec and therefore a CPMG echo could be obtained only every 6 msec, only a few points could be obtained on a CPMG decay curve. However, the Hahn echo and CPMG techniques were compared on a solution of NaCl to determine the differences, if any, of the value for T_2 obtained with the two methods. They were also compared with a small number of data points for the intracellular sodium of the heart.

Due to the low signal level of the intracellular sodium, long acquisitions were required to obtain reasonable signal to noise levels for the entire Hahn echo sequence. In order to compensate for possible changes over time, two modifications of the standard Hahn echo sequence were used. The list of delays was written such that the first half contained delays in descending order and the second half of the delays had values interleaved between the first, such that a change over time would be evident in alternate points being consistently high or low. In addition, the averaging was performed by looping through

the delay list several times and signal averaging the data. In some cases a few points with long delay times were run separately to allow for increased signal averaging.

Analysis of Relaxation Time Data:

The T_1 data were fit to a single exponential with the curve fitting program provided by Bruker. The T_2 data were also fit to a single exponential. However, when it became obvious that this fit was not sufficient a double exponential fit was performed using the statistics program at the Clinical Research Core Laboratory computer facilities at Boston's Beth Israel Hospital. The T_2 data were fit to the equation

$$M = M_0 (A e^{-t/\alpha} + B e^{-t/\beta}) \qquad (7.1)$$

The coefficients A and B were normalized such that $A + B = 1.0$, and thus A and B represent the fractions of the total signal which were decaying with time constants α and β, respectively. After this 4 parameter fit was obtained for all of the samples, a paired t-test was performed on the data of the samples for which both control and ouabain data was available. An unpaired t test, as well as Hotelling's T^2-test, were performed on all of the data to compare the parameters for the control versus the ouabain hearts. In addition, the means of the parameters in the control and ouabain cases were calculated.

If the representation of the relaxation as a double exponential decay is accurate, there are three models of the intracellular sodium which may be used to explain the data:

1. one homogeneous pool of sodium, with the biexponential relaxation being due to quadrupolar effects;
2. Two separate pools of sodium in slow exchange, in which

the sodium in each pool has a single relaxation time;

3. Two or more pools of nuclei in fast exchange, with at least one pool experiencing quadrupolar effects such that it inherently involves a biexponential decay.

The equations of chapter 2 (equations 2.19-2.22), along with the experimentally determined values for the relaxation times, were used to assess the validity of the above models concerning the state of intracellular sodium.

For model #1, the relaxation times can be described directly by equations 2.21-2.24, rewritten here with $C = \frac{1}{10}(\frac{e^2qQ}{\hbar})^2$.

$$\frac{1}{T_1'} = 2C\frac{\tau_c}{(1+4\omega_0^2\tau_c^2)} \qquad (80\%) \qquad (7.2)$$

$$\frac{1}{T_1''} = 2C\frac{\tau_c}{(1+\omega_0^2\tau_c^2)} \qquad (20\%) \qquad (7.3)$$

$$\frac{1}{T_2'} = C(\tau_c + \frac{\tau_c}{(1+\omega_0^2\tau_c^2)}) \qquad (60\%) \qquad (7.4)$$

$$\frac{1}{T_2''} = C(\frac{\tau_c}{(1+\omega_0^2\tau_c^2)} + \frac{\tau_c}{(1+4\omega_0^2\tau_c^2)}) \qquad (40\%) \qquad (7.5)$$

If this model is an accurate representation of the relaxation, the relative amplitudes of the 2 components of the measured T_2 should be 60:40. This was the first means of checking the legitimacy of this model. In addition, the ratios of the two experimentally determined values for T_2 were used to calculate the correlation time, given that in our application, $\omega_0 = 2\pi(95.3\times10^6)$Hz. C was then determined, and the T_1 equations were used to calculate the expected experimental values for T_1. The agreement with the measured T_1 was then evaluated.

Model #2 involves 2 pools of nuclei, each consisting of a single

exponential decay time. A single exponential decay implies either: a) the extreme narrowing condition applies, in which $T_1' = T_1'' = T_2' = T_2''$ or b) there are actually 2 components of the relaxation times which differ by less than a factor of 2, in which case the 2 components would not be differentiated experimentally. In this case, $T_1 > T_2$ and the relaxation times can be given as a weighted average of the components (Bull, 1972; Pettegrew et. al., 1984)

$$\frac{1}{T_1} = \frac{0.8}{T_1'} + \frac{0.2}{T_1''} \tag{7.6}$$

$$\frac{1}{T_2} = \frac{0.6}{T_2'} + \frac{0.4}{T_2''} \tag{7.7}$$

With the measured T_2, T_2' and T_2'' were estimated; the procedure described above was then used to calculate the values for T_1, and again check for the agreement with the measured T_1.

Model #3 is essentially equivalent to #1 in that the relative amplitudes of the components of T_2 should be in a ratio of 60:40. While this model involves two time constants in the decay curves, the actual number of pools of ions which may be contributing to the weighted average, or their relative amplitudes, cannot be determined from these studies alone.

Higher order models, which involve three or more inherent relaxation times and hence six or more variable parameters (relaxation times and coefficients), cannot be reasonably fit given the number of data points in these studies.

Linewidth vs. T_2 Measurement:

In order to determine how well the linewidth reflected the actual T_2 of the system as determined by the Hahn echo sequence, two values of τ were chosen and long acquisitions were obtained using the Hahn echo sequence. The linewidths were accurately determined and compared to the T_2 as determined from the full Hahn echo sequence.

Gated Experiments:

The intracellular sodium signal was also measured as a function of the timing within the action potential. In order to accomplish this, the heart was externally stimulated, as described earlier, at a rate of approximately 25 beats per minute. The external trigger source from the stimulator was used to trigger the spectrometer to begin a pulse program. The timing of this pulse program is shown in Figure 7-3. The trigger was followed by a delay, a presaturation pulse, an excitation pulse, and data acquisition. The memory pointer was then advanced and the cycle repeated such that each successive acquisition was stored in series within the computer memory, for a total of eight acquisitions. The memory pointer was then returned to the initial location and the sequence was repeated following the next trigger (and stimulation). Therefore a time average of the intracellular sodium was obtained for eight points in the cardiac cycle. The pressure was continuously monitored throughout the experiment, and a tracing of the electrical activity was obtained before and after the experiment.

The above procedure was followed for proton NMR and sodium NMR with active, responding hearts, and with the same hearts after death

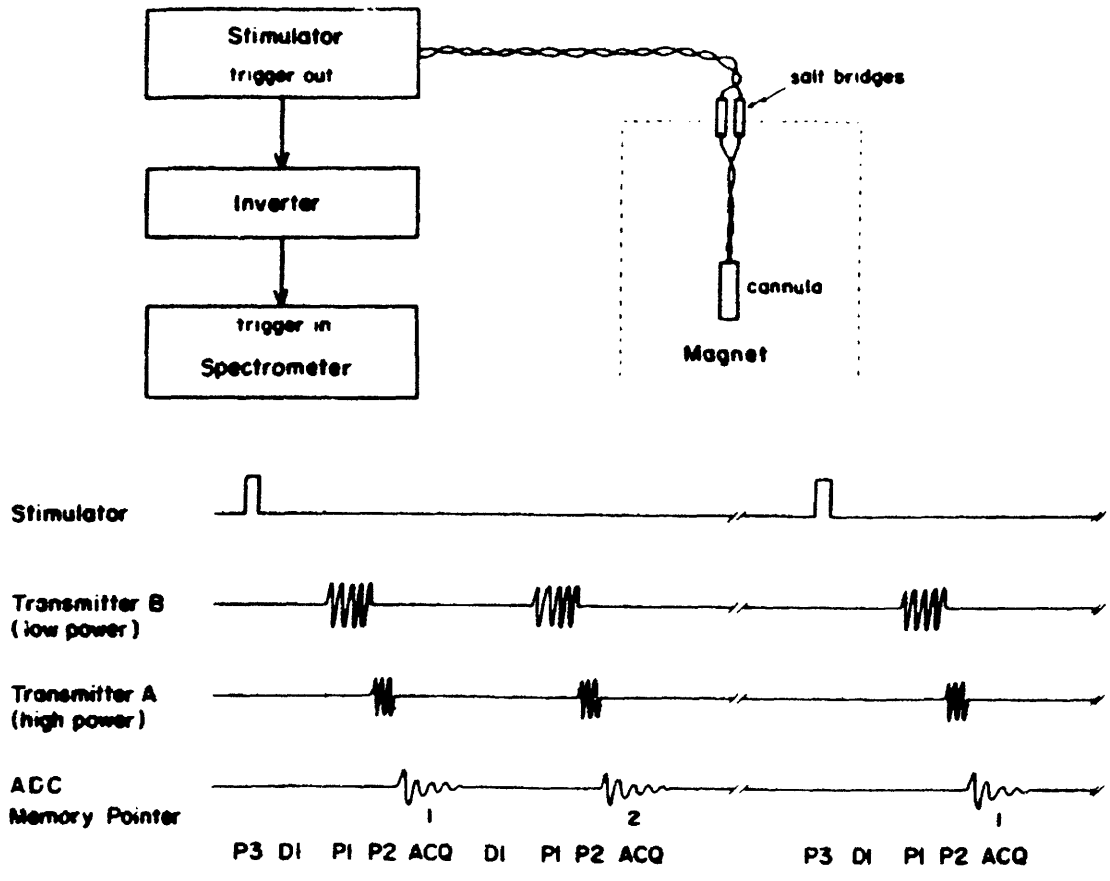

Figure 7-3 Electronic arrangement and pulse sequence for gated cardiac studies.

or with the stimulus level too low to produce a response.

8. RESULTS:

The parameters for the spectra which are presented in this chapter are given according to the notation of chapter 3, as follows:

SI = the total number of data points transformed

TD = the actual number of data points acquired; (SI-TD) points are zero-filled at the end of the FID

SW = spectral width (Hz)

PW = pulse width; the length of the excitation pulse (μsec)

RD = recycle delay; the delay before the excitation pulse which enables the spin system to reach equilibrium in between pulses (sec)

ACQ = acquisition time (sec)

NS = number of scans averaged

For the spectra in which presaturation was used,

P1 = the duration of the presaturation pulse (μsec)

PW = P2 = the duration of the excitation pulse (μsec)

D1 = the delay in between cycles (sec)

The data processing parameters are given as

LB = line broadening factor (Hz); for S/N enhancement the FID was multiplied by a function of the form $\exp[(-\pi)(LB)(t)]$

GB = Gaussian broadening factor (given as a fraction of the acquisition time); for resolution enhancement the FID was multiplied by a function of the form $\exp(-at-bt^2)$, where $a=\pi(LB)$ and $b=(-a)/2(GB)(ACQ)$

By convention, the spectra are plotted with the frequency increasing from right to left.

Heart Stability:

Upon perfusion with modified Ringer's solution, the hearts beat spontaneously at a rate of approximately 40 per minute. With the switch to the perfusate containing the $Dy(PPP)_2^{7-}$ shift reagent, the spontaneous rate slowed and the hearts bloated such that gross

mechanical motion was barely detectable by eye. The pressure as measured with the line in the arterial branch was measurable, however, and could be followed throughout the experiments (Figure 8-1). With the heart submerged in saline, voltage tracings from electrodes positioned in the saline indicated that the bulk electrical activity of the hearts continued (Figure 8-2). The hearts continued to beat spontaneously for up to 24 hours with either the Ringer's or shift reagent perfusate. A typical phosphorus spectrum obtained at 24 hours is shown in Figure 8-3, in which a significant amount of creatine phosphate and ATP can be seen, indicating the metabolic viability of the heart. A photograph of a heart being perfused within an NMR tube is shown in Figure 8-4.

The effects of the shift reagent on the heart, those of slower spontaneous rate and decreased developed pressure, were reversible by either adding excess calcium to the shift reagent perfusate or by returning to the normal Ringer's perfusion. Unless explicitly stated otherwise, in the experiments reported here, no excess calcium was added to the shift reagent perfusates. This was mainly because the excess calcium resulted in reduced NMR shifts of the extracellular sodium and potassium due to the ion's competition with calcium for interaction with the shift reagent. Since presaturation has not before been used for sodium in physiologic systems, it was desirable to be able to compare the intracellular resonance with and without the preasaturation. This was only possible if the intra- and extracellular resonances could be relatively well separated without the presaturation. In addition, the reduced calcium ensured that there would not be excessive motion of the heart within the magnetic field, which may

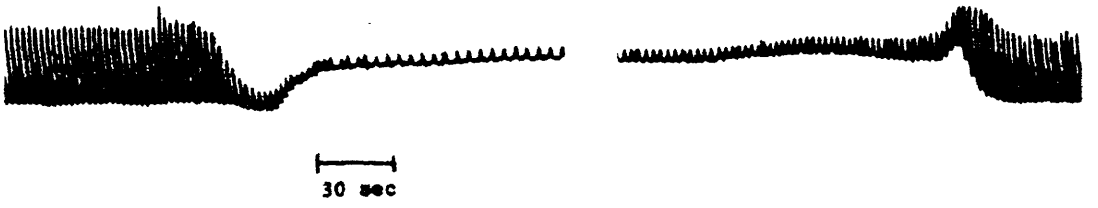

Figure 8-1 Pressure tracing obtained from the line in one of the arterial branches of the heart. The heart was initially perfused with Ringer's solution; the wash-in and wash-out of 3.0 mM $Dy(PPP)_2^{7-}$ buffer is also shown.

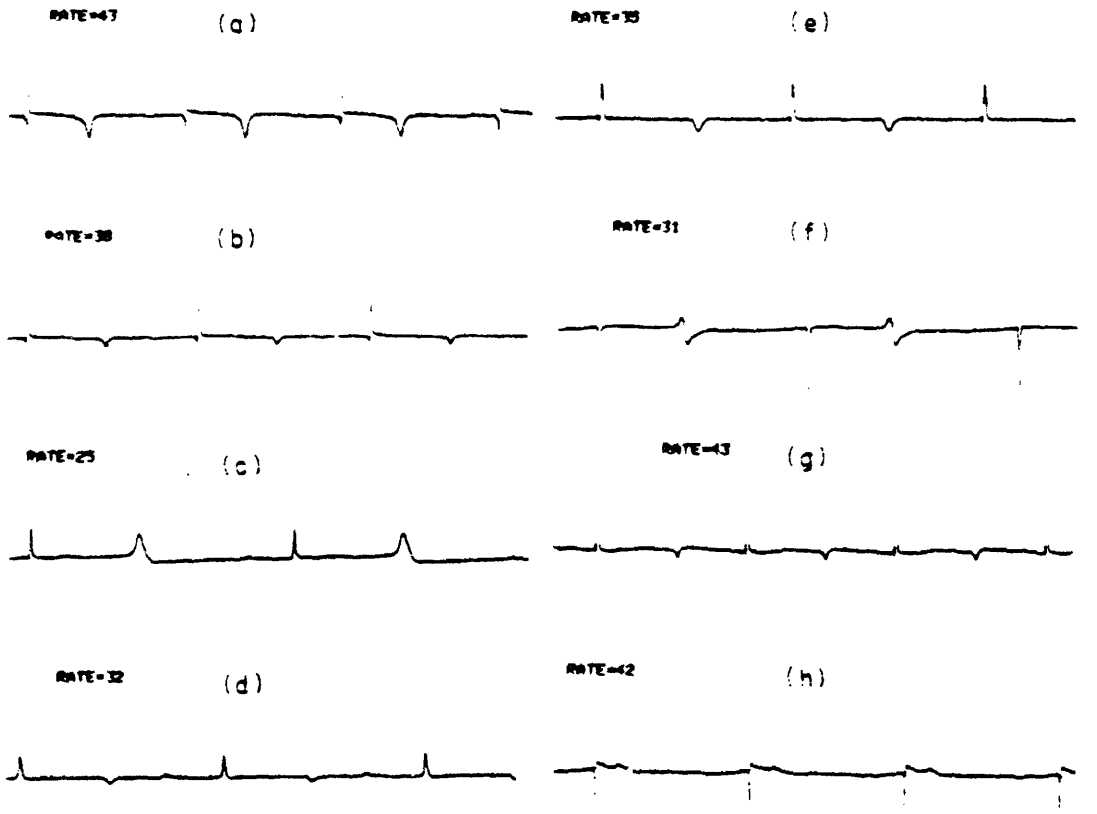

Figure 8-2 Series of electrical recordings from the buffer surrounding a spontaneously beating heart with the addition and washout of shift reagent buffer. The morphology of the tracings is not significant due to the changing orientation of the electrodes relative to the heart as it bloated with the shift reagent. a) Ringer's perfusing the heart; b) 10 minutes, c) 1 hour, d) 2 hours, e) 3 hours, and f) 4 hours, after the wash-in of 3.0 mM $Dy(PPP)_2^{7-}$ buffer; g) 10 minutes and h) 1/2 hour after return to Ringer's perfusion.

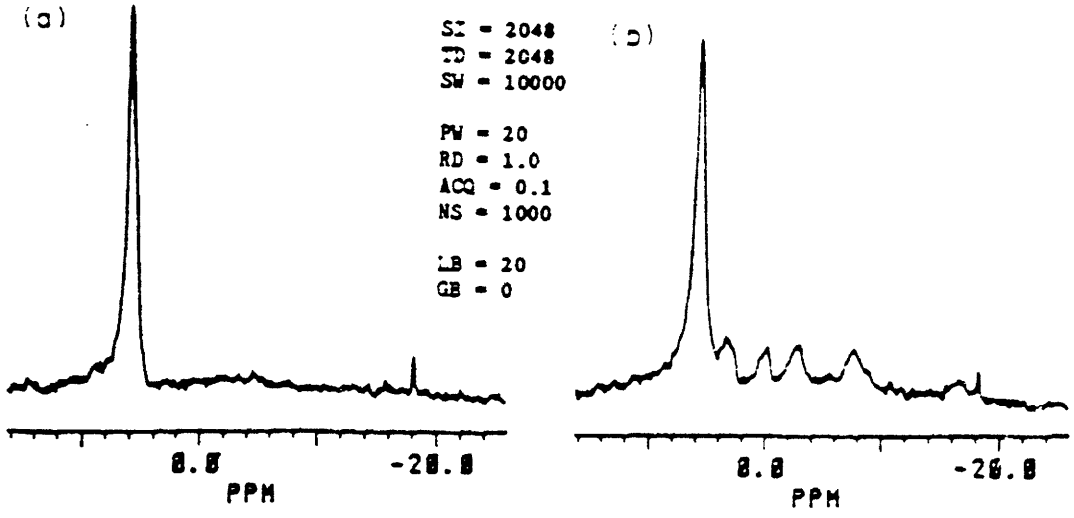

Figure 8-3 P-31 spectrum of (a) 3.0 mM $Dy(PPP)_2^{7-}$ buffer after being recirculated for 24 hours, and (b) perfused, submerged, heart after 24 hours. 0.0 ppm is referenced to the creatine phosphate resonance. The resonances at approximately 3, 7, and 16 ppm represent the γ, α, and β ATP resonances, respectively. The parameters are the same for both spectra.

Figure 8-4 (next page) Photograph of a heart perfused with 3.0 mM $Dy(PPP)_2^{7-}$ shift reagent buffer within a 20 mm O.D. NMR tube. The wires were used for pacing of the hearts.

contribute to effects in the T_2 measurements and gated studies, as will be discussed later.

Shift Reagents and Identification of the Intracellular Signal:

Figures 8-5 and 8-6 show the resonances of the ions in Ringer's solution as well as the resonances of the ions in the shift reagent buffers. The 10 mM $Dy(TTHA)^{3-}$ buffer yielded shifts of approximately 4.5 ppm for sodium and 6.0 ppm for potassium, while the 3 mM $Dy(PPP)_2^{7-}$ buffer yielded shifts of 0.45 ppm for proton, 6.4 ppm for sodium, 3.5 ppm for potassium, and 3.2 ppm for lithium.

The degree to which the resonances were shifted and broadened by the shift reagent varied with the stock solution. The broadening seemed to depend upon the method by which the excess tripolyphosphate was added to the shift reagent stock. The method described earlier, that of adding the excess tripolyphosphate in solution form, yielded the sharpest resonances. In some cases the potassium NMR signal was broadened to the point of losing a significant fraction of the shifted potassium from detectability under these conditions. In order to show that the low signal intensity was due to the interaction with the shift reagent and not an error in the actual potassium concentration added to the solution, a spectrum of the potassium in Ringer's solution was obtained, shift reagent was added to a concentration of 3 mM, and another spectrum was obtained. The dilution factor was negligible, in that the stock solution was at a concentration of 100 mM. Figure 8-7a shows the obvious decrease in the area of the resonance with the addition of the shift reagent. Adding the shift reagent to a solution of 5 mM KCl + 145 mM NaCl produced an equivalent shift as that in the

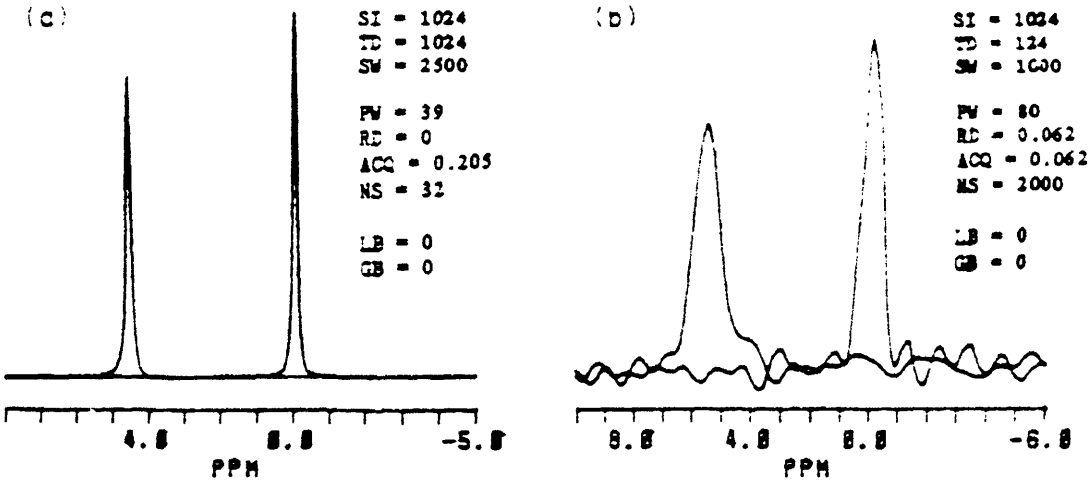

Figure 8-5 (a) Sodium and (b) potassium spectra obtained with the Ringer's and the 10 mM $Dy(TTHA)^{3-}$ shift reagent buffers, as given in Table 7.1. The resonance at 0.0 ppm is the resonance of the ion in Ringer's solution.

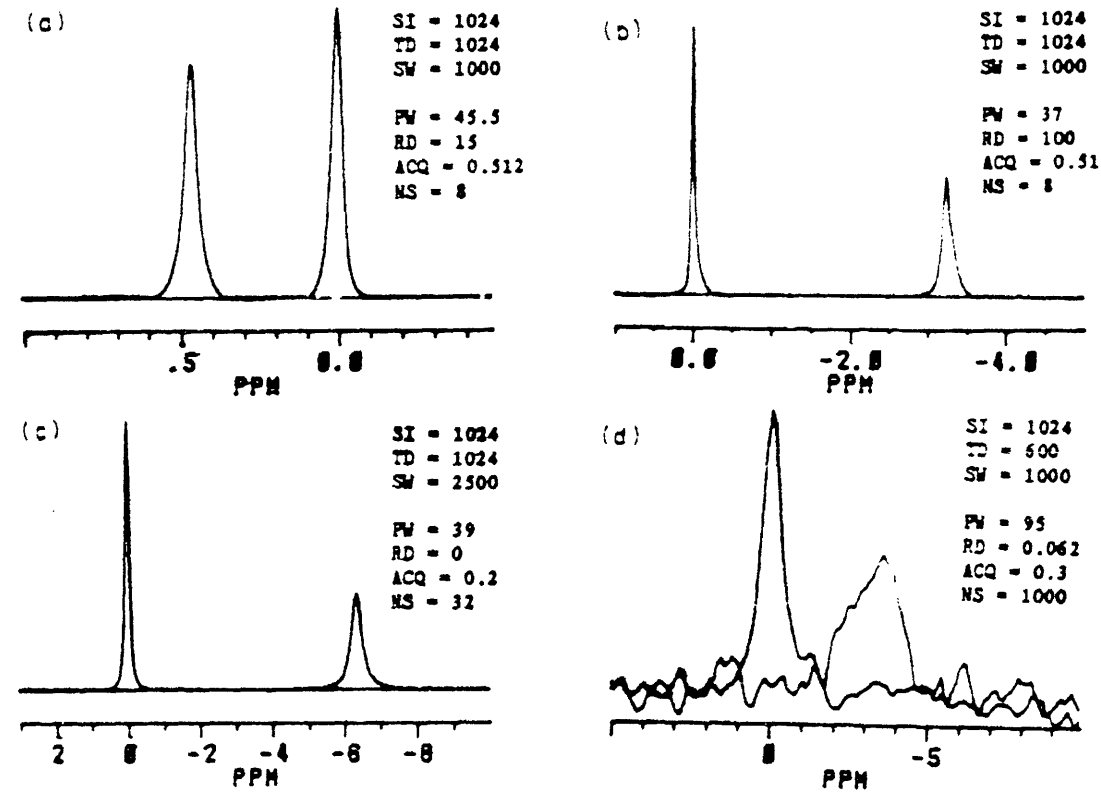

Figure 8-6 (a) Proton, (b) lithium, (c) sodium, and (d) potassium spectra obtained with Ringer's and with the 3 mM $Dy(PPP)_2^{7-}$ shift reagent buffers. The resonance at 0.0 ppm is the resonance of the ion from Ringer's solution. All LB=GB=0, except for the potassium spectra in which LB=5. NS=1000 for the Ringer's potassium spectrum and 4000 for the shift reagent potassium spectrum.

case of Ringer's solution, with some broadening, but with no loss in signal intensity (Figure 8-7b).

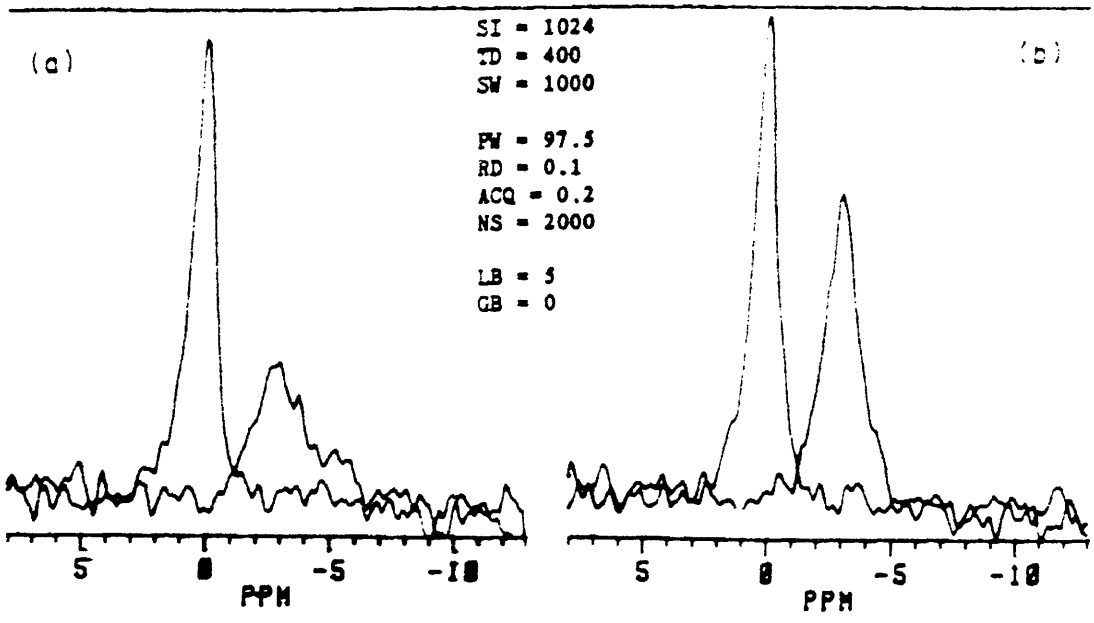

Figure 8-7 K-39 spectra of (a) Ringer's before (resonance at 0 ppm) and after the addition of 100 mM $Dy(PPP)_2^{7-}$ stock solution to yield a 3.0 mM $Dy(PPP)_2^{7-}$ solution. The relative areas of the two resonances are 1:0.6. (b) Same as (a), with 5 mM KCl + 145 mM NaCl in place of the Ringer's. The relative areas in this case are 1:0.9.

Typical sodium spectra obtained with the the $Dy(TTHA)^{3-}$ and $Dy(PPP)_2^{7-}$ buffers perfusing the heart are shown in Figure 8-8, with the zero referenced to the position of the sodium signal from the Ringer's solution. The $Dy(TTHA)^{3-}$ appeared to shift the entire peak, with only a small shoulder on the upfield side, with no identifiable intracellular signal. The spectra obtained with the $Dy(PPP)_2^{7-}$ buffer consistently showed a small peak remaining at the unshifted position. This peak slowly decreased over a period of approximately one half hour after addition of the shift reagent, and then remained stable for up to 24 hours with a steady flow of shift reagent-buffer.

Potassium spectra were much more difficult to obtain due to the low inherent sensitivity of potassium and the broadening of the potassium signal. With the $Dy(TTHA)^{3-}$, no second peak was distinguishable at, or close to, the unshifted position. With the $Dy(PPP)_2^{7-}$, two peaks were easily discernible (Figure 8-9).

All of the spectra to be presented from this point on which utilize shift reagent were obtained with the $Dy(PPP)_2^{7-}$ shift reagent.

Suppression of the Extracellular Resonance:

A number of techniques were used in order to eliminate the interference of the large shifted sodium signal with the much smaller unshifted signal. Resolution enhancement was effective in separating the two peaks (Figure 8-10), however the concomitant decrease in S/N necessitated long signal averaging. The advantage of reducing the amount of shifted signal by hanging the heart in air was offset by the broadening of the lines due to the resultant inhomogeneous magnetic field. Submerging the heart as a closed system in a non-sodium solution (mannitol) was also attempted as a means of reducing the shifted signal. However, within a few minutes a significant amount of sodium was present in the external bath. With the heart perfused as a closed system, suspended nonsubmerged, it was demonstrated that there was no bulk leak of fluid from the closed perfusion system. Therefore the sodium must have diffused through the myocardium. Having a second pump quickly exchange the external fluid may eliminate this problem. However, either shift reagent would need to be added to the external bath, thereby introducing sodium due to the pentasodium tripolyphosphate, or the sodium which diffused through the heart would appear at

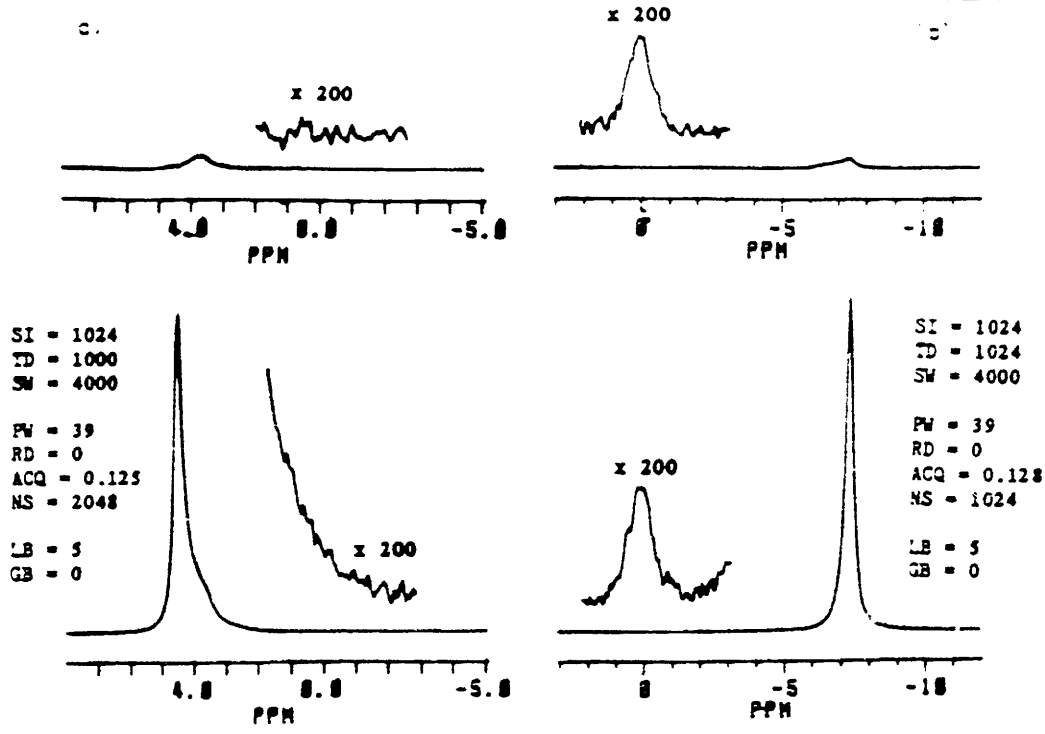

Figure 8-8 Na-23 spectra obtained from a perfused heart with a) 10.0 mM $Dy(TTHA)^{3-}$ and b) 3.0 mM $Dy(PPP)_2^{7-}$ buffers, both with and without presaturation (to be discussed below) of the shifted peak. For the presaturated resonances, P1=75 msec. 0.0 ppm is referenced to the resonance of the buffer without shift reagent.The spectrum around 0 ppm is scaled up vertically by a factor of 200 to more easily display the unshifted resonance.

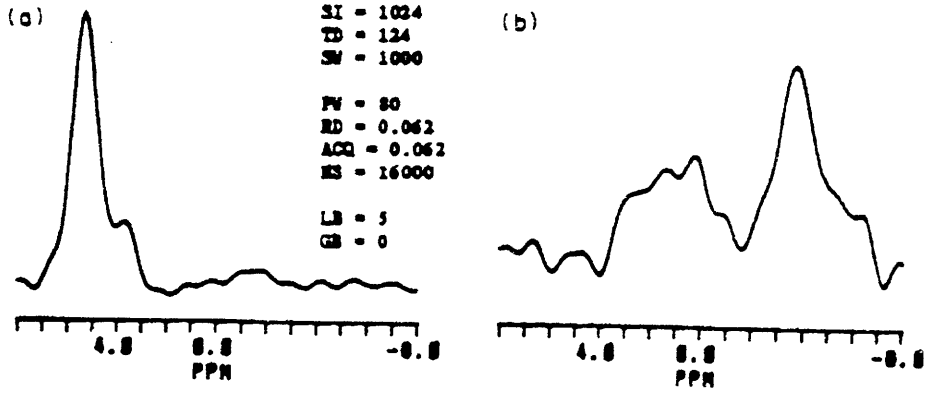

Figure 8-9 K-39 spectra obtained from a perfused heart with a) 10.0 mM $Dy(TTHA)^{3-}$ and b) 3.0 mM $Dy(PPP)_2^{7-}$ buffers. Again, 0.0 ppm is referenced to the Ringer's perfusate without shift reagent. The given parameters are identical for both spectra, however the vertical scale of (b) is 4 times that of (a).

the unshifted position, indistinguishable from the intracellular sodium resonance. Even a small error introduced by this technique would not be tolerable given the expected small intracellular signal, and therefore this method was not utilized.

The technique of presaturation was very effective in suppressing the shifted resonance without affecting the resonance at the unshifted position. This is demonstrated in Figure 8-11 with presaturation of the shifted resonance in a sample of concentric tubes containing Ringer's and shift reagent buffer. A presaturation pulse of 75 msec was sufficient to presaturate the shifted peak, and thus the by reducing the recycle delay or acquisition time to compensate, the total experimental time did not need to be changed. As shown in Figure 7-2, this method required the addition of a cable from the second synthesizer to the directional coupler at the probe. This additional cable led to some noise pickup into the probe.

Sodium spectra obtained from a perfused heart both with and without presaturation of the shifted resonance are shown in Figure 8-8b. The utilization of presaturation yielded spectra with better dynamic ranges and unshifted resonances with better baselines than without the presaturation. The use of presaturation also allowed for higher line broadening factors to be used to increase the S/N in the spectra without causing overlap of the two resonances. While keeping in mind that a quantitative comparison would not be warranted due to possible overlap of the two resonances without presaturation, a comparison of the unshifted resonance before and after presturation demonstrated that this had a very small effect, if any, on the

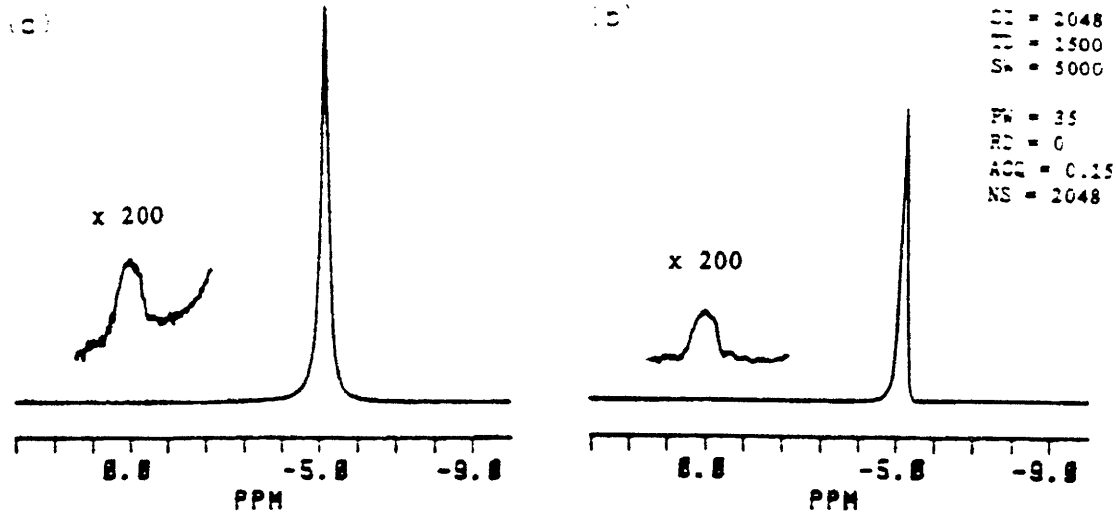

Figure 8-10 Mathematical resolution enhancement: Na-23 spectrum of perfused heart. (a) LB=0, GB=0; (b) LB=-15, GB=0.2. All other parameters are the same for both spectra. The vertical scale of the region around 0 ppm is scaled up by a factor of 200 to better illustrate the unshifted resonance.

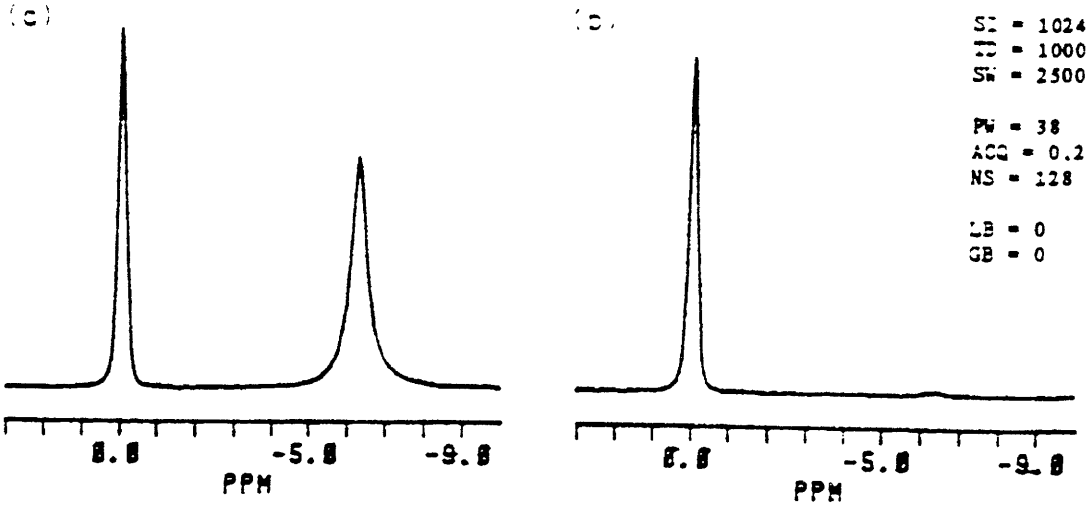

Figure 8-11 (a) Na-23 spectrum from concentric tubes containing Ringer's and 3.0 mM $Dy(PPP)_2^{7-}$ buffer, RD=0.1 (b) Same as (a), with presaturation of the shifted peak, RD=0, P1=75 msec. All other parameters are the same for both spectra.

unshifted signal.

As will be shown, all of the experimental results are consistent with the hypothesis that the unshifted resonance represents intracellular sodium. From this point on, for ease of discussion, the unshifted resonance will be referred to as the intracellular resonance, and the shifted resonance will be referred to as the extracellular resonance.

Intracellular Ionic Concentrations:

The calibration curves obtained with the solutions of NaCl and KCl are shown in Figure 8-12. Table 8.1 gives the percentage of the total NMR observable volume (7 ml) which was determined to be the intracellular volume by the two methods described earlier. With the exception of one sample, the two values agreed to within 20%. Also shown are the intracellular sodium and potassium concentrations using the average of the two values for the volume and the calibration curve of Figure 8-12. The average of the intracellular sodium concentrations of the five samples was found to be 6.2 ± 2.1 mM (mean ± standard deviation), and the intracellular potassium concentration was found to be 14.5 ± 5.0 mM. There was no correlation between the calculated intracellular potassium concentration and the degree of broadening of the potassium signal in the shift reagent buffer.

The area of the extracellular resonance obtained with a 450 degree pulse was 1/2 that obtained with a 90 degree pulse, while the ratio of the intracellular resonances with the two pulse lengths was approximately 1/4. In both cases, this leads to less than 5% error on

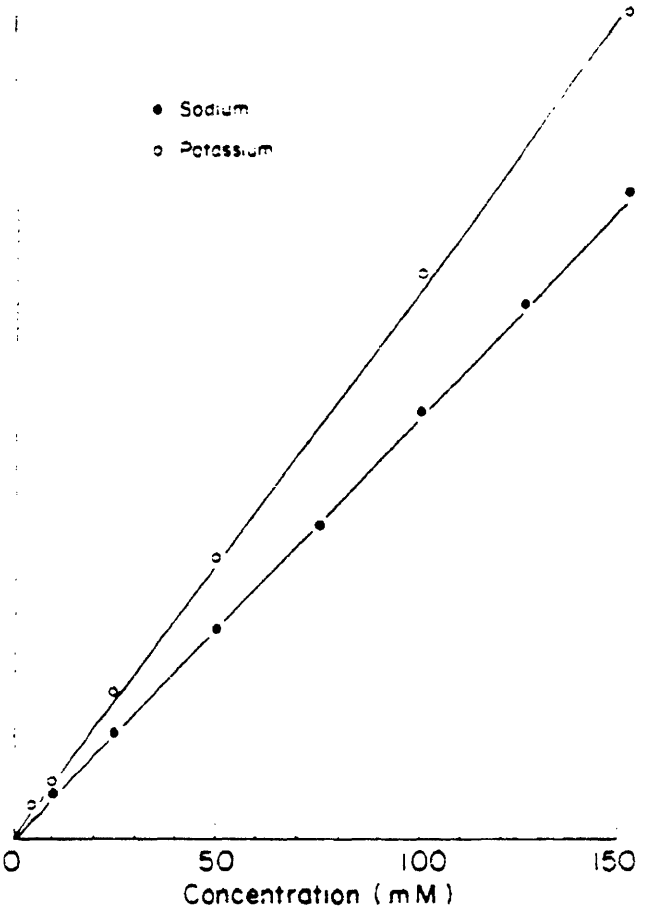

Figure 8-12 The sodium and potassium signals, given in arbitrary units of the area of the NMR resonance, as a function of the concentration of the ion. The solutions were all equal in total ionic strength.

Heart	Volume 1	Volume 2	Avg. Volume	$[Na]_i$	$[K]_i$
A	3.8	8.3	6.1	7.5	19.3
B	5.8	6.9	6.4	9.1	7.3
C	8.0	8.8	8.4	2.9	16.2
D	6.0	7.3	6.7	6.4	9.9
E	8.0	8.2	8.1	4.9	19.8
Mean ± S.D.				6.2 ± 2.1	14.5 ± 5.0

Table 8.1 Intracellular volumes, given as percentages of the NMR sensitive volume (7 ml), and calculated intracellular sodium and potassium concentrations, given in mM units. Volume 1 was determined by the NMR method, Volume 2 was determined by the weight method.

the signal obtained from the actual 90 degree pulse relative to a perfect 90 degree pulse (Table 3.1). Therefore, $\vec{B}_1$ inhomogeneity should not have played a large role in the scatter of the intracellular concentration determinations.

Pharmacologic and Physiologic Interventions:

Ouabain, in a dose of 10 μM, raised the intracellular signal by 460 ± 60 % (mean ± S.D. , n=6) over a time course of approximately 2.5 hours. The pressure initially increased with the addition of ouabain, then decreased. After several hours, the hearts no longer were contracting and would not respond to a stimulus. In one experiment, the shifted resonance began to split over the time course of the rise in the intracellular sodium, with a component moving downfield towards the unshifted resonance. As the intracellular resonance stabilized, the shifted resonance coalesced to its original position (Figure 8-13). During this time, the intracellular resonance did not change position. Presaturation did not affect the intracellular signal, even after ouabain administration (Figure 8-14).

With the zero K^+, low Ca^{++}, perfusion, the unshifted signal increased by 300 ± 30 % over approximately one hour, which was reversible upon perfusion with the normal shift reagent buffer (Figure 8-15). The pressure decreased during the zero K^+ perfusion, however it returned to its initial level on return to the normal shift reagent buffer. In some cases, perfusion with zero K^+ also resulted in the splitting of the extracellular resonance, which coalesced with the return to normal perfusate.

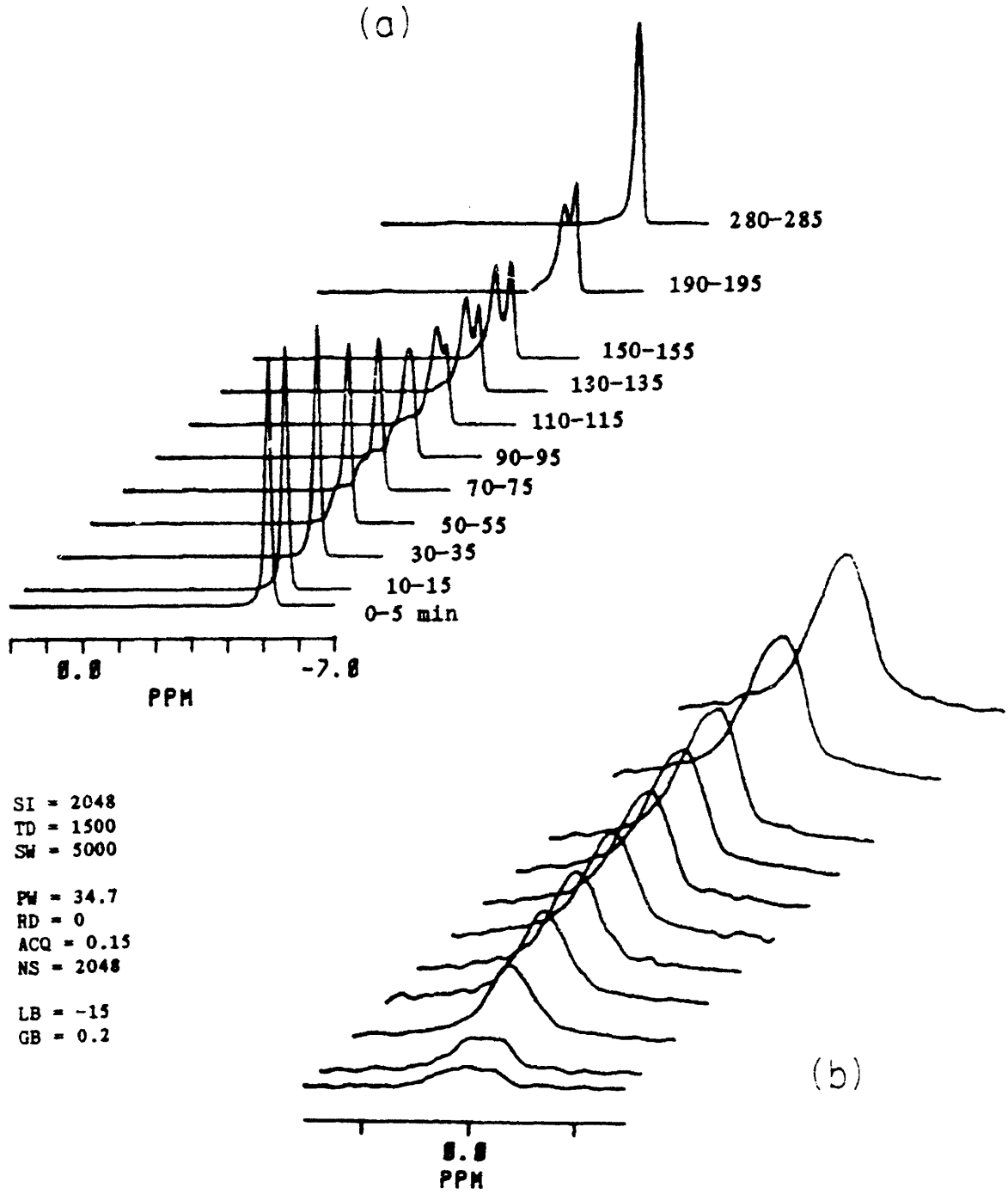

Figure 8-13 Sodium spectra obtained during administration of a perfusate containirg 10 μM ouabain. Each spectrum was acquired over the 5 minute period shown, when t=0 is at the start of the ouabain perfusion. (a) The total spectrum; and (b) the intracellular resonance, scaled vertically by a factor of 100 relative to the spectra in (a).

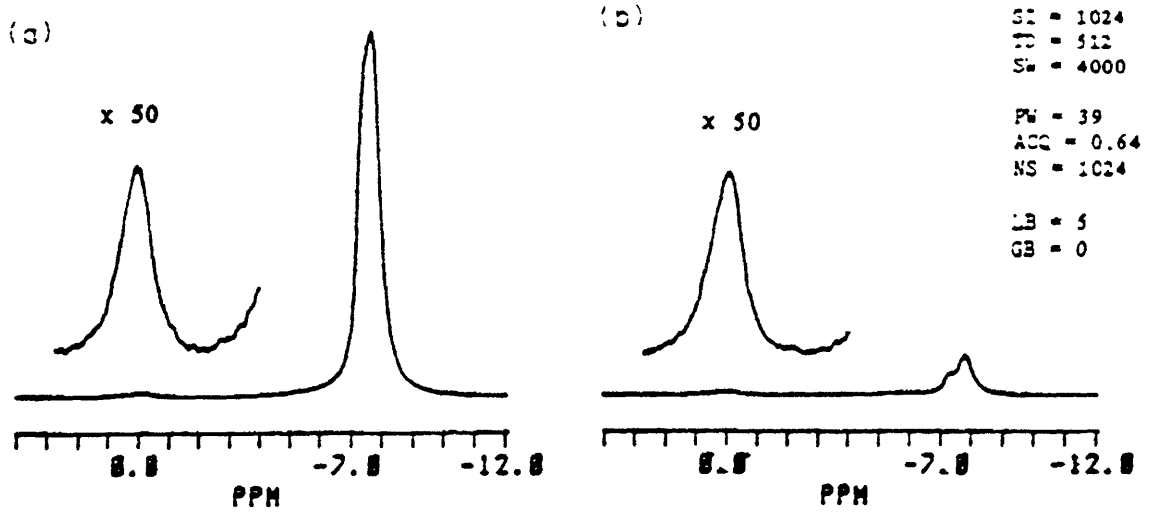

Figure 8-14 (a) Na-23 spectrum of a perfused heart after ouabain exposure, RD=0.1 (b) same, with presaturation of the shifted resonance, RD=0, P1=75 msec. The other parameters are identical for both spectra. Expansion of the vertical scale around 0 ppm displays the intracellular resonance.

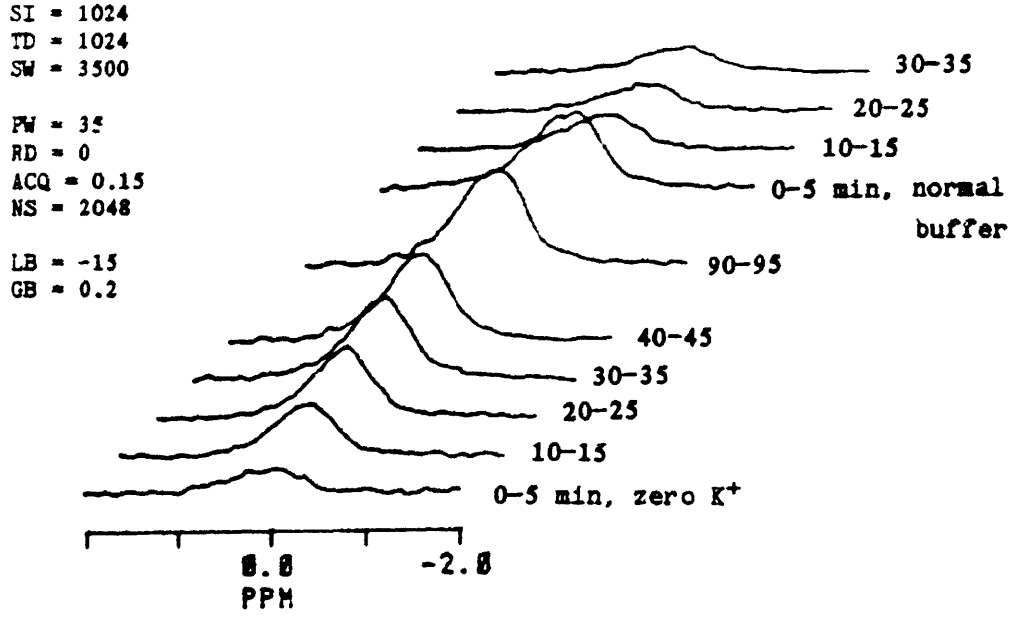

Figure 8-15 Intracellular sodium resonance with the wash-in and out of a zero potassium, low calcium perfusate. The times given (in minutes) are the times of acquisition, measured from the time of introducing the zero potassium or normal shift reagent perfusate to the heart.

Perfusion with lithium replacing 2/3 of the sodium lowered the unshifted resonance by 51 ± 6 % over 3.5 hours (Figure 8-15), and on lithium NMR a small resonance appeared at the unshifted position (Figure 8-17). After the T_1 of the intracellular lithium was determined to be 700 msec, the recycle delay was adjusted such that a good spectrum could be obtained with 32 scans (Figure 8-18). There was a small potentiation of pressure with the introduction of the lithium buffer, followed by a slow decrease over the next 1/2 hour. With the wash in of normal Ringer's solution, the heart resumed normal beating.

Three hearts were utilized in the pacing study, none of which had spontaneous activity. In one, a pacing rate of 60 beats per minute was achieved, and in the increase of the intracellular sodium with pacing rate is shown in Figure 8-19. The other two would not pace above 30 beats per minute, but with an increase of rate from 0 to 30 the intracellular sodium increased by approximately 25% in both cases. These increases were reversible and reproducible upon changing the pacing rate. When approximately 1.8 mM excess $CaCl_2$ was added to the buffer, a change in rate from 0 to 30 resulted in an increase in intracellular sodium of approximately 50%.

Relaxation Time Measurements and Data Analysis:

The T_1 and T_2 relaxation times for sodium in Ringer's solution were found to be equal with a value of 56 msec, with each relaxation curve consisting of single exponential. The result was the same whether the Hahn echo or the CPMG sequence was used. The sodium in the shift reagent buffers had T_1s of approximately 25 msec, with the T_2s varying between 10 and 25 msec, depending on the stock solution of

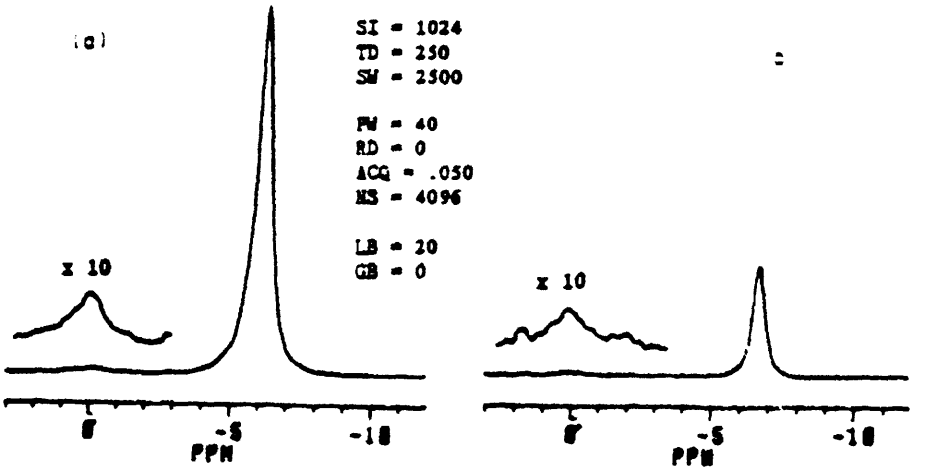

Figure 8-16 Sodium spectrum (a) before and (b) 2.5 hours after the initiation of perfusion with a lithium buffer. Presaturation, with P1=75 msec, was used.

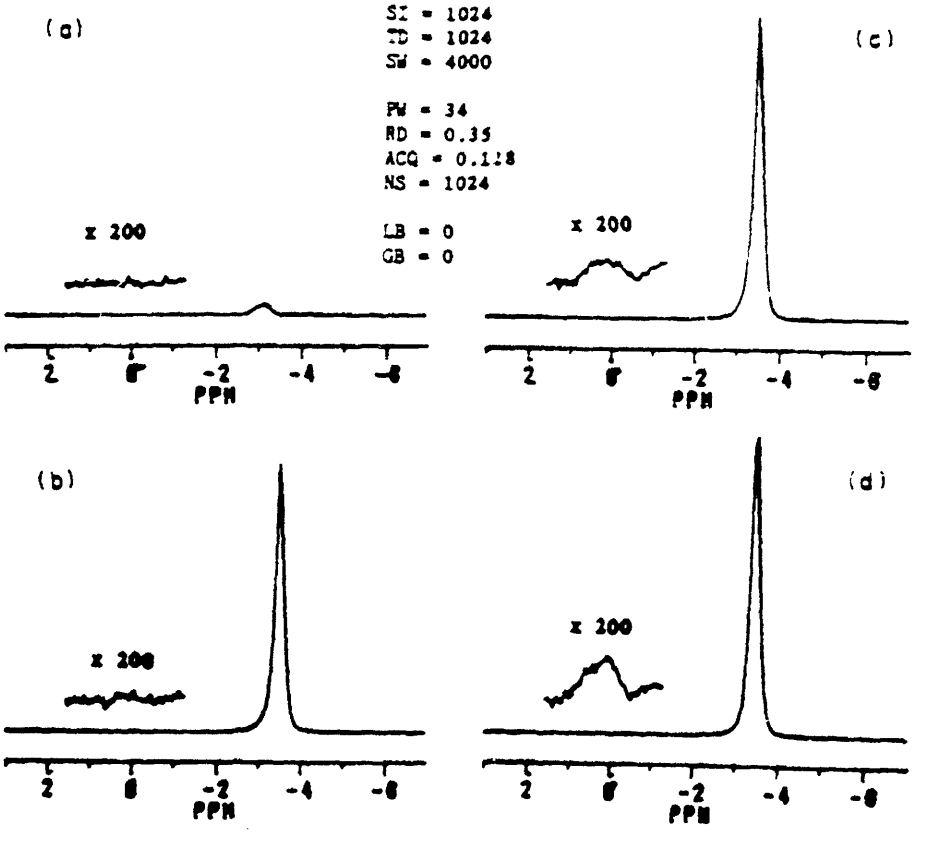

Figure 8-17 Lithium spectra obtained during the wash-in of a lithium perfusate. Each spectrum was acquired over a five minute interval, as follows: (a) 0-5 min., (b) 5-10 min., (c) 45-50 min., and (d) 135-140 min. after perfusion with the lithium buffer was initiated. 0 ppm is referenced to the resonant frequency of lithium in a lithium chloride solution. The large shifted peak is due to the lithium in the shift reagent buffer.

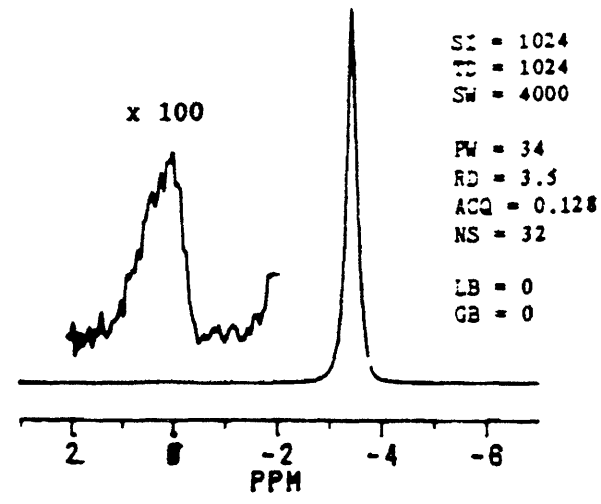

Figure 8-18 Lithium spectrum obtained with 32 scans and with a RD of 3.5 seconds.

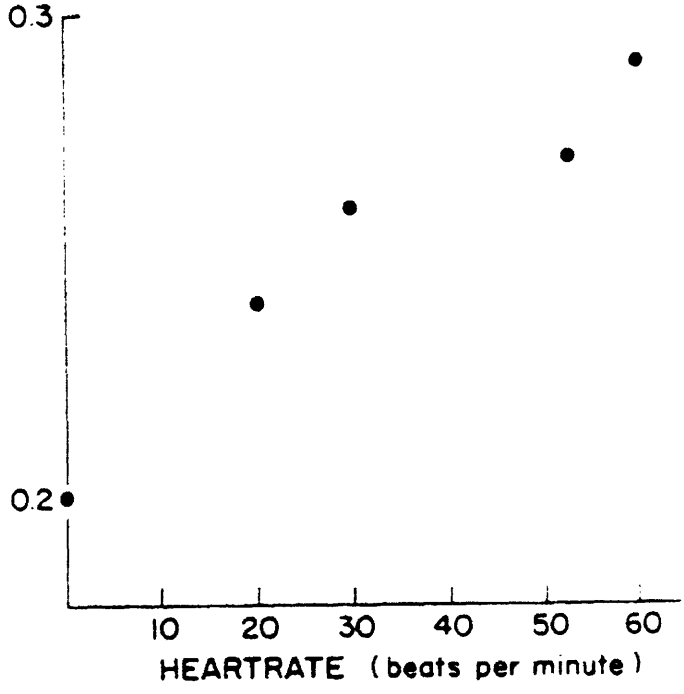

Figure 8-19 Intracellular sodium level, as determined by the area of the intracellular resonance (given in arbitrary units), as a function of pacing rate.

shift reagent. Again, the relaxation curves consisted of single exponential decays. A concentric tube setup with Ringer's and shift reagent buffer in the two tubes was used to measure the T_2 of sodium in Ringer's with presaturation of the shifted resonance; this had no significant effect on the result.

The relaxation times of the intracellular sodium were measured both under control conditions and after equilibration with ouabain, with approximately a five fold increase in the intracellular sodium level as determined by NMR. The T_1 relaxation of the intracellular resonance showed no observable deviation from that of a single exponential (Figure 8-20); the time constant was found to be 22.4 ± 3.0 msec for the control hearts and 24.2 ± 1.5 for the ouabain treated hearts.

In contrast, the T_2 relaxation curve of the intracellular sodium was found to be markedly nonexponential, as demonstrated by its striking nonlinearity on a semi-log plot of the magnetization versus time. This was true for both the control hearts and those with the high sodium content due to ouabain exposure (Figure 8-21). Examples of the spectra used to obtain these types of curves are shown in Figure 8-22. (The data shown is from a different heart than that of Figure 8-21). The relaxation behavior was unchanged with the increase in sodium content due to ouabain exposure. This is more easily seen when the first points of the two curves are normalized to the same value (Figure 8-23). The relaxation curves of the extracellular ions in the heart preparation were unchanged from those obtained from the solutions in tubes.

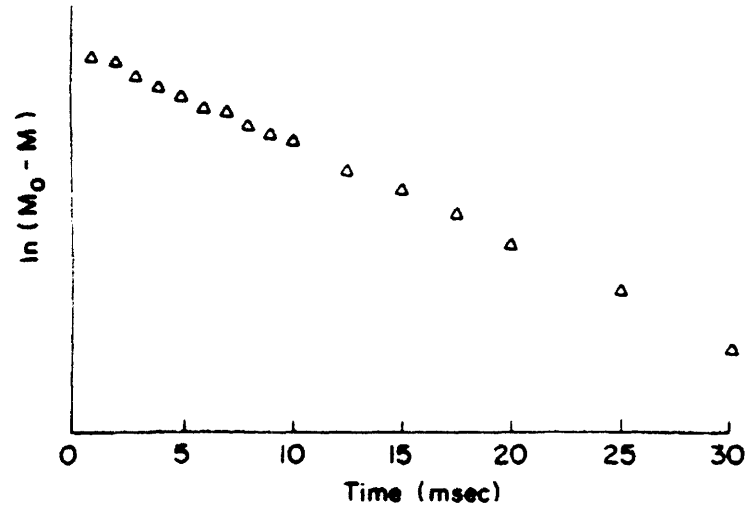

Figure 8-20 T_1 relaxation curve obtained from the intracellular sodium resonances.

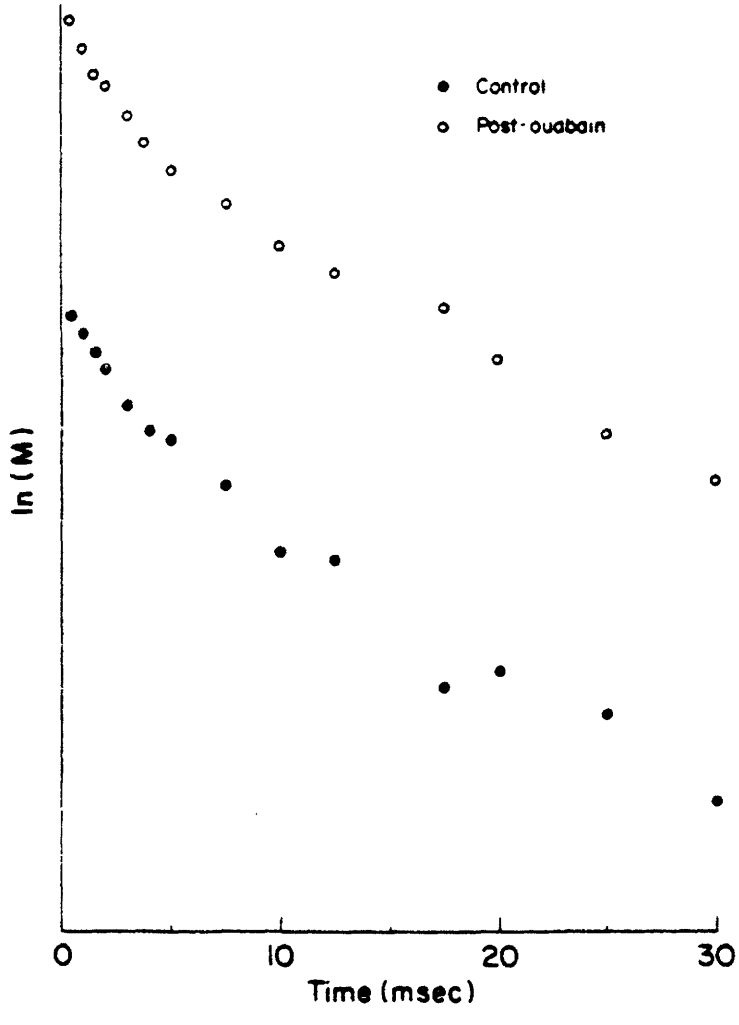

Figure 8-21 T_2 relaxation curve obtained from the intracellular sodium resonances under both control conditions and after a five fold increase in the intracellular sodium level due to ouabain exposure.

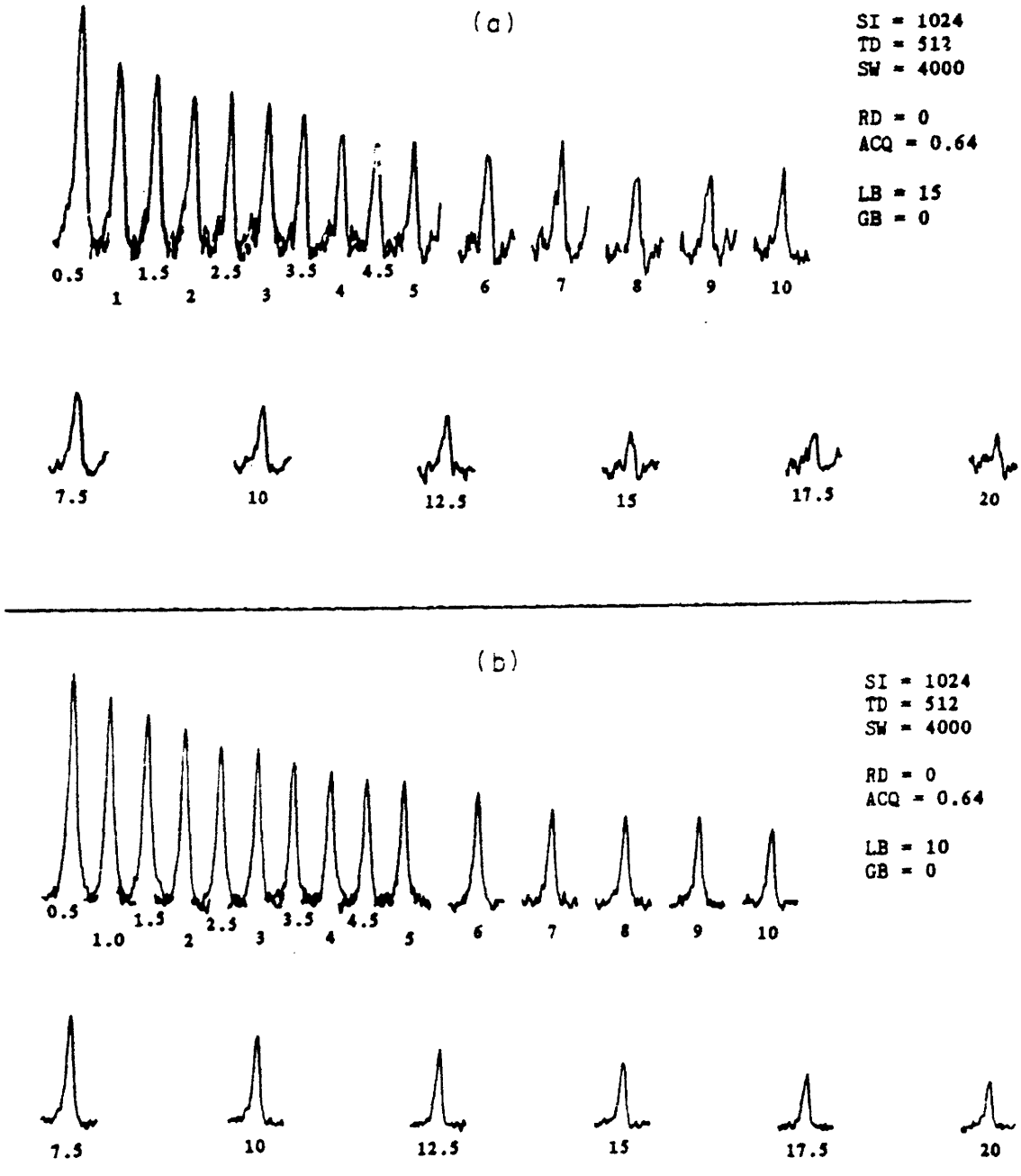

Figure 8-22 The intracellular resonances obtained with the Hahn echo pulse sequence. The numbers under the resonances correspond to the echo time, in msec. The 90 degree pulse was 39 μsec, the 180 degree pulse was 78 μsec, and a presaturation pulse of 100 msec was used before the 90 degree pulse. (a) Control; NS = 2048 for the top row and 4096 for the bottom row, which was acquired after the first was completed. (b) Ouabain; NS = 1024 (top) and 2048 (bottom).

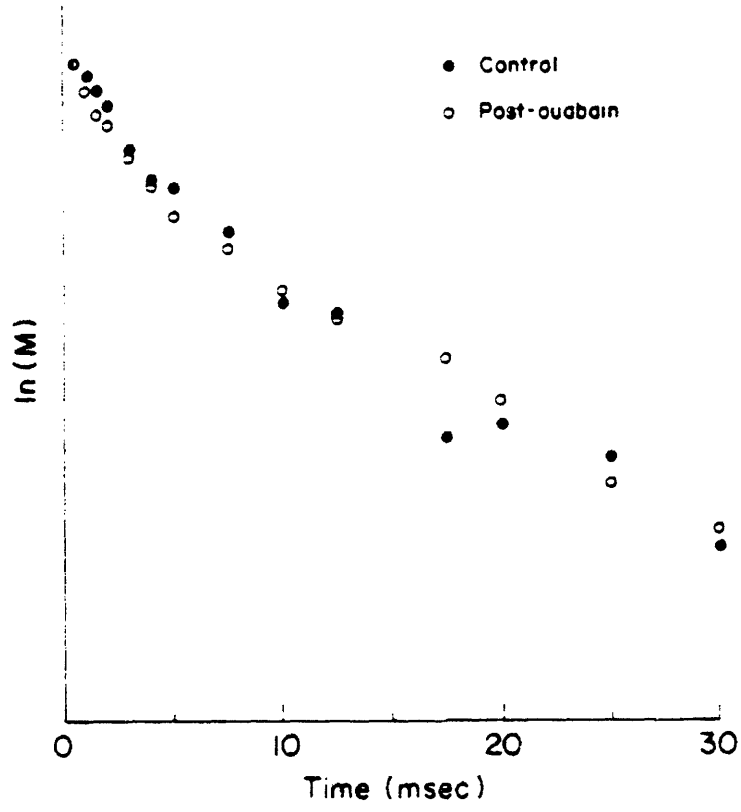

Figure 8-23 T_2 relaxation curve for the intracellular sodium under control conditions and after equilibration with ouabain, in which the intracellular sodium level has increased by a factor of five. The first points of both curves are normalized tc the same value.

There was no significant difference between the relaxation decay as determined by the Hahn echo technique and as determined by the CPMG pulse sequence, between the times of 5 and 30 msec (Figure 8-24). There was also no significant difference between the curves obtained with 3 mM versus 6 mM shift reagent perfusate (Figure 8-25).

In all, 8 hearts were utilized in the T_2 relaxation studies involving the comparison of the control versus the ouabain relaxation behavior. The details of the parameters of the biexponential fit of

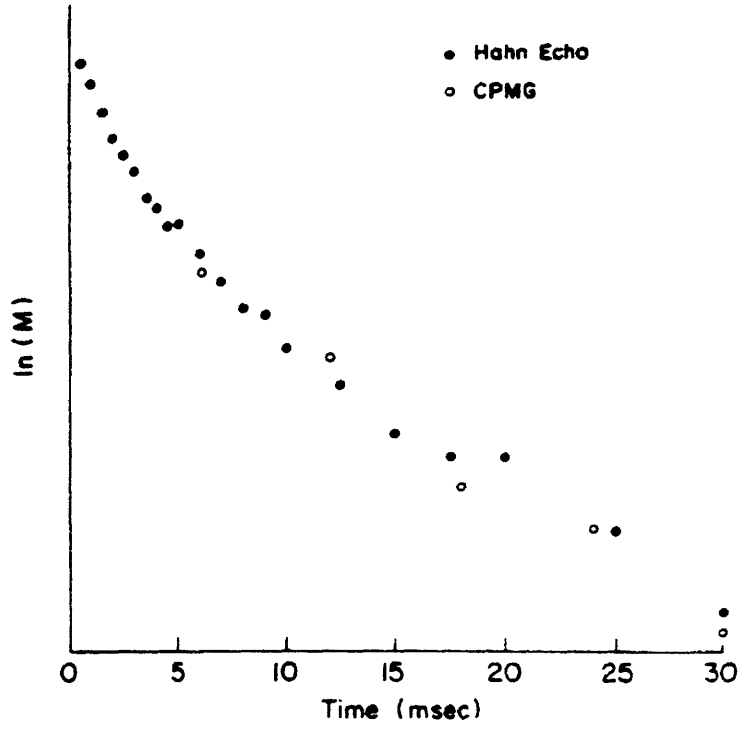

Figure 8-24 T_2 relaxation curve of the intracellular sodium obtained with the Hahn echo pulse sequence compared to that obtained with the CPMG pulse sequence. Only 5 points could be obtained in the CPMG sequence due to the power limitations on the transmitter.

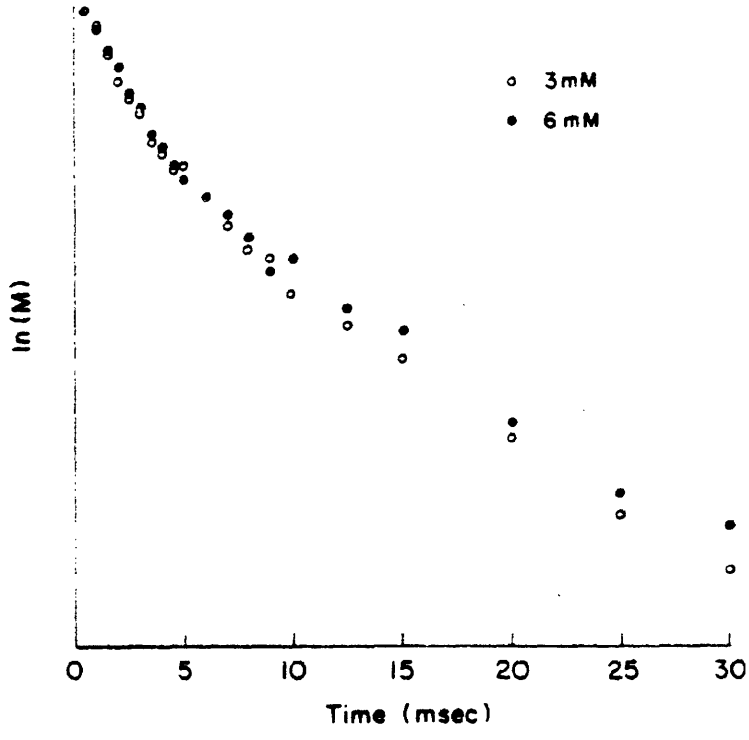

Figure 8-25 T_2 relaxation curve of the intracellular sodium obtained with a 3 mM $Dy(PPP)_2^{7-}$ perfusate and with a 6 mM $Dy(PPP)_2^{7-}$ perfusate.

the decay are given in the appendix. Neither a paired t-test, an unpaired t-test, nor Hotelling's T^2-test gave any significant difference between the two sets of parameters (control and ouabain). The means of the fitted parameters for the all of the hearts are given in Table 8.2.

	Control (n=5)	Ouabain (n=7)
A	0.46 ± 0.8	0.43 ± 0.05
α	2.0 ± 1.3	2.1 ± 0.6
B	0.54 ± 0.8	0.57 ± 0.05
β	16.3 ± 4.3	16.8 ± 4.0

Table 8.2 Parameters of fits to the equation $M = M_0 (Ae^{-t/\alpha} + Be^{-t/\beta})$. The experimental curves were each fit to this equation and the parameters were averaged to yield the above (mean ± S.D.). The time constants are given in msec.

As stated earlier, a double exponential fit implies three possible models for the system. The first model, that of a single homogeneous pool of nuclei with a double time constant due to quadrupolar interactions, implies that 60% of the signal should decay with the shorter time constant than the remaining 40%. This was not found to be the case for the intracellular sodium. Constraining the mathematical fit in one case such that 50% of the nuclei would have a relaxation time of less than 10 msec led to a fit with a much larger standard deviation, and with time constants of 4 and 24 msec with relative amplitudes of 0.60 and 0.40.

Using these values in equation 7.6 leads to $\omega_0^2\tau_c^2=5.69$ and $\tau_c=3.98$ nsec. Therefore we can calculate C to be 54.7×10^9, and $T_1'=55$ msec (80%) and $T_1''=15$ msec (20%). Assuming that the 2 would not be

differentiated experimentally due to the shorter T_1 containing only 20% of the energy, a weighted average would yield

$$\frac{1}{T_-} = \frac{0.8}{55} + \frac{0.2}{15} \qquad (8.1)$$

or T_1=36 msec. This is much longer than the measured T_1 of 24 msec. This further suggests that the data does not conform to that of a single pool of ions.

The second model is that of 2 separate pools of sodium in slow exchange, in which each pool consists of a single exponential decay. Therefore, one pool, with approximately 45% of the nuclei, can be associated with a T_2 of 2 msec, and one pool, with approximately 55% of the sodium, with a T_2 of 16 msec. If each pool was under conditions of extreme narrowing, then T_1=T_2 in each pool and we should have seen 45% of the T_1 decay with a T_1 of 2 msec. This was clearly not observed. If the T_2 of the 2 msec component actually consisted of 2 comonents, with time constants of approximately 2 and 4 msec, the correlation time would be 1.5 nsec and T_1'=6.7 msec, T_1''=2.8 msec, or a weighted average of 5 msec. Therefore, this data is not consistent wtih the possibility of there being a component of the sodium with a short time constant only, or with a biexponential T_2 in which both components are short. It should also be noted that the data obtained between 0.1 and 0.5 msec did not indicate that there was a very short component of T_2 in the system. For the five points, a single exponential of approximately 6 msec was fit, which must be considered to be a weighted average of the long and short time constants.

Any models which involve a higher number of time constants cannot be fit uniquely with this data. There are several possible models

which may be able to explain the data. For example, a pool which has a biexponential T_2 decay with time constants of 2 and 10 msec will have a correlation time of 3.5 nsec and T_1 components of 22 and 6 msec, or a T_1 of 14 msec. This, in slow exchange with a second pool with time constants of $T_1=T_2=20$ msec could yield a reasonable fit to this data.

Linewidth vs. T_2 Measurement:

The linewidth of the intracellular resonance was normally found to be between 80 and 120 hertz at half height. We can estimate the bulk inhomogeneity contribution to this value by comparing the linewidth of the extracellular resonance to its measured T_2 value. In a typical case, the shifted resonance had a T_2 measured to be 22 msec and a linewidth of 25 hertz. The linewidth due to the inherent T_2 should be $1/\pi T_2$, or 14 hertz, and therefore there was 11 hertz broadening due to magnetic field inhomogeneities for the extracellular sodium. The intracellular resonance in the same case had a linewidth of 105 hertz, and if we were to assume the same inhomogeneity broadening as the extracellular this leaves a linewidth of 94, or an expected T_2 of 3.4 msec. After a Hahn echo sequence with a τ value of 10 msec (an echo time of 20 msec), the linewidth obtained was 85 hertz, or a T_2 of 4.5 msec after accounting for the inhomogeneity. This contrasts with the measured T_2 curve of the intracellular sodium, which has a long component on the order of 16 msec. Therefore, there is some additional broadening of the intracellular sodium through a mechanism which can be compensated for through the use of spin echos.

Lithium Relaxation Times:

The T_1 relaxation time for lithium in lithium chloride was found to be 17 seconds. The T_1 for lithium in the shift reagent buffer was determined to be 100 msec, with a T_2 of 52 msec. The intracellular lithium, however, had a T_1 of 700 msec with a T_2 of 31 msec. The relaxation of all of the above appeared to consist of single exponentials.

Gated Experiments:

Sodium spectra, gated to the cardiac cycle, were obtained from 10 hearts. While all of the gated experiments showed a consistent increase in the intensity and linewidth of the intracellular sodium resonance in the interval immediately following the cardiac depolarization, the scatter in the data was large. Variations of almost the same amplitude were found in the experiments in which the stimulator was turned down such that the heart was no longer responding, however these showed no consistent variation across the intervals. The gated proton signal showed no significant variation in intensity or linewidth with gating. While most of the proton signal was due to the perfusate, and thus no conclusion can be drawn regarding the possible change in proton NMR with the action potential, the lack of change of the total proton signal demonstrated that the motion of the heart during contraction was not affecting the field homogeneity significantly.

9. DISCUSSION

The perfused frog heart proved to be a very stable preparation with which to study intracellular sodium, potassium, and lithium by NMR. While it was not possible to identify an intracellular resonance with the $Dy(TTHA)^{3-}$ shift reagent, the $Dy(PPP)_2^{7-}$ was very effective in separating the NMR signals arising from the intracellular and from the extracellular ions. For the sodium studies, presaturation was found to be the best method of suppressing the extracellular sodium resonance. The use of this technique enabled the quantitative analysis of the intracellular sodium, both in terms of monitoring intracellular sodium levels and evaluation of the NMR parameters, T_1 and T_2.

To summarize the results, the intracellular sodium was found to increase almost five-fold with the addition of 10μM ouabain to the perfusate, and approximately three-fold during perfusion with a zero potassium buffer. It decreased by approximately fifty percent with two thirds of the sodium in the perfusate being replaced by lithium, and an increase of almost fifty percent was found with a heart rate increase from zero to sixty beats per minute. The changes with the zero potassium buffer and the pacing rates were reversible.

The T_1 of the intracellular sodium was found to consist of a single time constant, of approximately 24 msec. The T_2 was better fit by a double exponential, with time constants of 2 and 16 msec with relative amplitudes of approximately 0.45 and 0.55, respectively. This relaxation behavior was not affected by a five-fold increase in the intracellular sodium level due to ouabain exposure, and is inconsistent with the model of a single pool of sodium ions within the

cell.

Shift Reagents:

The reason why an intracellular resonance was not identifiable with the $Dy(TTHA)^{3-}$ shift reagent is unclear. While another group was able to identify an intracellular resonance in a perfused rat heart with 10 mM $Dy(TTHA)^{3-}$ buffer, this resonance was shifted by 0.8 ppm relative to the sodium resonant frequency without shift reagent, in the same direction as the extracellular shifted resonance (Pike et. al., 1985). This was apparently a characteristic of the $Dy(TTHA)^{3-}$, and was not seen with other shift reagents (Pike et. al., 1984). Therefore it is possible that, in this study, a combined shift and broadening of the intracellular resonance with the 10 mM $Dy(TTHA)^{3-}$ buffer made it indistiguishable from the extracellular resonance. Furthermore, if the shift of the intracellular resonance was significant, presaturation of the extracellular resonance may have also presaturated the intracellular resonance.

$Dy(PPP)_2^{7-}$ was found to be a very efficient shift reagent for all of the ions observed in this study, producing usable shifts with very little concomitant broadening of the resonances. Perfusion with the 3 mM $Dy(PPP)_2^{7-}$ buffer reliably yielded intracellular resonances at the position of the unshifted resonance. The position of the intracellular sodium resonance in oocytes was also unaffected by the presence of the dysprosium tripolyphosphate shift reagent (Gupta et. al., 1985). In one study, the $Dy(PPP)_2^{7-}$ shifted the intracellular resonance of red blood cells downfield, opposite to the shift of the buffer, over time. This was attributed to the leak of Dy^{3+} into the cells (Boulanger et.

al., 1985). In another study, however, there was no change in the position of the intracellular resonance of red blood cells over 36 hours (Matwiyoff et. al., 1986). No change in the position of the intracellular resonance was noted over 24 hours in these studies.

Suppression of the Extracellular Resonance:

Excellent suppression of the extracellular resonance was achieved through the use of presaturation with two transmitters. In the future, hardware improvements may make it possible to simplify the presaturation by switching between high and low power on one transmitter in a sufficiently short time to prevent relaxation from occuring between the pulses. This would eliminate the need for the extra cables and the directional coupler, with their increased noise and attenuation factors. It may also be possible to decrease the presaturated shifted resonance even further by reducing the extracellular volume. In addition, the use of different cations in the shift reagent complex, such as choline tripolyphosphate (Gullans et. al., 1985) or potassium tripolyphosphate (Boulanger et. al., 1985), would enable the heart to be perfused as a closed, submerged, system in a non-sodium solution. The cation-tripolyphosphate could be used in the extracellular volume to shift any sodium which may wash out of the heart without introducing a large amount of sodium, and the extracardiac buffer could be exchanged rapidly to remove the small amount of sodium which leaks through the heart.

Intracellular Concentration Determinations:

The scatter in the calculated intracellular sodium and potassium

concentrations is probably due to a combination of the inaccuracy of determining the intracellular volume, the inaccuracy of determining the integral of the intracellular resonance, and the actual differences in the intracellular concentrations due to various physiologic conditions. When the volume is determined by means of subtracting the volume of the buffer in the perfused heart preparation from that of the NMR tube filled with buffer, the intracellular volume is determined as a small difference between two large numbers. Other methods of determining the intracellular volume, such as with the use of extracellular markers (Co-39, Shinar and Navon, 1984; Cl-35, Rayson and Gupta, 1985), encounter similar problems. When the intracellular volume is determined by the wet weight and the literature value for the cell water weight per wet weight, there are errors introduced by variable degrees of blotting of the hearts after the experiments. In addition, the possibility remains that a portion of the cells had been injured, and that we are actually observing the intracellular events from the cells that are healthy enough to exclude the shift reagent. In this case the volume as determined by the weight method would be an overestimate. The above, combined with the fact that the actual intracellular concentration has been shown to vary by up to 50 percent with a change in rate, means that from these studies it is not possible to determine the absolute fraction of sodium which is NMR visible.

On the other hand, the value obtained for the intracellular potassium concentration is only a factor of 2 higher than the value for the intracellular sodium concentration, as opposed to the expected factor of approximately 10. Therefore it appears that a significant fraction of the intracellular potassium is not detectable by NMR under

the conditions utilized in these studies. All of the errors associated with the volume calculation, as well as any which may be due to an inhomogeneous $\vec{B}_1$, would affect both the sodium and potassium concentration values. Thus the relative discrepancy between sodium and potassium in the amount of ions measured by NMR and that expected from classical studies stands, despite the large scatter.

The potassium results reported here also indicate that care must be taken before using the buffer signals as calibration standards, in that the addition of shift reagent resulted in a degree of potassium "invisibility". This precaution was taken in two previous studies, where the visibility of sodium in the shift reagent buffer was explicitly determined (Gullans et. al., 1985; Boulanger et. al., 1985). In this study, the NMR method of calibrating the volumes utilized the sodium spectra; the shift reagent perfusates did not exhibit any sodium invisibility by NMR.

Pharmacologic and Physiologic Experiments:

Experiments with ouabain, zero potassium, and lithium perfusion illustrate the ease with which the intracellular sodium level can be followed during pharmacologic and physiologic interventions. Since the technique is nondestructive, these interventions can be monitored reversibly as was demonstrated by the zero potassium and pacing studies.

The ouabain and zero potassium studies confirm the increase in intracellular sodium with these interventions. This has been previously demonstrated by NMR (Pike et. al., 1985), however quantification

of the increase was difficult due to the problems with identifying the intracellular resonance before the intervention.

It is difficult to interpret the results of the lithium studies in that there are two competing influences; that of lithium entering the cells in place of sodium and lithium preventing the efflux of sodium through inhibition of the sodium pump. This may explain the small and slow effect of the lithium perfusate on the intracellular sodium.

Several proposals have been suggested to explain a change in intracellular sodium with a change in pacing rate. Among them is the sodium lag hypothesis, which proposes that the sodium pump cannot immediately compensate for changes in rate. It has been suggested that a 10 mM change in intracellular sodium level is needed to stimulate a change in pumping rate (Langer, 1983). Hypoxia has also been suggested as a possible explanation (Cohen et. al., 1982). In addition, there has been shown to be a very small decrease in intracellular volume (2%) in Purkinje fibers stimulated at rate of 4 Hz. (Browning and Strauss, 1981).

Physiologic conclusions must be reached with the understanding that the ionic composition of the perfusates is slightly altered due to the shift reagent. Shift reagent is not expected to have a large effect on the cardiac electrophysiology, in that it is in a concentration of 3 mM versus an extracellular ionic concentration of approximately 150 mM. Through a fast exchange mechanism with the extracellular sodium, this low concentration of shift reagent results in a small, but usable, NMR frequency shift.

Possible effects of the shift reagent on the electrophysiology of the heart must still be considered. The shift reagent was shown to have no effect on the membrane conductance or potential of oocytes (Gupta et. al., 1985; Morrill et. al., 1985), and did not inhibit the sodium pump in cultured myocytes (Gupta and Wittenberg, 1983). The fact that, in these studies, the hearts were able to reduce their intracellular sodium content after being subjected to low potassium solutions or high pacing rates also demonstrates the viability of the sodium pump mechanism with the shift reagent perfusate.

The two effects of the introduction of the shift reagent to the perfusate, the decreased rate of spontaneous activity and the decreased contractility, were most likely due to the decrease in free calcium in the solution. This is supported by the observation that the heartrate and contractility would increase with the addition of excess calcium to the shift reagent buffer. This hypothesis is also supported by several previous studies. When the external calcium was totally removed from the solution of hearts from Rana Pipiens, the ventricles lost their ability to contract, with the excitability being sustained for two to three hours and a prolonged action potential of 2 to 3 seconds (Martin and Morad, 1982). In addition, in frog ventricular muscle the heart rate was shown to be dependent on the extracellular free calcium levels (Dresdner and Kline, 1985). It is possible to partially normalize the buffer by including a higher concentration of calcium, such that the free calcium concentration is closer to the normal value. Presaturation can then be used to separate the intracellular and extracellular resonances. In these studies, doubling the calcium which was added to the shift reagent perfusate resulted in a

decrease of 2.5 ppm in the sodium shift, for a total shift of approximately 4.5 ppm. This is still consistent with the use of presaturation, as was demonstrated with a concentric tube setup.

The splitting of the extracellular resonance with ouabain exposure, and in some cases with the zero potassium perfusion, may have been due to breakdown of the shift reagent due to a local release of enzymes. A decomposition of the $Dy(PPP)_2^{7-}$ shift reagent in the presence of nonperfused abdominal muscle from a rat was demonstrated by Matwiyoff et. al. (1986). Alternatively, the decrease in the shift may have been due to a local accumulation of calcium. It should be noted that, in the studies presented here, the position and lineshape of the intracellular resonance did not change appreciably throughout the experiments, and was not affected when the shifted resonance coalesced into a single shifted resonance at the original position. The shifted resonance and the level of intracellular sodium were very stable in the absence of interventions.

The possibility remains that membrane damage of some cells during the interventions resulted in the shift reagent entering some cells. This is not likely in the case of zero K^+ and the pacing studies, in that the sodium level returned to its original level after the intervention. If there was a breakdown in some of the membranes with the ouabain overdose such that shift reagent entered the cells, the increase in intracellular sodium must have been even greater than that indicated in the spectra.

Relaxation Times and Linewidths:

Both the T_1 and T_2 of Ringer's and the shift reagent buffers consisted of single exponential decays. The T_1 relaxation of the intracellular sodium consisted of a single exponential, both under control conditions and after ouabain exposure.

The T_2 decay curves of intracellular sodium are remarkable in their obvious deviations from a single exponential behavior. Several aspects of the acquisition protocol should be noted. The time averaging was such that if the intracellular sodium concentration changed over time, the effect would be averaged across the data points. A large change would be noticeable in that every other point would be higher than the alternate points. However, in some cases the end points were averaged separately, such that more scans could be acquired per point. If this was done, at least one point of the first set of data was repeated for comparison.

The fact that there was no significant change in the relaxation behavior with a five fold increase in the sodium level is surprising. One hypothesis which may explain these results is that the increased sodium had displaced intracellular potassium at various binding sites within the cell, and therefore the percentage of sodium which may have been bound remained constant. In fact it has been shown that, in frog ventricular strips under conditions of inhibition of the sodium pump, the increase in sodium due to ouabain was directly offset by the decrease in potassium (Flear et. al., 1975). The T_2 of the intracellular sodium was also found to be independent of the intracellular sodium concentration in red blood cells (Shinar and Navon, 1984). The

authors proposed that this may be due to a balancing of the sodium and potassium concentrations, such that the percentage of sodium ions bound remained constant despite the variations in absolute concentrations.

The T_2 relaxation data does not conform to the model of a single pool of nuclei experiencing quadrupolar effects, nor to the model of two separate pools of nuclei, each with a single relaxation time. While it may be possible that there is some systematic error in the system, none has been identified. The long range stability of the intracellular resonance was demonstrated several times, the shift reagent did not seem to be affecting the relaxation behavior in that doubling the concentration did not substantially affect the results, and the CPMG experiment demonstrated that diffusion was not an issue.

The results presented here also serve to caution against using linewidths as a means of measuring T_2 in cellular systems where there may be significant intracellular inhomogeneity broadening. A similar observation was made in a system of erythrocytes, in which T_2 was found to be less than T_1 and the linewidth was found to be greater than one would expect from the value of the measured T_2 (Pettegrew et. al., 1984). There have been several suggested explanations for the increased linewidth of the intracellular sodium resonances. One is that there is a difference in bulk susceptibility between the intra- and extracellular space, which leads to broadening of the signals (Fabry and San George, 1983; Pike et. al., 1984). Another is that there may be exchange between the intra- and extracellular compartments, with the site containing the lower population broadening more

rapidly than the site of high population (Riddell and Hayer, 1985). An alternate explanation has been that there is a leak of dysprosium into the cells (Boulanger et. al., 1985). However, in this last situation the resonances would be shifted as well as broadened.

Gated Experiments:

While the results of these studies are not conclusive, they are promising and warrant further investigation. We have seen that presaturation had no perceptible effect on the intracellular signal, either before or after the addition of a lethal dose of ouabain. This implies a lack of significant exchange between the intracellular and extracellular sodium on the time scale of T_1, or approximately 25 msec. It is important to keep in mind, however, that this represents an averaged result for the entire cardiac cycle, and the possibility remains that there is significant exchange during a small part of the cycle. To improve these studies and determine whether or not changes can be seen during some interval of the action potential, better S/N is needed and more intervals need to be measured within the action potential.

Other NMR Considerations:

The effect of the external presence of shift reagent on the NMR signals from the intracellular sodium should also be considered. This could take several forms. The most obvious is the possibility of shift reagent entering the cells and affecting the intracellular sodium directly. It is also possible for the shift reagent to affect the intracellular resonance by changing the bulk susceptibility of the solution, thus introducing field gradients and perhaps a change in the

intracellular field strength. The stability of the position of the intracellular resonance argues against both possibilities. However, as already mentioned, broadening due to susceptibility differences may have been a factor in the linewidth being larger than those which would be expected from the measured T_2.

It is also possible that the T_2 of the intracellular resonance is affected by the extracellular sodium in that the regime of exchange between the intracellular and extracellular sodium is altered with the addition of the shift reagent. This is because the resonant frequencies must also be taken into account when fast vs. slow exchange is being considered for T_2. Two pools which were in fast exchange and exchange narrowed may be in fast exchange but not exchange narrowed with the addition of the shift reagent. Comparison of characteristic time scales to show that this is unlikely in this case. The difference in the relaxation rates between the two resonances is several hundred Hz, which is also the separation of the two resonances. Therefore, it would not be possible to have fast exchange between the two resonances in the absence of shift reagent and slow exchange due to the frequency separation incurred by the use of shift reagent.

Finally, it is possible that second order quadrupolar effects are involved in the intracellular sodium NMR behavior (Werbelow, 1979; Werbelow and Marshall, 1981). However, these effects are subtle, and would tend to be undetectable with the S/N level in this preparation.

Future Directions:

Many opportunities exist for further cardiac studies with the

preparation described here. One obvious direction for further study would be to expand the range of pharmacologic agents to be investigated. It would also be interesting to combine the quantitative sodium studies with interleaved potassium measurements during a given intervention. The slow inherent rate of the frog heart and lack of spontaneous activity also make it a well suited preparation with which to pursue the gated NMR studies.

In addition, it may be possible to utilize a second shift reagent which will not penetrate into the myocardium, and thus may serve to separate the intraventricular and interstitial spaces. There have been several reports of local accumulations of potassium in the intercellular clefts (Kline and Morad, 1978; Martin and Morad, 1982; Kline and Cohen, 1984). These may be observed simultaneously with the intracellular potassium levels through the method just described, and equivalent sodium studies can be performed.

The intracellular sodium studies can also be extended to in-vivo preparations. While some of the shift reagents may be non-toxic, the results presented here, along with further studies, may make it possible to eliminate the need for the shift reagent for basic studies of intracellular sodium content. This is because a component of the intracellular sodium may be identifiable on the basis of its short T_2 relaxation time instead of on the basis of its resonant frequency. It should be noted that, while the intracellular sodium relaxation times were found to be insensitive to an electrophysiologic derangement, it remains to be shown whether or not this will hold for conditions in which edema may be significant.

Localized spectroscopic techniques, such as the use of surface coils or specialized pulse sequences (ISIS, for example; Ordidge et. al., 1986), would be used for the in-vivo studies. With these techniques, the NMR signals could be obtained from the myocardium alone, and therefore the ratio of intracellular to extracellular signals would be much larger than that obtained with the perfused heart preparation. It may therefore be possible to deconvolute the two signals more easily on the basis of their relaxation times (or linewidths). One method which has been utilized for such applications is that of the DISPA analysis (Roe and Marshall, 1978; Marshall and Roe, 1978, 1979; Marshall and Bruce, 1980).

In addition, the localized spectroscopy techniques may allow for the evaluation of local changes in the intracellular sodium content, such as those which may occur in the regions of infarcts (Kimura et. al., 1986; Cannon et. al., 1986). Another means of obtaining information regarding local variations of sodium is through the use of sodium NMR imaging, in which the NMR parameters of tissue in one region are contrasted to those of the surrounding tissue. The contrast within the image is therefore determined by these NMR parameters of sodium content, T_1, and T_2. While clinical sodium images have recently been obtained (Hilal et. al, 1985), the source of the contrast between regions of infarct and normal tissue has been difficult to identify. Consequently, another important application of the measurement of intracellular relaxation times is that of aiding in the interpretation of clinically obtained sodium images.

While the relaxation times may serve to distinguish between

intracellular and extracellular ions, the stability of the relaxation behavior with the ouabain exposure indicates that the relaxation times may not provide contrast between normal and electrically disturbed tissue. However, this may enable a more straightforward interpretation of the contrast due to a change in sodium content due to electrical alterations.

REFERENCES

Abragam, A., The Principles of Nuclear Magnetism, Oxford University Press, New York, 1961.

Antholine, W. E., Hyde, J. S., and Swartz, H. M., "Use of Dy^{3+} as a Free Radical Relaxing Agent in Biological Tissues", J. Magn. Reson. 29: 517-22, 1978.

Armstrong, W. McD., and Garcia-Diaz, J. F., "Ion-Selective Microelectrodes: Theory and Technique", Fed. Proc. 39: 2851-9, 1980.

Balschi, J. A., Crillo, V. P., and Springer, C. S. Jr., "Direct High Resolution Nuclear Magnetic Resonance Studies of Cation Transport in Vivo", Biophys. J. 38: 323-6, 1982.

Balschi, J. A., Jensen, D., Pike, M. M., Hoefeler, H., Cirillo, V. P., DeLayre, J., Springer, C. S. Jr., and Fossel, E. F., "Sodium Efflux from Sodium Rich Yeast. Simultaneous Observation with Sodium-23 and Phosphorus-31 NMR Spectroscopy in-Vivo", (abstr.) Magn. Resor. Med. 1: 96-97, 1984.

Becker, E. D., Ferretti, J. A., and Gambhir, P. N., "Selection of Optimum Parameters for Pulse Fourier Transform Nuclear Magnetic Resonance", Anal. Chem. 51: 1413-20, 1979.

Beeler, G. W., and McGuigan, J. A. S., "Voltage Clamping of Multicellular Myocardial Preparations: Capabilities and Limitations of Existing Methods", Prog. Biophys. Molec. Biol. 34: 219-54, 1978.

Berendsen, H. J. C., and Edzes, H. T., "The Observation and General Interpretation of Sodium Magnetic Resonance in Biological Material", Ann. N.Y. Acad. Sci. 204: 459-85, 1973.

Biology Data Book, 2nd Edition, Volume III, Fed. Amer. Soc. Exper. Biol., Bethesda, Maryland, pg. 1802, 1974.

Bleam, M. L., Anderson, C. F., and Record, M. T. Jr., "Relative Binding Affinities of Monovalent Cations for Double Stranded DNA", Proc. Natl. Acad. Sci. 77: 3085-9, 1980.

Bogusky, R. T., Garwood, M., Matson, G. B., Acosta, G., Cowgill, L. D., and Schleich, T., "Localization of Phosphorus Metabolites and Sodium Ions in the Rat Kidney", Magn. Reson. Med. 3: 251-61, 1986.

Boyett, M. R., and Jewell, B. R., "Analysis of the Effects of Changes in Rate and Rhythm Upon Electrical Activity in the Heart", Prog. Biophys. Molec. Biol. 36: 1-52, 1980.

Boulanger, Y., Vinay, P., and Desroches, M., "Measurement of a Large Range of Intracellular Sodium Concentrations in Erythrocytes by Na-23 Nuclear Magnetic Resonance", Biophys. J. 47: 553-61, 1985.

Brady, A. J., "Physiology of the Amphibian Heart", in Physiology of the Amphibia, J. A. Moore, ed., Academic Press, New York, 1964.

Braunlin, W. H., and Nordenskiold, L., "A Potassium-39 NMR Study of Potassium Binding to Double Helical DNA", Eur. J. Biochem. 142: 133-7, 1984.

Braunlin, W. H., Vogel, H. J., and Forsen, S., "Potassium-39 and Sodium-23 NMR Studies of Cation Binding to Phosvitin", Eur. J. Biochem. 142: 139-44, 1984.

Brophy, P. J., Hayer, M. K., and Riddell, F. G., "Measurement of Intracellular Potassium Ion Concentration by N.M.R.", Biochem. J. 210: 961-3, 1983.

Brown, M. A., Stenzel, T. T., Ribeiro, A. A., Drayer, B. P., and Spicer, L. D., "NMR Studies of Combined Lanthanide Shift and Relaxation Agents for Differential Characterization of Na-23 in a Two-Compartment Model System", Magn. Reson. Med. 3: 289-95, 1986.

Browning, D. J., and Strauss, H. C., "Effects of Stimulation Frequency on Potassium Activity and Cell Volume in Cardiac Tissue", Am. J. Physiol. 240: C39-55, 1981.

Bryant, R. G., "Potassium-39 Nuclear Magnetic Resonance", Biochim. Biophys. Res. Comm. 40: 1162-6, 1970.

Bull, T. E., "Nuclear Magnetic Relaxation of Spin-3/2 Nuclei Involved in Chemical Exchange", J. Magn. Reson. 8: 344-53, 1972.

Bull, T E., Andrasko, J., Chiancone, E., and Forsen, S., "Pulsed Nuclear Magnetic Resonance Studies on Na-23, Li-7, and Cl-35 Binding to Human Oxy- and Carbon Monoxyhaemoglobin", J. Mol. Biol. 73: 251-9, 1973.

Burton, D. R., Forsen, S., and Reimarsson, P., "The Interaction of Polyamines with DNA: a Na-23 NMR Study", Nucleic Acids Res. 9: 1219-28, 1981.

Cannon, P. J., Maudsley, A. A., Hilal, S. K., Simon, H. E., and Cassidy, F., "Sodium Nuclear Magnetic Resonance Imaging of Myocardial Tissue of Dogs After Coronary Artery Occlusion and Reperfusion", J. Amer. Coll. Cardiol. 7: 573-9, 1986.

Carmeliet, E. E., "Influence of Lithium Ions on the Transmembrane Potential and Cation Content of Cardiac Cells", J. Gen. Physiol. 47: 501-30, 1964.

Carr, H. Y., and Purcell, E. M., "Effects of Diffusion on Free Precession in Nuclear Magnetic Resonance Experiments", Phys. Rev. 94: 630-8, 1954.

Chang, D. C., and Woessner, D. E., "Spin Echo Study of Na-23 Relaxation in Skeletal Muscle. Evidence of Sodium Ion Binding Inside a Biological Cell", J. Magn. Reson. 30: 185-91, 1978.

Chapman, R. A., Coray, A., and McGuigan, J. A. S., "Sodium/Calcium Exchange in Mammalian Ventricular Muscle: A Study with Sodium Sensitive Micro-Electrodes", J. Physiol. 343: 253-76, 1983.

Chu, S. C., Pike, M. M., Fossel, E. T., Smith T. W., Balschi, J. A., and Springer, C. S. Jr., "Aqueous Shift Reagents for High Resolution Cationic Nuclear Magnetic Resonance III. $Dy(TTHA)^{3-}$, $Tm(TTHA)^{3-}$, and $Tm(PPP)_2^{7-}$", J. Magn. Reson. 56: 33-47, 1984.

Civan, M. M., McDonald, G. G., Pring, M., and Shporer, M., "Pulsed Nuclear Magnetic Resonance Study of K-39 in Frog Striated Muscle", Biophys. J. 16: 1385-98, 1976.

Cohen, C. J., Fozzard, H. A., and Sheu, S. S., "Increase in Intracellular Sodium Ion Activity During Stimulation in Mammalian Cardiac Muscle", Circ. Res. 50: 651-62, 1982.

Cohen, I., and Kline, R., "K^+ Fluctuations in the Extracellular Spaces of Cardiac Muscle. Evidence from the Voltage Clamp and Extracellular K^+ Selective Microelectrodes", Circ. Res. 50: 1-16, 1982.

Cope, F. W., "Nuclear Magnetic Resonance Evidence for Complexing of Sodium Ions in Muscle", Proc. Natl. Acad. Sci., 54: 225-7, 1965.

Cope, F. W., "NMR Evidence for Complexing of Na+ in Muscle, Kidney, and Brain, and by Actomyosin. The Relation of Cellular Complexing of Na+ to Water Structure and to Transport Kinetics", J. Gen. Physiol. 50: 1353-75, 1967.

Cope, F. W., "Complexing of Sodium Ions in Myelinated Nerve by Nuclear Magnetic Resonance", Physiol. Chem. Phys. 2: 545-50, 1970.

Cope, F. W., and Damadian, R., "Cell Potassium by K-39 Spin Echo Nuclear Magnetic Resonance", Nature 228: 76-7, 1970.

Cope, F. W., and Damadian, R., "Biological Ion Exchange Resins: IV. Evidence for Potassium Association with Fixed Charges in Muscle and Brain by Pulsed Nuclear Magnetic Resonance of K-39", Physiol. Chem. Phys. 6: 17-30, 1974.

Cornelis, A, and Laszlo, P., "Sodium Binding Sites of Gramicidin A: Sodium-23 Nuclear Magnetic Resonance Study", Biochem. 18: 2004-7, 1979.

Cowan, B. E., Sze, D. Y., Mai, M. T., and Jardetzky, O., "Measurement of the Sodium Membrane Potential by NMR", FEBS Lett. 184: 130-3, 1985.

Czeisler, J. L., Fritz, O. G. Jr., and Swift, T. J., "Direct Evidence from Nuclear Magnetic Resonance Studies for Bound Sodium in Frog Skeletal Muscle", Biophys. J., 10: 260-8, 1970.

Czeisler, J. L., and Swift, T. J., "A Comparative Study of Sodium Ion in Muscle Tissue and Ion Exchange Resins Through the Application of Nuclear Magnetic Resonance", Ann. N. Y. Acad. Sci. 204: 261-73, 1973.

Damadian, R., and Cope, F. W., "NMR in Cancer V. Electronic Diagnosis of Cancer by Potassium (K-39) Nuclear Magnetic Resonance: Spin Signatures and T_1 Beat Patterns", Physiol. Chem. Phys. 6: 309-322, 1974.

Dedrick, D., and Allen, P. D., "NMR Studies of Myocardial High Energy Phosphates and Sodium as Mediators of Negative Inotropic Effects of Volatile Anesthetics", Anesthesiology 59: A23, 1983.

Degani, H., and Elgavish, G. A., "Ionic Permeabilities of Membranes. Na-23 and Li-7 NMR Studies of Ion Transport Across the Memrane of Phosphatidylcholine Vesicles", FEBS Lett. 90: 357-60, 1978.

DeLayre, J. L., Ingwall, J. S., Malloy, C., and Fossel, E. T., "Gated Na-23 NMR Images of an Isolated Perfused Working Rat Heart", Science 212: 935-6, 1981.

Delville, A., Detellier, C., and Laszlo, P., "Determination of the Correlation Time for a Slowly Reorienting Spin-3/2 Nucleus: Binding of Na^+ with the 5' GMP Supramolecular Assembly", J. Magn. Reson. 34: 301-15, 1979.

Delville, A., Detellier, C., Gerstmans, A., and Laszlo, P., "The Theoretical Interpretation of Sodium-23 NMR Chemical Shifts and Quadrupolar Coupling Constants, as Supported by New Experimental Evidence", J. Magn. Reson. 42: 14-27, 1981.

DiFrancesco, D., and Noble, D., "A Model of Cardiac Electrical Activity Incorporating Ionic Pumps and Concentration Changes", Phil. Trans. R. Soc. Lond. B307: 353-98, 1985.

Dresdner, K. P., and Kline, R. P., "Extracellular Calcium Ion Depletion in Frog Cardiac Ventricular Muscle", Biophys. J. 48: 33-45, 1985.

Edzes, H. T., Rupprecht, A., and Berendsen, H. J. C., "Observation of Quadrupolar NMR Signals of Li-7 and Na-23 in Hydrated Oriented DNA", Biochem. Biophy. Res. Comm. 46: 790-4, 1972.

Elgavish, G. A., and Elgavish A., "Evidence from Na-23 NMR Studies for the Existence of Sodium Channels in the Brush Border Membrane of the Renal Proximal Tubule", Biochem. Biophys. Res. Commun. 128: 746-53, 1985.

Engstrom, S., Jonsson, B., and Jonsson, B., "A Molecular Approach to Quadrupole Relaxation. Monte Carlo Simulations of Dilute Li^+, Na^+, and Cl^- Aqueous Solutions", J. Magn. Reson. 50: 1-20, 1982.

Fabry, M. E., and San George, R. C., "Effect of Magnetic Susceptibility on Nuclear Magnetic Resonance Signals Arising from Red Cells: A Warning", Biochem. 22: 4119-25, 1983.

Feeney, J., Batchelor, J. G., Albrand, J. P., and Roberts, G. C. K., "The Effects of Intermediate Exchange Processes on the Estimation of Equilibrium Constants by NMR", J. Magn. Reson. 33: 519-29, 1979.

Feinberg, D. A., Crooks, L. A., Kaufman, L., Brant-Zawadzki, M., Posin, J. P., Arakawa, M., Watts, J. C., and Hoenninger, J., "Magnetic Resonance Imaging Performance: A Comparison of Sodium and Hydrogen", Radiol. 156: 133-8, 1985.

Flear, C. T. G., Greener, J. S., and Bhaltacharya, S. S., "Effects of Ouabain on Sodium Uptake by Frog Heart and Skeletal Muscle", in Recent Advances in Studies on Cardiac Structure and Metabolism, Volume 5, Basic Functions of Cations in Myocardial Activity, ed. by A. Fleckenstein and N. S. Dhalla, University Park Press, Baltimore, 1975.

Forsen, S., and Lindman, B., "Ion Binding in Biological Systems as Studied by NMR Spectroscopy", in Methods of Biochemical Analysis, ed. by D. Glick,John Wiley and Sons, New York, Vol. 27, 1981.

Fossarello, M., Orzalesi, N., Corongiu, F. P., Biagini, S., Casu, M., and Lai, A., "Na-23 NMR Investigation of Human Lenses from Patients with Cataracts", FEBS Lett. 184: 245-8, 1985.

Fossel, E.T., "Observation of Intracellular Ca-43 and Mg-25 in Isolated Perfused Rat Hearts at 8.45 T", (abstr.) Magn. Reson. Med. 1: 291-2, 1984.

Fossel, E. T., and Hoefeler, H., "Observation of Intracellular Potassium and Sodium in the Heart by NMR: A Major Fraction of Potassium is 'Invisible'", Magn. Reson. Med., in press.

Fossel, E. T., Sarasua, M. M., and Koehler, K. A., "A Li-7 NMR Investigation of the Lithium Ion Interaction with Phosphatidylcholine-Phosphatidylglycerol Membranes. Observation of Calcium and Magnesium Ion Competition", J. Magn. Reson. 64: 536-40, 1985.

Fozzard, H. A., January, C. T., and Makielski, J. C., "New Studies of the Excitatory Sodium Currents in Heart Muscle", Circ. Res. 56: 475-85, 1985.

Goldberg, M., and Gilboa, H., "Sodium Magnetic Resonance in Biological Systems. Interpretation of the Relaxation Curves", in Nuclear Magnetic Resonance Spectroscopy in Molecular Biology, ed. by B. Pullman, D. Reidel Publ. Co., Holland, pgs. 481-491, 1978a.

Goldberg, M., and Gilboa, H., "Sodium Exchange Between Two Sites. The Binding of Sodium to Halotolerant Bacteria", Biochim. Biophys. Acta. 538: 268-83, 1978b.

Goldsmith, M., and Damadian, R., "NMR in Cancer: VII. Sodium Magnetic Resonance of Normal and Cancerous Tissues", Physiol. Chem. Phys. 7: 263-9, 1975.

Grandjean, J., and Laszlo, P., "Sodium Complexation by the Calcium Binding Site of Parvalbumin", FEBS Lett. 81: 376-9, 1977.

Grisham, C. M., and Hutton, W. C., "Lithium-7 NMR as a Probe of Monovalent Cation Sites at the Active Site of Na-K-ATPase from Kidney", Biochem. Biophys. Res. Comm. 81: 1406-11, 1978.

Gullans, S. R., Avison, M. J., Ogino, T., Giebisch, G., and Shulman, R. G., "NMR Measurements of Intracellular Sodium in the Rabbit Proximal Tubule", Am. J. Physiol. 249: F160-8, 1985.

Gupta, R. K., and Gupta, P., "Direct Observations of Resolved Resonances From Intra- and Extracellular Sodium-23 Ions in NMR Studies of Intact Cells and Tissues using Dysprosium(III)Tripolyphosphate as Paramagnetic Shift Reagent", J. Magn. Reson., 47: 344-50, 1982.

Gupta, R. K., Gupta, P., and Moore, R. D., "NMR Studies of Intracellular Metal Ions in Intact Cells and Tissues", Ann. Rev. Biophys. Bioeng. 13: 221-46, 1984.

Gupta, R. K., Kostellow, A. B., and Morrill, G. A., "NMR Studies of Intracellular Na-23 in Amphibian Oocytes, Ovulated Eggs, and Early Embryos", Biophys. J. 41: 128a, 1983.

Gupta, R. K., Kostellow, A. B., and Morrill, G. A., "NMR Studies of Intracellular Sodium Ions in Amphibian Oocytes, Ovulated Eggs, and Early Embryos", J. Biol. Chem. 260: 9203-8, 1985.

Gupta, R. K., and Wittenberg, B. A., "Observation of Effect of Extracellular Na^+ Ions in Isolated Cardiac Myocytes", Federation Proceedings, 42: 2065, 1983.

Hahn, E. L., "Spin Echos", Phys. Rev. 80: 580-94, 1950.

Hilal, S. K., Maudsley, A. A., Bonn, J., Simon, H. E., Cannon, P., and Perman, W. H., "NMR Imaging of Tissue Sodium, in Vivo and in Resected Organs", (abstr.) Magn. Reson. Med. 1: 165-6, 1984.

Hilal, S. K., Maudsley, A. A., Ra, J. B., Simon, H. E., Roschmann, P., Wittekoek, S., Cho, Z. H., and Mun, S. K., "In Vivo NMR Imaging of Sodium-23 in the Human Head", J. Comput. Assisted Tomography, 9: 1-7, 1985.

Hilal, S. K., Maudsley, A. A., Simon, H. E., Perman, W. H., Bonn, J., Mawad, M. E., Silver, A. J., Ganti, S. R., Sane, P., and Chien, I. C., "In vivo NMR Imaging of Tissue Sodium in the Intact Cat Before and After Acute Cerebral Stroke", AJNR 4: 245-9, 1983.

Hoffman, B. F., and Cranefield, P. F., Electrophysiology of the Heart, McGraw Hill Book Co., Inc., New York, 1960.

Hubbard, P. S., "Nonexponential Nuclear Magnetic Relaxation by Quadrupole Interactions" J. Chem. Phys. 53: 985-7, 1970.

James, T. L., and Noggle, J. H., "Na-23 Nuclear Magnetic Resonance Relaxation Studies of Sodium Ion Interaction with Soluble RNA", Proc. Natl. Acad. Sci. 62: 644-49, 1969.

Jardetzky, O., and Wertz, J. E., "Detection of Sodium Complexes by Nuclear Spin Resonance", Am. J. Physiol. 187: 608, 1956.

Kaplan, J. H., "Ion Movements Through the Sodium Pump", Ann. Rev. Physiol. 47: 535-44, 1985.

Keenan, M. J., and Niedergerke, R., "Intracellular Sodium Concentration and Resting Sodium Fluxes of the Frog Heart Ventricle", J. Physiol. 188: 235-60, 1967.

Keynes, R. D., and Swan, R. C., "The Permeability of Frog Muscle Fibers to Lithium Ions", J. Physiol. 147: 626-38, 1959.

Kielman, H. S., and Leyte, J. C., "Nuclear Magnetic Resonance of Sodium-23 in Polyphosphate Solutions", J. Phys. Chem. 77: 1593-4, 1973.

Kimura, S., Bassett, A. L., Gaide, M. S., Kozlovskis, P. L., and Myerburg, R. J., "Regional Changes in Intracellular Potassium and Sodium Activity after Healing of Experimental Myocardial Infarction in Cats", Circ. Res. 58: 202-8, 1986.

Kissel, T. R., Sandifer, J. R., and Zumbulyadis, N., "Sodium Ion Binding in Human Serum", Clin. Chem. 28: 449-52, 1982.

Kline, R. P., and Cohen, I. S., "Extracellular [K^+] Fluctuations in Voltage-Clamped Canine Cardiac Purkinje Fibers", Biophys. J., 46: 663-8, 1984.

Kline, R. P., and Kuppersmith, J., "Effects of Extracellular Potassium Accumulation and Sodium Pump Activation on Automatic Canine Purkinje Fibres", J. Physiol. 324: 507-33, 1982.

Kline, R. P., and Morad, M., "Potassium Efflux in Heart Muscle During Activity. Extracellular Accumulation and its Implications", J. Physiol. 280: 537-58, 1978.

Klitzner, T., and Morad, M., "Excitation-Contraction Coupling in Frog Ventricle. Possible Ca^{2+} Transport Mechanisms", Pflugers Arch. 398: 274-83, 1983.

Langer, G. A., "The 'Sodium Pump Lag' Revisited", J. Mol. Cell. Cardiol. 15: 647-51, 1983.

Langer, G. A., "Sodium-Calcium Exchange in the Heart", Ann. Rev. Physiol. 44: 435-49 1982.

Laszlo, P., "Quadrupolar Metallic Nuclei: Na-23 NMR Studies of Cation Binding by Natural and Synthetic Ionophores", in NMR Spectroscopy: New Methods and Applicatons, G. C. Levy, ed., Amer. Chem. Soc., 1982.

Lee, C. O., "Ionic Activities in Cardiac Muscle Cells and Application of Ion-Selective Microelectrodes", Am. J. Physiol. 241: H459-78, 1981.

Leigh, J. S. Jr., "Relaxation Times in Systems with Chemical Exchange: Some Exact Solutions", J. Magn. Reson. 4: 308-11, 1971.

Lindblom, G., and Lindman, B., "Ion Binding in Liquid Crystals Studied by NMR. V. Static Quadrupolar Effects for Alkali Nuclei", Molec. Crystals Liquid Crystals 22: 45-65, 1973.

Lindman, B., "Applications of Quadrupolar Effects in NMR for Studies of Ion Binding in Biological and Model Systems", J. Magn. Reson. 32: 39-47, 1978.

Magnuson, J. A., and Magnuson, N. S., "NMR Studies of Sodium and Potassium in Various Biological Tissues", Ann. N. Y. Acad. Sci. 204: 297-309, 1973.

Magnuson, J. A., Shelton, D. S., and Magnuson, N. S., "A Nuclear Magnetic Resonance Study of Sodium Ion Interaction with Erythrocyte Membranes", Biochem. Biophys. Res. Comm. 39: 279-83, 1970.

Magnuson, N. S., and Magnuson, J. A., "$Na\text{-}23^{+}$ Interaction with Bacterial Surfaces: a Comment on Nuclear Magnetic Resonance Invisible Signals", Biophys. J., 13: 1117-9, 1973.

Malloy, C. R., Smith, T. W., DeLayre, J. L., and Fossel, E. T., "Observation of Intracellular Sodium in a Langendorff Perfused Rat Heart by Na-23 NMR", Proc., 22nd Exper. NMR Confer., 1981.

Marshall, A. G., "Calculation of NMR Relaxation Times for Quadrupolar Nuclei in the Presence of Chemical Exchange", J. Chem. Phys. 52: 2527-34, 1970.

Marshall, A. G., and Bruce, R. E., "Dispersion versus Absorption (DISPA) Lineshape Analysis. Effects os Saturation, Adjacent Peaks, and Simultaneous Distribution in Peak Width and Position", J. Magn. Reson. 39: 47-54, 1980.

Marshall, A. G., and Roe, D. C., "Dispersion versus Absorption: Spectral Line Shape Analysis for Radiofrequency and Microwave Spectrometry", Anal. Chem. 50: 756-63, 1978.

Marshall, A. G., and Roe, D. C., "Dispersion versus Absorption (DISPA): Effects of Digitization, Noise, Truncation of Free Induction Decay, and Zero Filling", J. Magn. Reson. 33: 551-7, 1979.

Martin, G., and Morad, M., "Activity-Induced Potassium Accumulation and its Uptake in Frog Ventricular Muscle", J. Physiol. 328: 205-27, 1982.

Martinez, D., Silvidi, A. A., and Stokes, R. M., "Nuclear Magnetic Resonance Studies of Sodium Ions in Isolated Frog Muscle and Liver", Biophys. J. 9: 1256-60, 1969.

Martino, A. F., and Damadian, R., "Na-23 NMR Maps of Head Sized Phantoms and a Low Resolution Na-23 Map of the Live Human Head", Physiol. Chem. Phys. Med. 15: 481-7, 1983.

Matwiyoff, N. A., Gasparovic, C., Wenk, R., Wicks, J. D., and Rath, A. "P-31 and Na-23 NMR Studies of the Structure and Lability of the Sodium Shift Reagent, Bis(tripolyphosphate)dysprosium(III) ([Dy(P3O10)]7-) Ion, and its Decomposition in the Presence of Rat Muscle", Magn. Reson. Med. 3: 164-68, 1986.

Maudsley, A. A., and Hilal, S. K., "Biological Aspects of Sodium-23 Imaging", Br. J. Med. 40: 165-6, 1984.

McLaughlin, A. C., and Leigh, J. S. Jr., "Relaxation Times in Systems with Chemical Exchange: Approximate Solutions for the Nondilute Case", J. Magn. Reson. 9: 296-304, 1973.

Meiboom, S., and Gill, D., "Modified Spin Echo Method for Measuring Nuclear Relaxation Times", Rev. Sci. Instrum. 29: 688-91, 1958.

Monoi, H., "Nuclear Magnetic Resonance of Tissue Na-23: I.Na-23 Signal and Na^+ Activity in Homogenate", Biophys. J., 14: 645-51, 1974a.

Monoi, H., "Nuclear Magnetic Resonance of Tissue Na-23: II. Theoretical Line Shape", Biophys. J., 14: 653-9, 1974b.

Monoi, H., "Effects of Alkali Cations in the Nuclear Magnetic Resonance Intensity of Na-23 in Rat Liver Homogenate", Biophys. J., 16: 1349-55, 1976a.

Monoi, H., "Nuclear Magnetic Resonance of Tissue Na-23 Correlation Time", Biochim. et Biophys. Acta 451: 604-9, 1976b.

Monoi, H., and Katsukura, Y., "Nuclear Magnetic Resonance of Na-23 in Suspensions of Pig Erythrocyte Ghosts: A Comment on the Interpretation of Tissue Na-23 Signals", Biophys. J. 16: 979-81, 1976.

Monoi, H., and Uedaira, H., "Na Interacting with Gramicidin D Nuclear Magnetic Resonance Study", Biophys. J. 25: 535-40, 1979.

Monoi, H., and Uedaira, H., "Magnetic Relaxation of Na-23 in Heterogeneous Systems", J. Magn. Res. 38: 119-29, 1980.

Morad, M., and Goldman, Y., "Excitation-Contraction Coupling in Heart Muscle: Membrane Control of Development of Tension", in Prog. Biophys. Molec. Biol., ed. by J.A.V. Butler and D. Noble, Pergamon Press, Oxford, 1973.

Morrill, G. A., Weinstein, S. P., Kostellow, A. B., and Gupta, R. K., "Studies of Insulin Action on the Amphibian Oocyte Plasma Membrane Using NMR, Electrophysiological and Ion Flux Techniques", Biochim. Biophys. Acta. 844: 377-92, 1985.

Moseley, M. E., Chew, W. M., Nishimura, M. C., Richards, T. L., Murphy-Boesch, J., Young, G. B., Marschner, T. M., Pitts, L. H., and James, T. L., "In-Vivo Sodium-23 Magnetic Resonance Surface Coil Imaging: Observing Experimental Cerebral Ischemia in the Rat", Magn. Reson. Imaging 3: 383-7, 1985.

Mullins, L. J., "The Generation of Electric Currents in Cardiac Fibers by Na/Ca Exchange", Am. J. Physiol. 236: C103-10, 1979.

Mullins, L. J., Ion Transport in Heart, Raven Press, New York, 1981.

Neurohr, K. J., Drakenberg, T., Forsen, S., and Lilja, H., "Potassium-39 Nuclear Magnetic Resonance of Potassium Ionophore Complexes: Chemical Shifts, Relaxation Times, and Quadrupole Coupling Constants", J. Magn. Reson. 51: 460-9, 1983.

Noble, D., "The Surprising Heart: A Review of Recent Progress in Cardiac Electrophysiology", J. Physiol. 353: 1-50, 1984.

Nordenskiold, L., Chang, D. K., Anderson, C. F., and Record, M. T. Jr., "Na-23 NMR Relaxation Study of the Effects of Conformation and Base Composition on the Interactions of Counterions with Double Helical DNA", Biochem. 23: 4309-17, 1984.

Ogino, T., Den Hollander, A., Castle, A. M., MacNab, M., Milanick, M., Hoffman, J. F., and Schulman, R. G., "K-39, Na-23, and P-31 NMR Studies of Ion Transport in Microorganisms and in Mammalian Cells", (abstr.) Magn. Reson. Med. 1: 219-20, 1984.

Ogino, T., Den Hollander, J. A., and Shulman, R. G., "K-39, Na-23, and P-31 NMR Studies of Ion Transport in Saccharomyces Cerevisiae", Proc. Natl. Acad. Sci., 80: 5185-9, 1983.

Ogino, T., Shulman, G. I., Avison, M. J., Gullans, S. R., Den Hollander, J. A., and Shulman, R. G., "Na-23 and K-39 NMR Studies of Ion Transport in Human Erythrocytes", Proc. Natl. Acad. Sci. 82: 1099-1103, 1985.

Ordidge, R. J., Connelly, A., and Lohman, J. A. B., "Image-Selected in Vivo Spectroscopy (ISIS). A New Technique for Spatially Selective NMR Spectroscopy", J. Magn. Reson. 66: 283-94, 1986.

Ostroy, F., James, T. L., Noggle, J. H., Sarrif, A., and Hokin, L. E., "Studies on the Characterization of the Sodium-Potassium Transport Adenosinetriphosphatase. Nuclear Magnetic Resonance Studies of Na-23 Binding to the Purified and Partially Purified Enzyme", Arch. Biochem. Biophys. 162: 421-25, 1974.

Page, S. G., and Niedergerke, R., "Structures of Physiological Interest in the Frog Heart Ventricle", J. Cell. Sci. II: 179-203, 1972.

Persson, N., Lindblom, G., Lindman, B., and Arvidson, G., "Deuteron and Sodium-23 NMR Studies of Lecithin Mesophases", Chem. Phys. Lipids 12: 261-70, 1974.

Pettegrew, J. W., Woessner, D. E., Minshew, N. J., and Glonek, T., "Sodium-23 NMR Analysis of Human Whole Blood, Erythrocytes, and Plasma. Chemical Shifts, Spin Relaxation, and Intracellular Sodium Concentration Studies", J. Magn. Reson. 57: 185-96, 1984.

Pike, M. M., Fossel, E. T., Smith, T. W., and Springer, C. S. Jr., "High Resolution Na-23-NMR Studies of Human Erythrocytes: Use of Aqueous Shift Reagents", Am. J. Physiol. 246: C528-36, 1984.

Pike, M. M., Frazer, J. C., Dedrick, D. F., Ingwall, J. S., Allen, P. D., Springer, C. S. Jr., and Smith, T. W., "Na-23 and K-39 Nuclear Magnetic Resonance Studies of Perfused Rat Hearts. Discrimination of Intra- and Extracellular Ions Using a Shift Reagent", Biophys. J. 48: 159-173, 1985.

Pike, M. M., Simon, S. R., Balschi, J. A., and Springer, C. S. Jr., "High Resolution NMR Studies of Transmembrane Cation Transport: Use of an Aqueous Shift Reagent for Na-23", Proc. Natl. Acad. Sci., 79: 810-14, 1982.

Pike, M. M., and Springer, C. S. Jr., "Aqueous Shift Reagents for High Resolution Cationic Nuclear Magnetic Resonance", J. Magn. Reson., 46: 348-53, 1982.

Pike, M. M., Yarmush, D. M., Balschi, J. A., Lenkinski, R. E., and Springer, C. S. Jr., "Aqueous Shift Reagents for High Resolution Cationic Nuclear Magnetic Resonance. 2. Mg-25 K-39 and Na-23 Resonances Shifted by Chelidamate Complexes of Dysprosium (III) and Thulium (III)", Inorg. Chem., 22:2388-92, 1983.

Ra, J. B., Hilal, S. K., and Cho, Z. H., "A Method for in-Vivo MR Imaging of the Short T_2 Component of Sodium-23", Magn. Reson. Med. 3: 296-302, 1986.

Rayson, B. M., and Gupta, R. K., "Na-23 NMR Studies of Rat Outer Medullary Kidney Tubules", J. Biol. Chem. 260: 7276-80, 1985.

Reisin, I. L., Rotunno, C. A., Corchs, L., Kowalewski, V., and Cereijido, M., "The State of Sodium in Epithelial Tissues as Studied by Nuclear Magnetic Resonance", Physiol. Chem. Phys. 2: 171-9, 1970.

Renshaw, P. F., Haselgrove, J. C., Leigh, J. S., and Chance, B., "In Vivo Nuclear Magnetic Resonance Imaging of Lithium", Magn. Reson. Med. 2: 512-16, 1985.

Reuben, J., Shporer, M., and Gabbay, E. J., "Alkali Ion-DNA Interaction as Reflected in the Nuclear Relaxation Times of Na-23 and Rb-87", Proc. Natl. Acad. Sci. 72: 245-7, 1975.

Riddell, F. G., and Hayer, M. K., "The Monensin-mediated Transport of Sodium Ions Through Phospholipid Bilayers Studied by Na-23 NMR Spectroscopy", Biochim. Biophys. Acta. 817: 313-17, 1985.

Robb, J. S., Comparative Basic Cardiology, Grune and Stratton, New York, 1965.

Roe, D. C., and Marshall, A. G., "Dispersion versus Absorption: Analysis of Line-Broadening Mechanisms in Nuclear Magnetic Resonance Spectrometry", Anal. Chem. 50: 764-7, 1978.

Rose, K., and Bryant, R. G., "Electrolyte Ion Correlation Times at Protein Binding Sites", J. Magn. Reson. 31: 41-7, 1978.

Sakmann, B., and Neher, E., "Patch Clamp Techniques for Studying Ionic Channels in Excitable Membranes", Ann. Rev. Physiol., 46: 455-72, 1984.

Sandstrom, J., Dynamic NMR Spectroscopy, Academic Press, New York, 1982.

Shinar, H., and Navon, G., "NMR Relaxation Studies of Intracellular Na^+ in Red Blood Cells", Biophys. Chem., 20: 275-83, 1984.

Shporer, M., and Civan, M. M., "Nuclear Magnetic Resonance of Sodium-23 Linoleate Water: Basis for an Alternative Interpretation of Sodium-23 Spectra Within Cells", Biophys. J., 12: 114-22, 1972.

Shporer, M., and Civan, M. M., "Effects of Temperature and Field Strength on the NMR Relaxation Times of Na-23 in Frog Striated Muscle", Biochim. Biophysic. Acta., 354: 291-304, 1974.

Shporer, M., and Civan, M. M., "Pulsed Nuclear Magnetic Resonance Study of K-39 Within Halobacteria", J. Membr. Biol. 33: 385-400, 1977a.

Shporer, M., and Civan, M. M., "The State of Water and Alkali Cations within the Intracellular Fluids: The Contribution of NMR Spectroscopy", Curr. Topics Memb. Transp. 9: 1-69, 1977b.

Shporer, M., Zemel, H., and Luz, Z., "Kinetics of Complexation of Sodium Ions with Valinomycin in Methanol by Na-23 NMR Spectroscopy", FEBS Lett. 40: 357-60, 1974.

Slichter, C. P., Principles of Magnetic Resonance, Springer-Verlag, New York, 1980.

Sperelakis, N., "Electrical Properties of Cells at Rest and Maintenance of the Ion Distributions", in Physiology and Pathophysiology of the Heart, ed. by N. Sperelakis, Martinus Nijhoff Publ. Boston, 1984.

Springer, C. S. Jr., Pike, M. M., Balschi, J. A., Chu, S. C., Frazier, J. C., Ingwall, J. S., and Smith, T. W., "Use of Shift Reagents for Nuclear Magnetic Resonance Studies of the Kinetics of Ion Transfer in Cells and Perfused Hearts", Circ. 72 (Suppl. IV): IV-89-93, 1985.

Sweadner, K. J., and Goldin, S. M., "Active Transport of Sodium and Potassium Ions", N. Engl. J. Med. 302: 777-83, 1980.

Ting, D. Z., Hagan, P. S., Chan, S. I., Doll, J. D., and Springer, C. S. Jr., "Nuclear Magnetic Resonance Studies of Cation Transport Across Vesicle Bilayer Membranes", Biophys. J., 34: 189-215, 1981.

Tsien, R. Y., "Intracellular Measurements of Ion Activities", Ann. Rev. Biophys. Bioeng. 12: 91-116, 1983.

Uchiyama, K., Tsumuraya, Y., Ishibiki, A., and Okada, K., "Electrophysiological and Biochemical Activities of Amphibian Heart", in Electrophysiology of Ultrastructure of the Heart, T. Sano, V. Mizuhira, and K. Matsuda, eds., Grune and Stratton Inc., New York, 1967.

Urry, D. W., Trapane, T. L., Andrews, S. K., Long, M. M., Overbeck, H. W., and Oparil, S., "NMR Observation of Altered Sodium Interaction with Human Erythrocyte Membranes of Essential Hypertensives", Biochem. Biopys. Res. Comm. 96: 514-21, 1980.

Ventura-Clapier, R., and Vassort, G., "The Hypodynamic State of the Frog Heart. Further Evidence for a Phosphocreatine-Creatine Pathway", J. Physiol. (Paris) 76: 583-89, 1980.

Venkatachalam, C. M., and Urry, D. W., "Analysis of Multisite Ion Binding Using Sodium-23 NMR with Application to Channel-Forming Micellar-Packaged Malonyl Gramicidin", J. Magn. Reson. 41: 313-35, 1980.

Walker, J. L., and Ladle, R. O., "Frog Heart Intracellular Potassium Activities Measured with Potassium Microelectrodes", Am. J. Physiol. 225: 263-7, 1973.

Wennerstrom, H., Linblom, G., and Lindman, B., "Theoretical Aspects on the NMR of Quadrupolar Ionic Nuclei in Micellar Solutions and Amphiphilic Liquid Crystals", Chemica Scripta 6: 97-103, 1974.

Werbelow, L. G., and Marshall, A. G., "The NMR of Spin-3/2 Nuclei: The Effect of Second Order Dynamic Frequency Shifts", J. Magn. Reson., 43: 443-8, 1981.

Wittenberg, B. A., and Gupta, R. K., "NMR Studies of Intracellular Sodium Ions in Mammalian Cardiac Myocytes", J. Biol. Chem. 260: 2031-4, 1985.

Yeh, H. J. C., Brinley, F. J. Jr., and Becker, E. D., "Nuclear Magnetic Resonance Studies on Intracellular Sodium in Human Erythrocytes and Frog Muscle", Biophys. J., 13: 56-71, 1973.

APPENDIX

This appendix contains the data from the T_2 relaxation experiments. In all, 8 hearts were utilized for these studies. Both control relaxation curves and ouabain relaxation curves were obtained from 4 of these. The ouabain curve was repeated for 3 of the hearts after conditions were changed. (In 2 cases, the shift reagent perfusate was changed to one which had a different inherent T_2, and in 1 case the curve was obtained once with presaturation of the shifted resonance and once without.)

As an initial means of comparing the control versus ouabain relaxation behavior, the data was plotted with the first data point normalized to the same value for both the control and ouabain cases. The same was done with the second data point, so that the scatter of the first data point would not be a predominant factor in the comparisons. These graphs are shown in Figures A-1 through A-4.

The parameters of the fit to equation 7.1 for all of the hearts are given in Table A.1. For the cases in which there were two sets of data for a given heart, the parameters were averaged and the average value was used to yield the mean parameters of Table 8.2.

The first set of data for heart #6 was also fit with the constraint that 50 percent of the decay would have a time constant of less than 10 msec. This yielded time constants of 3.9 and 24.3 msec, with relative amplitudes of 0.60 and 0.40. However, the standard deviation of the fit was much higher than that of the unconstrained fit (3.9 ± 0.8 msec and 24.3 ± 9.5 msec versus 2.2 ± 0.4 msec and 14.7 ±

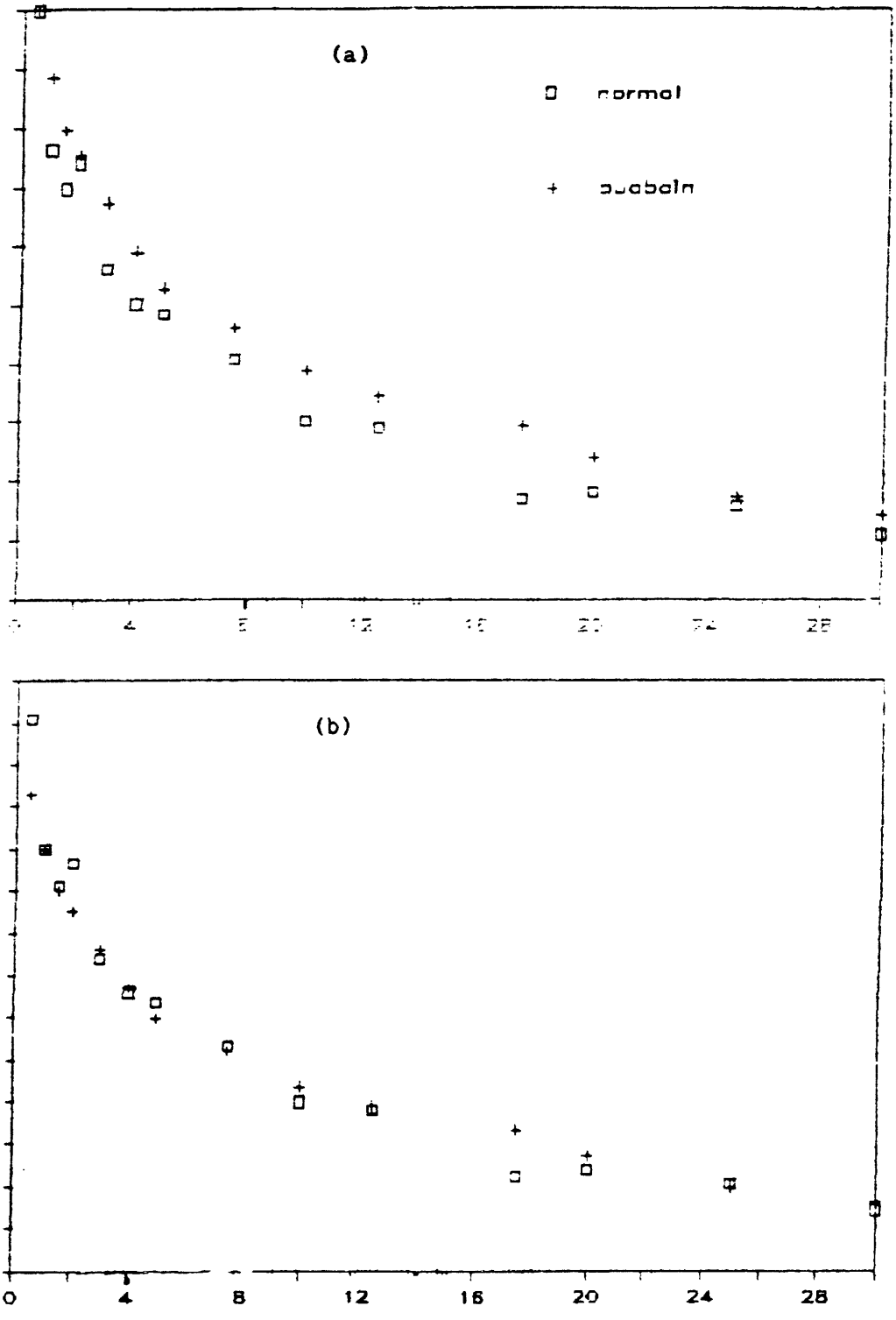

Figure A-1 T_2 relaxation decay for heart #2 under control and ouabain conditions; (a) normalized to first point, (b) normalized to second point.

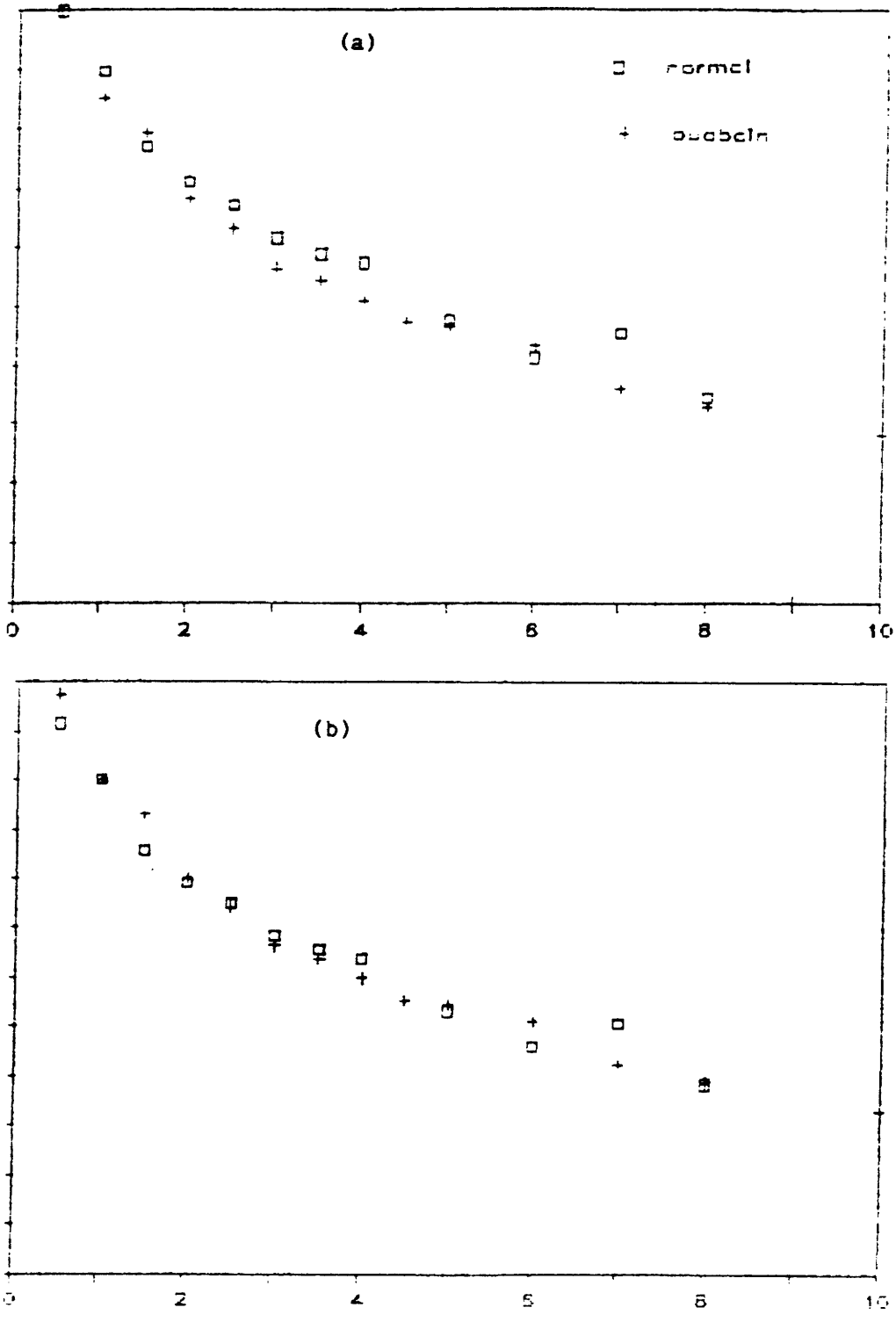

Figure A-2 T_2 relaxation decay for heart #3 under control and ouabain conditions; (a) normalized to first point, (b) normalized to second point.

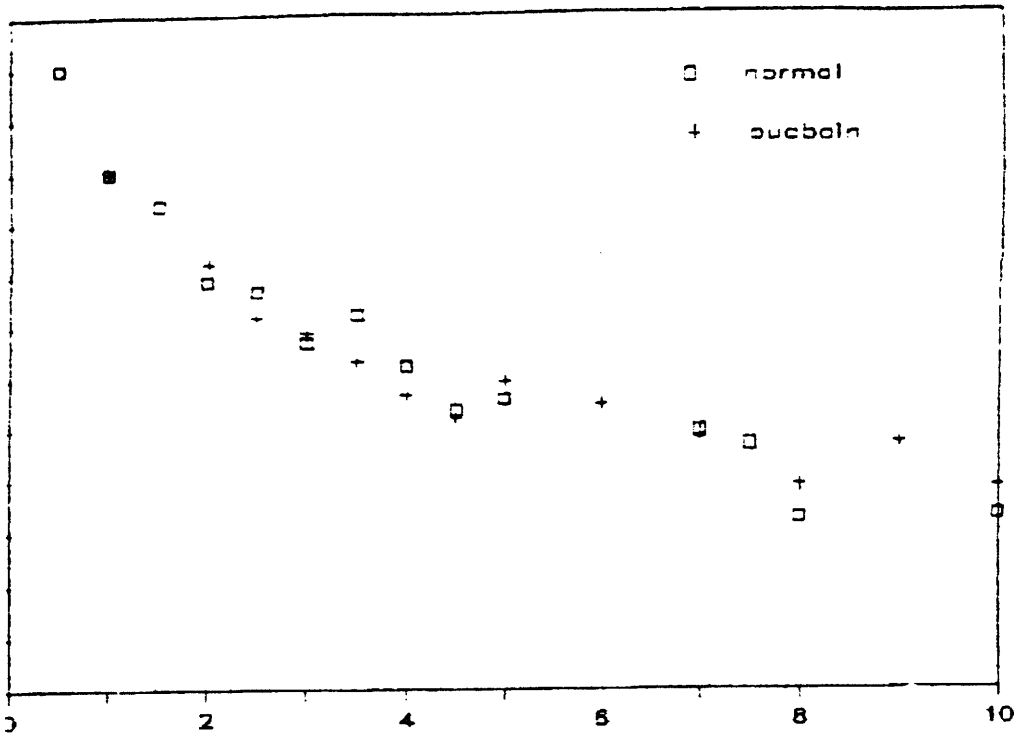

Figure A-3 T_2 relaxation decay for heart #5 under control and ouabain conditions. Since there was no data at 0.5 msec for this heart under conditions of ouabain, the data is normalized to the second point only.

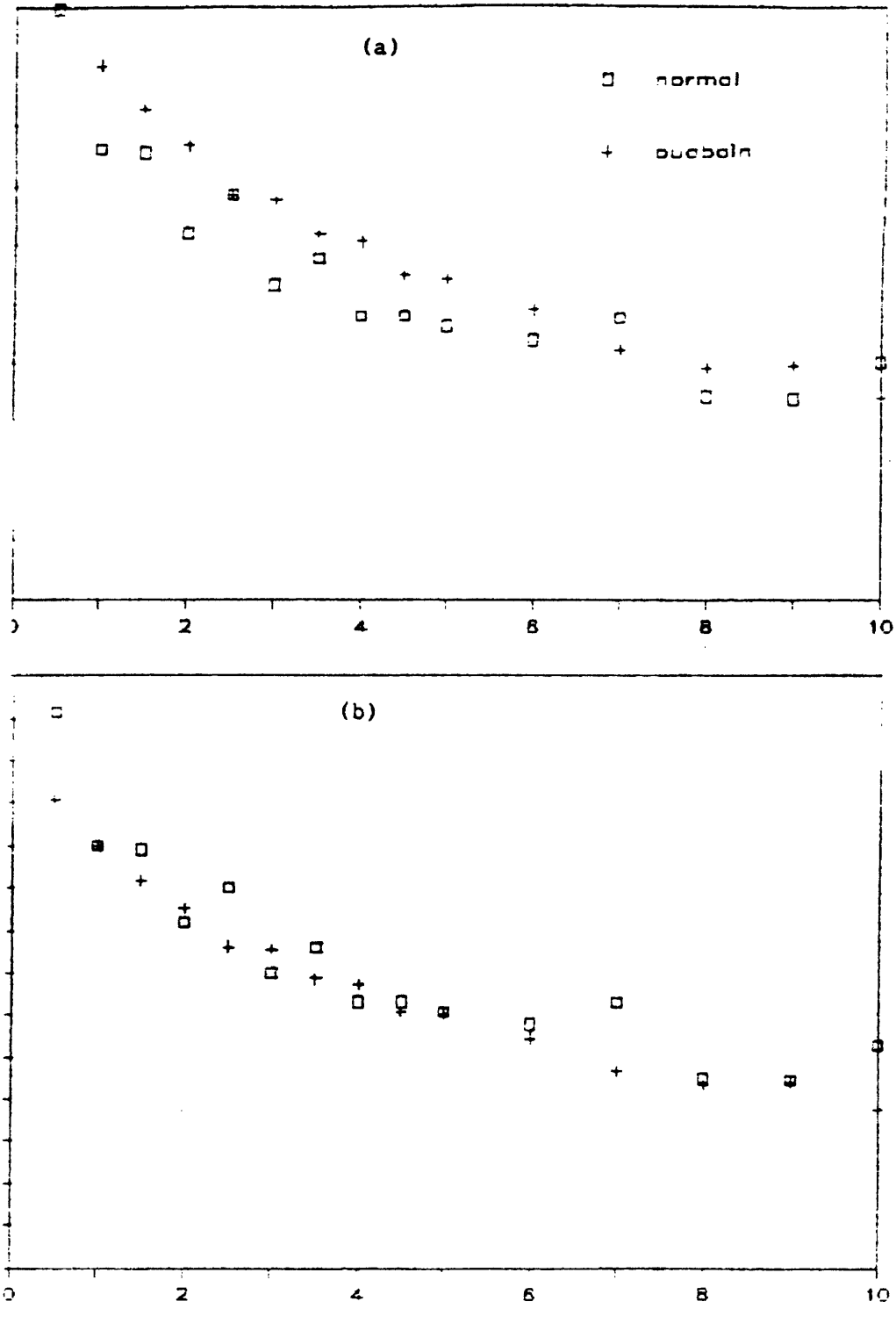

Figure A-4 T_2 relaxation decay for heart #6 under control and ouabain conditions; (a) normalized to first point, (b) normalized to second point.

Heart #	Control				Ouabain			
	A	α	B	β	A	α	B	β
1					0.37	2.4	0.63	20.7
2	0.50	4.0	0.50	21.8	0.42	1.9	0.58	19.9
3	0.32	1.0	0.68	10.0	0.41	1.8	0.59	11.2
4					0.40	2.4	0.60	20.6
					0.50	3.1	0.50	20.5
5	0.49	1.4	0.51	17.4	0.45	1.2	0.55	14.3
6	0.47	1.1	0.53	17.1	0.38	2.2	0.62	14.7
					0.41	2.4	0.59	14.2
7					0.51	3.1	0.49	15.8
					0.57	2.1	0.43	14.5
8	0.50	2.3	0.50	15.0				

Table A.1 Parameters of the fits to the equation $M = M_0(Ae^{-t/\alpha} + Be^{-t/\beta})$. The time constants are given in msec. For hearts #4 and #6, the ouabain curve was repeated with a different shift reagent buffer, which had a different inherent T_2. For heart #7, the first set of data was obtained with presaturation of the shifted resonance, the second set of data was obtained without presaturation. The ouabain data of hearts #1 and #5 were also obtained without presaturation of the shifted resonance.

1.2 msec). Thus, constraining the fit to that which would be expected from a homogeneous pool of nuclei leads to a much poorer fit of the data.

It is interesting to note that visual inspection of the theoretical fit is not a very sensitive method of determining the goodness of the fit. The first data set of heart #4 was used to compare the plot of the data points versus the best fit to the data with the plot of the data points versus another theoretical fit, with very different time constants and relative amplitudes. This is shown in Figure A-5. While the distribution of points around the curve obtained from the

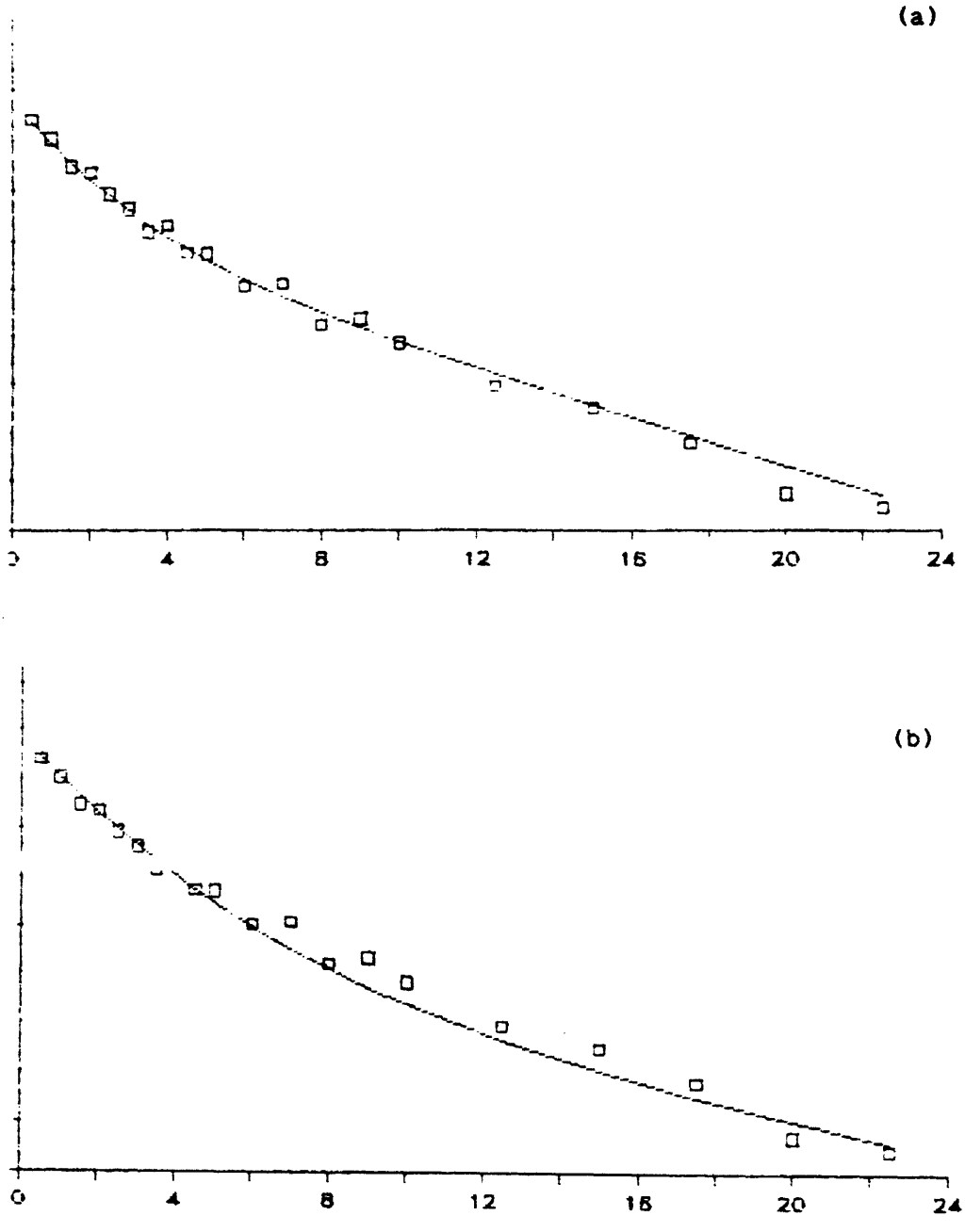

Figure A-5 The T_2 relaxation data for heart #4, plotted with 2 different theoretical fits. (a) The solid curve represents the decay of a biexponential with time constants and relative amplitudes of 2.5 msec (0.40) and 20.0 msec (0.60). (b) The solid curve consists of time constants and relative amplitudes of 4.0 msec (0.60) and 30 msec (0.40).

best fit to the data is more homogeneous than the distribution around the other theoretical curve, differentiating between these two would be very difficult on a visual basis alone.